RICE UNIVERSITY

Investigating the biological impacts of nanoengineered materials in *Caenorhabditis elegans* and *in vitro*

by

Elizabeth Quevedo Contreras

A THESIS SUBMITTED
IN PARTIAL FULFILLMENT OF THE
REQUIREMENTS FOR THE DEGREE

Doctor of Philosophy

APPROVED, THESIS COMMITTEE

Vicki L. Colvin, Chair
Kenneth S. Pitzer-Schlumberger Professor
of Chemistry and Professor of Chemical &
Biomolecular Engineering

Lon J. Wilson
Professor of Chemistry

Weiwei Zhong
Assistant Professor of Biochemistry and
Cell Biology

HOUSTON, TEXAS
October 2012

ABSTRACT

Investigating the biological impacts of nanoengineered materials in *Caenorhabditis elegans* and *in vitro*

by

Elizabeth Quevedo Contreras

In nematode *Caenorhabditis elegans, t*he chronic and multi-generational toxicological effects of commercially relevant engineered nanoparticles (ENPs), such as quantum dots (QDs) and silver (AgNP) caused significant changes in a number of physiological endpoints. The increased water-solubility of ENPs in commercial products, for example, makes them increasingly bioavailable to terrestrial organisms exposed to pollution and waste in the soil. Since 2008, attention to the toxicology of nanomaterials in *C. elegans* continues to grow. Quantitative data on multiple physiological endpoints paired with metal analysis show the uptake of QDs and AgNPs, and their effects on nematode fitness. First, *C. elegans* were exposed for four generations through feeding to amphiphilic polymer coated CdSe/ZnS (core-shell QDs), CdSe (core QDs), and different sizes of AgNPs. These ENPs were readily ingested. QDs were qualitatively imaged in the digestive tract using a fluorescence microscopy and their and AgNP uptake quantitatively measured using ICP-MS. Each generation was analyzed for changes in lifespan, reproduction, growth and motility using an automated computer vision system. Core-shell QDs had little impact on *C. elegans* due to its metal shell coating. In contrast, core QDs lacked a metal shell coating, which caused significant changes to nematode physiology.

In the same way, at high concentrations of 100 ppm, AgNP caused the most adverse effect to lifespan and reproduction related to particle size, but its adverse effect to motility had no correlation to particle size. Using *C. elegans* as an animal model allowed for a better understanding of the negative impacts of ENPs than with cytotoxicity tests. Lastly, to test the toxicity of water-dispersed fullerene (nanoC_{60}) using human dermal fibroblast cells, this thesis investigated a suite of assays and methods in order to establish a standard set of cytotoxicity tests. Ten assays and methods assessed nanoC_{60} samples of different purities to show differences in cytotoxic effects. Washed samples of fullerenes, with negligible traces of THF and other impurities, rendered the solution nontoxic. Even when exposed to UV-irradiation, washed nanoC_{60} were not photosensitized and did not cause cellular death. This work characterizes ENPs and investigates their impact in *C. elegans* and cells to assess toxicity risks to the environment and to human health.

Acknowledgments

I gratefully thank my advisor and the Chair of my thesis committee, Dr. Vicki L. Colvin for the advice, discussion and support in all ways. I wish to thank Dr. Lon Wilson for participating on my thesis committee; Dr. Weiwei Zhong for the support on the *C. elegans* nanobiotoxicity work and for participating on my thesis committee; and Dr. Jenifer West for the support on the cytotoxicity tests.

I thank you Dr. Wenhua Guo and all SEA staff. I wish to thank my current and past fellow group members and collaborators for your friendship and humor. I would also like to thank my former advisor, Dr. D. Tyler McQuade, and all of those at Cornell University in Ithaca, NY, my first graduate university, for their encouragement. Lastly, I would also like to thank Dr. Patrick Larkin who taught me many laboratory skills as his first undergraduate student at my first research internship at Texas A&M University—Corpus Christi, TX, my undergraduate university. Thank you to all of my current and past professors and teachers in science for their guidance.

I am grateful to my Lord for the gift of my own family. I thank my husband, Jesús G. Contreras, for his immense patience and endless support during my decade-long pursuit for (scientific) knowledge. In Corpus Christi, we met as youths and became best friends, and our love for each other has grown exponentially. Since then, God has given me two beautiful boys, Itzak Jesús and Lucas Andres Contreras, to love and to cherish. Words cannot express the joy that I feel in my heart.

I wish to thank my wonderful parents for their godly wisdom and for their dedication to my life for thirty one years. I thank my mother, Emma Quevedo, for always

encouraging me to live my life and for unselfishly helping me care for my own family as lovingly and as perfectly as only she can; and my father, Rev. Enrique L. Quevedo, for his constant prayers over our family. I would like to thank my brother, Enrique E. Quevedo, and his wife, Shirley, for cheering me on all of these years. I thank my husband's mother, Angeles Velandia, for her good will.

I thank my brothers and sisters in Christ at Champion Forest Baptist Church in Houston, TX, at South Main Baptist Church in Houston, TX, and at Iglesia Bautista Horeb in Corpus Christi, TX, for an amazing period of growing and walking in the Lord. I agree with what was written long ago: "For I know the plans I have for you," declares the LORD, "plans to prosper you and not to harm you, plans to give you hope and a future" (Jeremiah chapter 29, verse 11, New International Version of the Bible). These past seven and a half years in Houston have been a remarkable time of growth for me, especially from being surrounded by so many amazing people.

And finally I would like to thank the National Science Foundation, the Center for Biological and Environmental Nanotechnology, the United States Environmental Protection Agency, the National Institutes of Health, and the Kinship Foundation—Searle Scholars Program for funding.

Table of Contents

List of Figures

List of Tables

Nomenclature

AgNP	Silver nanoparticle
Al_2O_3	Aluminum oxide (Alumina)
AM	Acetomethoxy
AuNP	Gold nanoparticle
BC_{50}	Median behavior concentration
BOW	Bag of worm
C. elegans	*Caenorhabditis elegans*
CDC	Cyclodextrin
CFU	Colony-forming units
D. magna	*Daphnia magna*
DCF	2'7'-dichlorofluorescein
DCFH	2'7'-dichorodihydrofluorescein
DCFH-DA	2'7'-dichorodihydrofluorescein-diacetate
DMEM	Dulbecco's Modified Eagle's Medium
ENP	Engineered nanoparticle
FND	Fluorescent nanodiamond
GA	Gum arabic
GC-MS	Gas-chromatography mass-spectroscopy
GFP	Green fluorescent protein
GNP	Graphite nanoplatelets
h	Hour

H_2O_2	Hydrogen peroxide
HDF	Human dermal fibroblast
L1	Larval stage 1
L4	Larval stage 4
LC_{50}	Median lethal concentration
m	Minute
MTS	3-(4,5-dimethylthiazol-2-yl)-5-(3-carboxymethoxyphenyl)-2-(4-sulfophenyl)-2H-tetrazolium
NP	Nanoparticle
PBS	Phosphate buffer solution
PI	Propidium iodide
PtNP	Platinum nanoparticle
PVP	Polyvinyl pyrrolidone
ROS	Reactive oxygen species
s	Second
SEM	Scanning electron microscope
TEM	Transmission electron microscope
THF	Tetrahydrofuran
TiO_2	Titanium dioxide (titanium (IV) oxide or titania)

Chapter 1

Introduction

Nanoparticles have an array of applications from electronics to medicine, to textiles and composites, to energy production. Production of NPs has increased over the years as industry exponentially exploits NPs into consumables and textiles. It seems that any element or metal can be rendered to nanometer size by pyrolysis. The shape, small diameter, large surface area and reactivity of the NP yield its unique physiochemical properties.

According to the U.S. Environmental Protection Agency, nanoparticles (NPs) consist of any material or metal with at least one or more dimension measuring 100 nanometers or less. NPs are engineered to display unique electrical, mechanical, optical and thermal properties that differentiate it from its ionic or its bulk form of the same composition. The large surface/volume ratio, small diameter size, and different physiochemical properties make it unique to its bulk and ionic counterpart. The very characteristics that make NPs appealing are the properties that make it unique.

Current federal and safety regulations are still lacking. Ideally, understanding the ecological consequence by NPs should be obtained before production into thousands of products and ultimately before becoming waste in land fields. Potential occupational and public exposure to manufactured nanoparticles and to those found in consumer products has increased (**Figure 1**). For example, the ubiquitous sunscreen lotion contain nano-sized TiO_2 and ZnO for its UV blocking property with no opaque emulsion, rendering the solution transparent on the skin after coverage. The lack in oversight stems from misperceptions of NP toxicity and health risk to human safety and to the environment. In fact, NPs are categorized under the same composition as its non-toxic bulk counterpart from which exposure and risk for nano-sized materials are presumed, without regards to the novel and unique properties of NPs. This has led to a vast market of consumer products with NPs, but without sufficient testing to understand neither the adverse effects nor proper labeling on the ingredients' list.

NP waste is continuously generated or unintentionally released into terrestrial and water ecosystems threating many organisms and ultimately, the food-chain (**Figure 1**).

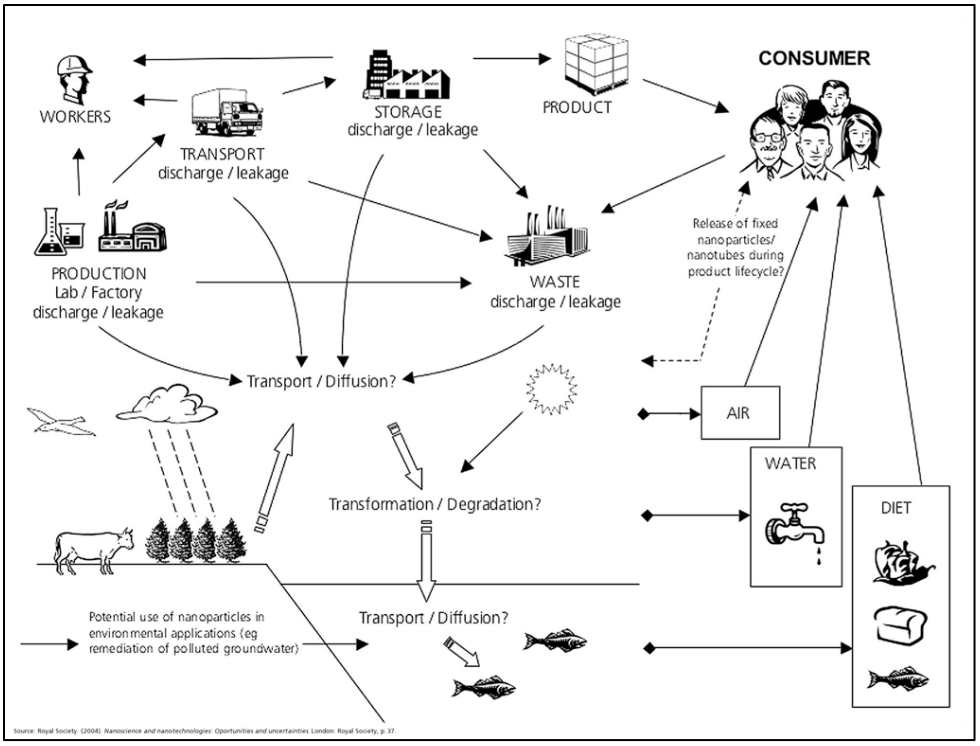

Figure 1. Engineered nanoparticles produced can end up in the enviornment. Reprinted from Royal Science [1]

Nanoparticles are not only released as waste into aqueous but also into terrestrial ecosystems. Nematodes are the first of the animals to interact with material wastes. Although abundantly found in the soil, wild-type C. *elegans* have been researched for years in a laboratory setting. These nematodes are available of the same strain as clones with the same genetic sequence, ideal for genetic and ecotoxicity studies, unlike earthworms. Handing them in a lab with minimal sterile techniques allows for quick and practical means of studying adverse effects in a multi-cellular organism. The short life-span and large brood size make these animals easy to work for studies in genetics, neurobiology, ethology and development, and toxicity.

The purpose of this thesis was to assess the toxicological effects of semi-conducting and metallic nanoengineered materials to terrestrial organism, *C. elegans, in vivo* in Chapters 4 and 5. Quantum dots are semi-conducting NPs that fluoresce at different wavelengths dependent on the diameter of their metal core, and are used primarily in optical and diagnostic applications. Silver nanoparticles are one of the most abundant materials with the most applications in diagnostic, antibacterial, conductive and optical fields. Existing literature with *C. elegans* exposed to different NPs show adverse effects at sublethal concentrations on different parameters such as lifespan, ageing, growth and fertility. These materials, without a doubt, will end up as waste and introduced into the environment. Therefore, studies on bioavailability and distribution in aquatic and terrestrial systems at sublethal concentrations are ongoing.

Here, NP toxicity research with *C. elegans* (i) introduced the use of sublethal concentrations of NPs on multiple generations, (ii) documented the adverse effects for up to 4 generations from chronic exposure to NP, (ii) measured physiological parameters such as lifespan, fertility and growth, and (iv) used a WormTracker to quantify locomotive behavior, such as flex, wavelength, amplitude, and velocity, using videography and software to analyze sinusoidal movements. Chapter 3 further explains the experimental methods for the procedures used in Chapters 4 and 5. Lastly, Chapter 6 and 7 examines risks to human health using human dermal fibroblast cells (HDF) exposed to nanoaggregated C_{60} fullerenes. A number of assays to test cytotoxicity and cell-free ROS production by fullerenes are explained in Chapter 6.

Chapter 2

Background

2.1. Introduction

NPs are mostly developed for bioimaging, drug delivery, and other antimicrobial properties. Concerns over nanoparticle exposure are over their stability, chemistry, size, and bioavailability that can make distribution into the environment unfavorable. For nanoparticles (NPs), the ionic form becomes problematic. Thus, assessing the toxicity of NPs should be fostered from dissolved metals, rather than from its bulk counterpart. For example, the antibacterial property of silver ions places AgNPs in many textiles such as socks, feminine hygiene products, and hospital curtains.[2] In turn, free silver ions in the soil originate from the wash of textiles which can lead to a negative impact on microbes in the environment, and ultimately the food chain.[2]

Table 1. Current timeline of *C. elegans* and nanoparticle literature from 2008-2012.

Year	Nanoparticle	Ref. [author]
2008	Cu	Gao/Chai Z
	Pt	Kim/Miyamoto Y (a)
	Pt	Kim/Miyamoto Y (b)
2009	Ag	Roh/Choi J
	Nanophosphors	Lim/Austin RH
	SiO_2	Pluskota/von Mikecz A
	ZnO	Ma/Williams PL
	ZnO, Al_2O_3, TiO_2	Wang/Xing B
2010	Ag	Meyer/Auffan M
	CeO_2, TiO_2	Roh/Choi J
	Diamond	Mohan/Chang H
	Pt	Sakaue/Miyamoto Y (c)
	Pt	Kim/Miyamoto Y (d)
2011	Ag	Yang/Meyer JN
	Al_2O_3	Wu/Wang D
	CeO_2	Zhang/Chai Z
	$Gd@C_{82}OH_{22}$	Zhang/Zhao Y
	Nanophosphors	Chen/Xu S
	Quantum dots	Qu/Chen C
	ZnO	Ma/Williams PL
2012	Ag	Ellegaard-Jensen/Johansen A
	Ag	Kim/An YJ
	Ag	Lim/Choi J
	Al_2O_3	Li/Wang D
	Au	Tsyusko/Bertsch PM
	C_{60}-OH	Cha/Choi SS
	Carbon nano-Onion	Sonka/Sarkar S
	CuO	Zhang/Pan X
	Graphite	Zanni/Uccelletti D

C. elegans are terrestrial nematode commonly found in the soils and can be used as indicators of environmental health. Nematodes have been the subject of a number of toxicology studies focused on the acute effects of NPs such as silver, silica, ceria, titania, and zinc (Table 1). A short lifespan (20-25 days) and large brood size (300 per worm) by self-fertilization make it easy to study and grow in the lab with OP50 *Escherichia coli* as food. *C. elegans* have 5 main life-stages which include four larval stages (L1, L2, L3, L4) and an adult stage (Figure 2). When under extreme stress, *C. elegans* survive by entering a sixth life stage of dauer-formation by development arrest until conditions improve. Adverse effects on their population and fitness can indicate stress in their soil environment. In literature, ecotoxicological endpoints such as, lethality, reproduction, growth, and locomotion behavior can be indicators of stress and of toxicity. Assessment tools to monitor fitness include chemical, optical, diagnostic, and genetic tests to measure stress-response gene expressions in *C. elegans*.[3]

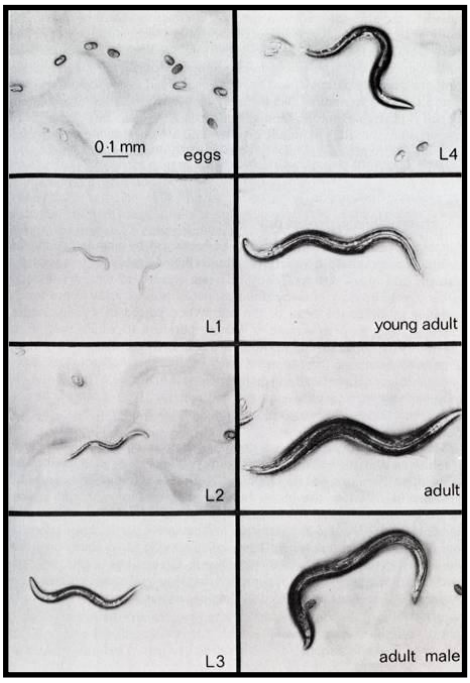

Figure 2. Nematodes have four larval stages in its life-cycle. Reprinted from the Journal of Visualized Experiments [4][4]

How *C. elegans* respond to endogenous and exogenous oxidative stress in its environment, affects a number of physiological endpoints, such as ageing and reproduction, which are directly related to cumulative oxidative stress and reactive oxygen species (ROS). Oxidative stress can alter ion gradients across cellular membranes, fragment and alter genetic material such as DNA, induce premature ageing and diseases, and damage a variety of cell types including oocytes and sperm of reproduction systems.[5] Like humans, nematodes have defenses against excess ROS, such as SOD/catalase and glutathione peroxidase which mainly scavenge excess O_2^- and H_2O_2 to detoxify the body.[6] Nematodes can also evolve to survive aggressive environments, or else perish.

2.2. Physiological Endpoints

Nematodes are a model organism that lends itself to efficient and high throughput experiments to monitor adverse effects from toxicants and wastes. Physiological endpoints, such as lifespan, fertility, body size can be easily assessed under a compound microscope. Nematode locomotion behavior is quantified using a computer-controlled tracking stage and software. Along with genetic screening, nematodes provide a vast opportunity of information on the varying modes of toxicity from different engineered nanoparticles with different compositions and structures.

Table 2. Literature summary of observed biologcial effects on N2 *C. elgans* by different nanoparticle systems**.**

ENP	Surface Coating	Media Exposure	Diameter	Concentration (mg/L)	Phenotype	Exposure	Life Stage	EC50	Biological Effect	Reference
Ag NP	bare	H2O	14-20 nm (<100 nm)	0.05, 0.1, 0.5	lifespan (1), growth (2), reproduction (3)	24 h (1,2) & 72 h (3)	L4 to Adult	n/a	No effect on survival (1) or growth (2); significant decrease (70%) in fertility (3); stress-related gene expression (daf-12 gene)	Roh, Sim 2009
Ag NP	PVP	K-media	21, 75 nm	0.5-5.0 mg/L	growth (1), reproduction (2)	3 d	L1 to Adult	50 mg/L (1)	Growth inhibition (1); no effect on fertility (2); smaller NP are easier to uptake;	Meyer, Lord 2010
Ag NP	citrate	K-media	7 nm	0.5-5.0 mg/L	growth (1), reproduction(2)	3d	L1 to Adult	5 mg/L (1)	Growth inhibition (1); transferred past cell membrane of egg; Bagging (2)	Meyer, Lord 2010
Ag NP	citrate	H2O & agar	50.6 nm	1-1000 mg/L	lifespan (1), reproduction (2)	24 h (1), 48 h (2)	L1/L2	55 mg/L (1), >100 mg/L (2)	Reduced survival (1) and reproduction (2), but not significantly; caused epidermis edema and burst	Kim/ An YJ 2011
Ag NP	bare	K-media	1.3 nm	gradient	lifespan	24, 48, 72h	L4	13.9 mg/L (1), 2.8 mg/L (2)	Not lethal	Ellengard-Jensen/ Johansen 2012
Ag NP	PVP	K-media	28 nm	gradient	lifespan	24, 48, 72h	L4	13.9 mg/L (1), 2.8 mg/L (2)	PVP coated NP was more toxic	Ellengard-Jensen/ Johansen 2012
Ag NP	bare	H2O	20-30 nm	0.1, 0.5, 1 mg/L	reproduction	4, 24 h	L4	n/a	Decreased reproduction and increased oxidative stress and genes. These AgNP more toxic than AgNO3	Lim/ Choi J
Ag NP	citrate	H2O	7 nm	gradient	growth	24 h	L1		No correlation to size (1). Instead toxicity correlated to coating.	Yang/Meyer JN

ENP	Surface Coating	Media Exposure	Diameter	Concentration (mg/L)	Phenotype	Exposure	Life Stage	EC50	Biological Effect	Reference
Ag NP	PVP	H2O	8, 38 nm	gradient	growth	24 h	L1		Adverse effect: GA>PVP>citrate	Yang/Meyer JN
Ag NP	gum arabic (GA)	H2O	5, 22 nm	gradient	growth	24 h	L1		Toxicity is greater in H2O (lower ionic strength) than in K-media; caused growth inhibition	Yang/Meyer JN
Al2O3 NP	bare	H2O	60 nm	10-400 mg/L	lifespan (1), growth (2), fertility (3), reproduction (4)	5d	L1 to Adult	82; 102; 102; 51 mg/L	Nano morelethal than bulk (1); inhibited growth (2); decreased number of eggs inside body (3) and offspring per worm (4)	Wang, Wick 2009
Al2O3 NP	bare	H2O	470-1126 nm	6.3-203.9 mg/L	lifespan (1), stress (2), ageing (3)	24 h	L1, L4 or Adult	6.3 (L1); 12.7 mg/L (L4)	Severe lethality greatest in L1 than L4 (1) correlated to stress response at 25.5 mg/L and cellular damage (2)	Wu, Lu 2011
Diamond NP	dextran	H2O & agar	290 nm (120 nm)	1.0 mg/L	lifespan (1), reproduction (2), stress (3)	3 h	L4	n/a	Biocompatible, nontoxic; no ROS production	Mohan, Chen 2010
CeO2 NP		K-media	15, 45 nm	1 mg/L	lifespan (1), growth (2), reproduction (3)	24 h	L4 to Adult	n/a	15 nm NP significantly decreased survival by 20% (1) and fertility by 28% (3); doesn't alter growth (2)	Roh, Park 2010
CeO2 NP		EtOH/H20 & agar	8.5 nm	1 nM-100 nM	lifespan (1), stress (2)	10, 72 h	L1 to Adult	1, 5 nM	Adverse effects at low concentrations. Lifespan decreased by 12% at 1 nM.	Zhang, He 2011
Cu NP		PBS	23.5 nm	1e-4 mg/L	mapping/in situ	36 h	L1 to Adult	n/a	Accumulation of NP not significant with 5.22ug/g internalized	Gao, Liu 2008
Pt NP	PVP	H2O	2.4 nm	0.1-1.0 mM NP	lifespan (1), stress (2)	5 d	L4 to Adult	n/a	Anti-ageing property oxidative stress resistance; SOD/catalase mimetic	Kim, Takahashi 2008

ENP	Surface Coating	Media Exposure	Diameter	Concentration (mg/L)	Phenotype	Exposure	Life Stage	EC50	Biological Effect	Reference
Pt NP	PVP/TAT-peptide-Pt		2.4 nm	0.2-50 uM NP	lifespan (1), ageing (2)	10 d	L4, Adult	0.5 uM (1); 5 uM (2-4)	Microcapsules (polypeptide/TAT) were internalized and extended lifespan by oxidative stress resistance	Kim, Shirasawa 2010
Pt NP	PVP/TAT-peptide-Pt	S-media; M9 buffer	2.4 nm	1-25 uM NP	lifespan	10 d	L4 to Adult	5 uM	Internalized in mitochondria and cytosol with NADH oxidase mimetic activity	Kim, Shirasawa 2010
SiO2 NP	bare	H2O & agar	50 nm	2.5 mg/L	lifespan (1), reproduction (2)	24 h	L4 to Adult	n/a	Doesn't alter mortality (1); decreased offspring (2); increased BOW phenotype (age-related degeneration of reproduction organs)	Pluskota, Horzowski 2009
TiO2 NP	bare	H2O	50 nm	24-240 mg/L	lifespan (1), growth (2), fertility (3), reproduction (4)	5d	L1 to Adult	80; 47.9; 47.9; 47.9 mg/L	Nano more lethal than bulk (1). Non-toxic at low concentration; may cause food depletion from antibacterial properties	Wang, Wick 2009
TiO2 NP		K-media	7, 20 nm	1 mg/L	lifespan (1), growth (2), reproduction(3)	24 h	L4 to Adult	n/a	Smaller particles are more toxic; 7 nm NP significantly decreased survival by 30% (1), growth by 9%(2), and fertility by 21% (3)	Roh, Park 2010
ZnO2 NP		K-media	1.5 nm	325-1625 (1); 50-1000 (2); 10-200 (3); 5-130 mg/L (4)	lifespan (1); locomotion (2); reproduction (3)	24 h(2); 72 h(3)	Adult	789; 635; 46 mg/L	10 % lethality (1); similar toxicity as ZnCl2	Ma, Bertsch 2009

2.2.1. Lifespan

When shortened, the lifespan of *C. elegans* has direct correlations to stress response from its environment, from reactive oxygen species (ROS) production , or from free ion dissolution. In humans, ROS are also the main culprit for premature ageing, diseases and death. The number of days from hatching until death constitutes nematode lifespan. Using a platinum wire, the nematodes are gently nudged for movement. Lack of motion indicates nematode death. The best value from these studies is the median lethal concentration (LC_{50}). This value can be used to compare with results in other animal models exposed to small chemicals, pharmaceuticals, poisons, and ENPs such as AgNP. In contrast, Miyamoto, *et al.,* showed platinum NPs served as an antioxidant and increased lifespan by scavenging ROS.[6-9]

2.2.1. Reproduction and Fertility

A decrease in reproduction and fertility has direct correlation to increased endogenic or exogenic stresses.[3] Wild-type N2 nematode yields 300 progeny in its lifetime over the span of 4-5 days. Reproduction is the number of surviving progeny; fertility is the number of gravid nematodes with one or more eggs. Endogenic stress can result from reactive oxygen species (ROS) and oxidative stress that can damage a variety of cell types, including oocytes and sperm.[5] Both of these endpoints can be adversely effected by toxicants that cause nematode developmental delays, decreased sexual appeal, obstructed reproductive parts, or deformities that prevent laying eggs as bag-of-worm (BOW) phenotypes, becoming lethal to parent as progeny hatch within the body cavity of its parent. At sublethal concentrations, a 40% inhibition for reproduction and 20%

inhibition for nematode fertility were established as the toxicity threshold when compared to untreated nematodes.[10]

Another consequence from ENP exposure besides decreased fertility in nematodes, is an increase in BOW phenotype.[11,12]For example, AgNP caused neurodegeneration and vulva muscle dystrophy, increasing bagging.[11] According to Pluskota, et al., silica nanoparticles also caused reproductive senescence where the vagina of nematodes swelled and prevented proper egg laying.

2.2.2. Growth

Changes in body size from environmental stressors can cause genetic mutations and physical deformities. Differences in body size can be quantitatively measured under a dissecting microscope. The worm can be immobilized with 10 mM sodium azide onto a microscope slide or its movements tracked by a computer with an automated stage.[13] For example, abnormal cell growth in the hypodermis results in longer phenotypes (*lon*), while developmental delays and deformities of the cuticle result in smaller phenotypes (*sma*, *dpy*).[14,15]

2.2.3. Motility

Exposure to nanoparticles can not only be lethal, but can behave as a neurotoxin, altering locomotion behavior. The nematode has 302 neuron cells and a centralized nervous system localized in the head.[16] Although simple and lacking a brain, some locomotion behavior parameters are conserved between *C. elegans* and human.[16] Changes in the sinusoidal movement of nematodes can be quantified using an automated computer

system and software.[13] ENPs can also place exogenic stress and adversely affect locomotion when it causes cuticles to become rigid and fracture.[11]

2.2.4. Gene Expression

C. elegans was the first multicellular organism to have its genome completely sequenced in the 1980s and has served as a model animal for genetic, neurobiology, and developmental biology research.[17] A number of mutants have been identified to explain changes in physiological endpoints, such as lifespan (ageing), body length, locomotion, fertility and neurological defects. Assessment tools such as the whole genome microarray (WMGA) can be used to efficiently scan for changes in gene expression from exposure to contaminants and nanoaggregates.[3] Stress-response gene expressions for reproduction have been identified as s*od*-3 and *daf*-12 gene in mutant worms.[3] *Daf-12* was linked to BOW and sod-3 was linked to defenses against oxidative stress in nematodes. Under exogenic or endogenic stress, *daf*-12 gene expression increased resulting in dauer formation. An increase in *daf-12* gene expression hinders larval development, decreasing reproduction.[3] When unfavorable conditions in the environment induce exogenous or endogenic stress, the nematode can turn to an alternate life-stage for survival and become dormant in dauer formation until more favorable conditions.[3] Lastly, *sod*-3 expression confirms the presence of ROS, such as superoxide radicals, and other oxidative stress.[3,18,19] Nematodes with gene expression for ageing include *uo-1* and *mev*-1; whereas mutants with long lifespans include *age*-1, *daf*-2.[6-9]

Another useful mutant is m*tl*-2, which are metal sensitive. Mtl-*2::gfp* transgenic gene are induced in the presence of metallic ENPs. These metallothionein-like proteins

also scavenge for ROS.[18] Sulfur functional groups scavenge and bind strongly to metal contaminants in the body to excrete and detoxify the organism.[3,18-20]

Moreover, *mtl-2*::gfp is a transgenic strain that consists of genetic material from a foreign organism artificially spliced onto nematode DN.[21] In this case, an *mtl-2* is the metallothieoneien-2 gene promoter tethered to a green fluorescence protein (GFP) gene reporter. As a biosensor, nematodes with *mtl-2*::GFP express GFP under a fluorescence microscope in the presence of internalized metal ions, such as Zn^{2+} from nano-ZnO, for example. Free metal ions and ROS increased gene expression as *mtl-2* functions by sulfur functional groups binding to metal ions for detoxification out of the body.[20,21]

2.3. Biochemical Assays

Commercially available chemical assays monitor the production of defense proteins in the presence of ROS and other stress triggers in nematodes. The mitochondrial assay, MitoSox (Molecular Probe, USA), is analogous to the MTS cytotoxicity assay, which measures mitochondrial viability. Red fluorescence only occurs from the oxidation of the dye by viable intracellular mitochondria. This can be measured with a fluorescent microscope to qualitatively detect between live and dead organism [6]. Red fluoresce can also be measured at 510 excitation and 580 nm emission wavelength using fluorescence microscopy (**Table 3**).Both the MitoSox and the DCF assay can be measured using a plate reader or flow cytometer.[6,22]. Another toxicity assay commonly used in the nematode literature is DCFH, or 2',7'-dichlorofluorescein (**Table 3**). In cytotoxicity assays, pro-fluorescent, lipophilic 2',7'-dichlorofluorescein diacetate (DCFH-DA) diffuses through the cell membrane and is further oxidized by cellular esterases in the

presence of ROS to DCFH.[22] In cell-free assays, DCFH oxidation is catalyzed by horseradish peroxidase in the presence hydrogen peroxide, for example, to detect oxidative stress.[22] The green fluorescence can was quantitatively measured with a microplate reader or flow cytometer.

As with cytotoxicity assays with nanoparticles, chemical assays originally designed to test small chemicals predating NPs have to be reassessed before testing nanoparticles. A common mishap includes false positives from NPs oxidizing the chemical assay, instead of by ROS or damaged organelles. This renders false results from interaction of the assay with the NP before interacting with cellular organelles, as designed to do.

Lastly, monitoring a number of endpoints, such as ageing and stress response, by quantifying lipofuscin, an endogenous fluorescence, is efficient.[23] In literature on ageing, lipofuscin is an endogenous autofluorescent marker easily monitored because of the transparency of the nematode body (**Table 3**). Densitometry with a scanning confocal microscope quantifies fluorescence from lipofuscin.[6] Autofluorescence from this ageing pigmentation in nematodes increases over time and with an increase in oxidative stress, which causes premature ageing.

Table 3. Fluorescent assays used to monitor adverse effects in *C. elegans*

Assay	Fluorescence (Ex/Em)	Measurement	Reference
MitoSOX	510/580 nm	Oxidative Stress: cellular marker for mitochondrial O_2^-.	[6]
DCF	488/510 nm	Oxidative Stress: cellular marker for ROS, especially H_2O_2.	[22]
Lipofuscin	351/420 nm	Ageing: autofluorescent pigment.	[24]

2.4. Nanobiotoxicology

Silver (AgNP), gold (AuNP) and platinum (PtNP) ENPs, were each introduced in *C. elegans* to study their impact on different physiological endpoints and resulted in different toxicity trends.[3,8,18,25] The antibacterial properties of AgNP can cause starvation in nematodes, but different organic surface coatings and media solvent can also make AgNP less toxic to *C. elegans.*[18,19,26] AuNP continued to be nontoxic like its bulk counterpart, but after AuNP exposure, Tsyusko et al. showed changes in gene expressions during detoxification in *C. elegans.*[25] Lastly, PtNP actually elongated nematode lifespan by functioning as an antioxidant.[6-9]

2.4.1. Silver

In humans, bulk silver is nontoxic, but silver ions can cause diseases. In *C. elegans*, physiological endpoints at sublethal concentrations, such as lifespan, reproduction and fertility, body size, locomotion and gene expression were measured after exposure to AgNPs. Along with non-coated (and bare) AgNP, gum arabic (GA), polyvinylpyrrolidone (PVP), and citrate polymers are the three main polymer surface coatings of AgNPs.

Lifespan. For small particles in K-media less than 50 nm, lifespan inhibition was not size related, but rather surface coating played a role in significantly decreasing lifespan. Non-coated (or bare) AgNP had no effect on survival; whereas, when coated with multiple organic layers, PVP was the most lethal and citrate the least.[3,19,26,27] For example, Roh *et al.*, found that 14-20 nm bare AgNP in K-media had no effect on lifespan,[3] as did Lim *et. al.*, who tested bare AgNP of 20-30 nm.[27] In the same way, Johansen found that PVP-

coated AgNP were more lethal than bare AgNPs.[26] When Yang *et al*., tested several AgNPs of different coatings in K-media but of the same small diameter between 5-8 nm, they found that GA-coated AgNP were the most lethal, followed by PVP-coated, then citrate coated AgNP as the least lethal,[19] as well.

We note that for bare AgNP, reporting a particle size of less than 100 nm is inconsistent to the fact that without a polymer coating Ag will aggregate and precipitate out of solution as 500 nm particles or greater.[19] We speculate that when reporting bare AgNP, the authors are in fact reporting the initial particle size before addition into water.[3,27] Instead, one might consider using the hydrodynamic diameter when studying ENP interactions.[11,19]

In contrast, Meyer *et al.,* found that smaller, citrate-coated AgNP were more lethal than PVP-coated AgNP in water.[18] Although, the opposite was true in K-media where citrate-coated AgNP were less lethal than PVP-coated AgNP,[3,19,26,27] suspension in water resulted in higher ionic dissolution than in K-media, making citrate-coated AgNP in water more toxic.[18,19]

Likewise, Kim et al., also found citrate-coated AgNP on agar reduced survival (LC_{50} = 55mg/L).[11] In this study AgNP were not taken in. Instead, using SEM, they noted that the cuticle of worms was entirely infected. Because AgNP caused epidermic edema and the cuticle to burst, leading to bacterial infections.[11] By a different mode of toxicity, particle effect caused damage to the cuticle of nematodes, preventing molting and becoming lethal.[11]

Reproduction and Fertility. The same group examined the transport of citrate-coated AgNP (0.05, 0.1, 1.0, 1.5, 10, 50, 100 mg/L) after inoculating L1/L2 worms for 48 hours. Although AgNPs were distributed along the digestive track, as seen under high-resolution microscope, the particles were readily excreted. Instead adverse effects to the muscles and vulva were attributed to Ag particles and not to silver ions, decreasing fertility by 40% at 10 mg/L.[11]

In water, bare AgNP [3,27] and citrate-coated NP [11,18] had no significant effect on mortality rate, but decreased fertility (egg count) and were most toxic than PVP-coated AgNP.[18] Likewise, at concentrations between 0.05 and 0.5 mg/L, citrate coated AgNP decrease reproduction by 70%.[3] Particle surface ionization increased citrate-coated AgNP uptake and smaller size particles passively transferred past the cellular membrane of eggs. Higher incidence of bagging (BOW) resulted, where eggs hatched within the body cavity of parent nematodes [18]. Therefore, Meyer *et al.*, found that silver ion leaching and coating dissolution was greatest for citrate-coated AgNP, becoming more lethal than PVP-coated AgNP in water. Moreover, when different sizes of AgNPs were tested, smaller sizes were more toxic and easier to uptake.[18]

Growth. AgNP caused growth inhibition when the NP was coated,[18,19] whereas bare AgNP caused no growth inhibition.[3] Meyer *et. al*, found that both PVP and citrate-coated AgNP both inhibited the growth of worms. Yang *et. al*, did an extensive study on seven different surface coatings. All AgNP with surface coating caused growth inhibition.[19]

Genotoxicity. AgNPs can induce oxidative stress in nematodes by releasing silver ions. Using a whole genome assay, genes such as *mtl-2*, *sod-3*, and *daf-12* were predominately expressed after exposure to AgNPs.[3,18-20]

2.4.2. Gold

Compared to AgNP, colloidal gold ENP has negligible dissolution by oxidation and does not release Au ions. Thus, AuNPs are as inert as its bulk counterpart. Gold is non-toxic but prolonged exposure to Au can cause changes in the genetic makeup in order to compensate for the stress. Genetic sequences during exposure to non-lethal contaminants, such as Au, can be subtle, but this defense can be monitored using genetic tools, such as RT-PCR.[25] At sublethal concentrations of AuNP, detoxification occurs in order for sustained health.

AuNP are less toxic than AgNP with little physiological adverse effects. Bar-Ilan et. al., assessed zebrafish embryos after transgeneration exposure of parent to Au and Ag ENPs.[28] For example 3, 10, 50, and 100 nm Au and Ag ENPs caused adverse effects to progeny but at different spectrums. AgNP completely diminished 100% of the population to lethality and caused deformities in surviving progeny; whereas AuNP caused less than 3% mortality and no significant adverse effect.

But Tsyusko, et al. introduced citrate-coated Au particles (4 nm) up to 10 mg/L and found toxicogenomics response in *C. elegans* due to oxidative stress. Using a whole genome microarray, the authors analyzed 797 genes linked to biological functions adversely effected from AuNP exposure, such as endocytosis and the amyloid processing pathway, which is associated to Alzheimer's disease in humans.[25] Information from a

genome microarray was confirmed using other genetic tools, such as RNAi and mutants. Ultimately this study suggests that AuNPs bioavailability may induce long-term genotoxicity in *C. elegans.*

2.4.3. Platinum

Nano platinum showed favorable results as a bioactive antioxidant, when chronically exposing *C. elegans* to sublethal concentrations. The Miyamoto group have extensively researched the use of PtNP to extend the lifespan of nematodes.[6-9]

Miyamoto *et al*., showed that at 500 um PVP-PtNP extended the lifespan of wild type N2 nematodes by 24%.[8] As a positive control, the same group inoculated N2-nematodes with 0.4M paraquat to generate intracellular free radical to be quenched by PtNP. Also, accumulation of ROS induced by paraquat (0.4M) in N2 animals was subsequently decreased by platinum nanoparticle (PtNP). In fact, when compared to superoxide dismutase (SOD), 0.5 mM PtNP reduced ROS and significantly prolonged the lifespan of nematodes by 24 ± 1%.[8] Yet, interestingly, at the higher concentration of 1mM, PtNP became toxic by supposedly scavenging too much ROS for the organism to function without its defenses. That is, since ROS is endogenously produced in the body for defense mechanism against infections, PtNP may overcompensate and deprive the organism of healthy amounts of ROS as well, instead of removing excess ROS in the body to prolong life.[8]

To further exploit the anti-ageing property of PtNP by increasing its liphophilicity, Miyamoto *et al*,. also conjugated PtNP with an HIV-1TAT protein linked peptide. At 5 uM, lifespan increased by 75 ± 7 %; while at 0.5 uM, by only 27 ± 5%

"leading to a lifespan extension at one hundredth the concentration, compared with unconjugated" PtNP.[6] Furthermore, this conjugation also led this particle to be a mitochondrial complex I enzyme mimetic because of its role in scavenging O_2.[6]

2.4.4. Aluminum oxide

Al_2O_3 has been linked to several degenerative diseases, such as Alzheimer's disease, and ageing.

Lifespan. Al_2O_3 caused severe lethality in adults when exposure occurred since L1 than since L4s. Having four juvenile stages, nematodes are more sensitive to metal contaminants when exposed at the L1 stage than at the L4 or young adult stage.[29] Wu *et al.*, exposed *C. elegans* to Al_2O_3 nanoparticles and compared the results to its bulk counterpart (470-1126 nm).[29] Exposure as L1s, during early developmental stage, to Al_2O_3 significantly increased lethality at 6.3 mg/L Al_2O_3. L4 exposure was lethal at a much higher concentration at 12.7 mg/L, making nano more toxic than bulk Al_2O_3 [29]. In fact, nematodes exposed as late juveniles (L4s) were able to thrive as healthy adults as compared to untreated adults. This is in agreement to results shown by Li, *et al*. After chronic exposure for 10 days, Al_2O_3 reduced lifespan by 20% at 15.6 mg/L for nano and 23.1 mg/L for bulk. [30]

Fertility and Reproduction. When 60 nm bare alumina were introduced to *C. elegans,* fertility and reproduction decreased significantly; in contrast, bulk alumina was non-toxic.[31] Bare Al_2O_3 NPs, lacking any surface coating had a tendency to aggregate and decrease fertility. In this study, fertility means the number of eggs within the body of *C. elegans* and reproduction is the number of offspring hatched.[31] In fact, at 102 mg/L, nano

Al_2O_3 significantly reduced body length, fertility and reproduction. At 203.9 mg/L Al_2O_3 NPs, sterility occurred. The smaller size of NPs allowed the transfer across the cell membrane of embryos causing adverse effects to fertility when compared to bulk Al_2O_3.[31] Once internalized, NP dissolution to Al^{3+} formed toxic free ions, which ultimately, became more toxic than bulk and nanoparticles.

Stress response. Nanoparticles are more toxic than bulk.[30] Toxic stress was monitored after a 48 hour exposure, where significant change at 30.6 mg/L for nano-Al_2O_3 and 51 mg/L for bulk Al_2O_3[30] were found. After a chronic exposure of 10 days, nanoparticles induced *Phsp-16.2*::gfp expression at 8.1 mg/L and 23.1 mg/L for bulk Al_2O_3.[30] This is in agreement to finding by Wu, *et. al*. Significant stress response was quantified using *Phsp-16.2*::gfp, at 6.3 mg/L nano-Al_2O_3 for L1 exposure and 12.7 mg/L for L4 and young adult exposure.[29] Oxidative damage from ROS production and stress response are directly correlated to lethality.

Lipofuscin autofluorescence served as an indicator for cellular damage, most notably from ageing. NPs given orally saturate the intestine during exposure.[29] Toxic exposure to Al_2O_3 induced a stress response due to cellular damage and autofluorescence in the pharyngeal bulb. Lipofuscin in the pharyngeal bulb was quantified under a fluorescence microscope by averaging pixel intensity.

Ultimately, toxicity was greatest at L1 stage.[29] Exposure during early development may cause the organism to increase defense mechanisms against environmental toxins in order to survive and maintain fit [29]. For example, exposure at the

L1 stage (6.3 mg/L) caused significant increase in autofluorescence than at L4 stage (12.7 mg/L).

Motility. Toxicity results for 8.1-23.1 mg/L Al_2O_3 of nano and bulk showed nano Al_2O_3 hindered locomotion behavior more than its bulk form. Li, *et al.*, studied the adverse effects on locomotion behavior after chronic exposure (10 days) to 60 nm Al_2O_3 and 429 nm bulk alumina. Using a microscope (non-automated), the number of head thrashing and body bending were counted for 1 min and 20 s, respectively. Significant decrease in motility occurred at 8.1 mg/L for nano Al_2O_3 and 23.1 mg/L for bulk.[30]

2.4.5. Cerium Oxide

Ceria is commonly found in poor air spaces saturated with exhaust, where as a catalyst for combustion engines, CeO_2 is expelled into the air by the exhaust of vehicles.

Lifespan. Smaller particles were more lethal than larger particles. Zhang *et al*., nematodes exposed to 8.5 nm CeO_2 caused lifespan to significantly decrease by 12% at 1 nM.[24] Likewise, Roh *et al*, exposed nematodes to 15 and 45 nm CeO_2 (1 mg/L) to test size-dependent toxicity. Lifespan also decreased by 20% when compared to untreated nematodes.[32]

Fertility and Growth. CeO2 NP significantly decreased fertility, but does not alter growth.[32] 15 nm CeO_2 readily decreased fertility (egg number) by 28%, compared to only 11% decrease by 45 nm CeO2. Again, growth was also not affected.

Stress Response. CeO_2 made *C. elegans* susceptible to stress and decreased lifespan by decreasing tolerance to harsh environment.[24] Nematodes thrive in many environments

that are highly contaminated near smelting plants to thermal stress in the soil, as they are capable of quickly acclimating to thermal stresses, for example, and their surroundings for survival.[33-35]

After pretreating nematodes with CeO_2 for 72 h, Zhang *et al*, evaluated nematode ability to withstand post-oxidative and thermal stress. Nematodes exposed to 5 nM juglone, a free radical generator, significantly decreased lifespan and was incapable of tolerating excess ROS, Thermotolerance at 35°C of pre-treated nematodes was also poor.[24] Likewise, an increase in *cyp35a2* gene expression also indicated a stress response from exposure to CeO_2, which correlates with fertility.[32]

2.4.6. Silicon Dioxide

SiO_2 is commonly found in emulsions. Pluskota, *et al*., found that SiO_2 does not affect lifepsany. Instead, 50 nm SiO_2 decreased the number offspring, increased BOW phenotype and caused age-related degeneration of reproduction organs.[12] In water, nanoSiO_2 and bulk silica were introduced to *C. elegans* for 24 hour assays to measure the adverse effects of physiologically relevant endpoints, such as lethality and fertility (egg count).[12] Here, nanoparticles caused protein aggregation in *C. elegans* as seen humans with neurodegenerative diseases. BOW increased as exposure to nanoSiO_2 immobilized vulva muscles and prevented the nematodes to lay their eggs. Using the lipofuscin assay, premature ageing of the reproduction system was observed under a fluorescent microscope.[12]

2.4.7. Titanium Dioxide

TiO2 is nontoxic at low concentration; and smaller particle are more toxic. For particles 7 and 20 nm, smaller particles were more toxic and the 7 nm TiO_2 decreased fertility and increased gene expression.[32] Roh *et al.,* exposed nematodes to 1 mg/L TiO_2 to test the effects of size on three physiological endpoints: lifespan, fertility, and body length. Lifespan decreased by 30%, fertility by 21%, and growth by 9%. These adverse effects were all correlated to the *cyp35a2* stress-response gene.[32]

For 285 nm TiO_2, Wang *et. al*. compared adverse results from nano and bulk particles. For each endpoints measured (fertility, reproduction and body length), both nano and bulk TiO_2 caused significant adverse effects at 47.9 mg/L and 95.9 mg/L, respectively.[31]

2.4.8. Zinc Oxide

Nanosized ZnO were more toxic than bulk and ionic forms of ZnO, with no significant difference between the different forms of Zn.[31] That is, nano-ZnO is as toxic as Zn ions. For 532 nm ZnO, Wang, *et. al.*, tested the toxicity in *C. elegans* and measured lethality, growth, fertility (egg count), and reproduction. At concentrations of 1.6 mg/L, significant inhibition in body length, fertility and reproduction occurred, compared to 4.1 mg/L bulk ZnO.

This is in good comparison to research by Ma, *et. al.* who also found nano-ZnO (1.5 nm) highly toxic. Ma, *et. al*, measured lethality, reproduction, and locomotion behavior using a Worm Tracker.[20] For all three endpoints measured, nano-ZnO behaved

and induced the *mtl-2*::gfp transgene expression similar to $ZnCl_2$, showing no significant difference between the different forms of Zn.[20]

The median behavior concentration (BC50) for ZnO-NP in K-media was 635 mg/L and for $ZnCl_2$, 546 mg/L.[20] These results are not significantly different from the reference toxicant, $ZnCl_2$ showing the release of Zn^{2+} into solution by ZnO-NP, becoming lethal. Also, antibacterial properties of Zn^{2+} can cause starvation as a secondary adverse effect in *C. elegans*.[20]

2.5. Nanoparticle Bio-imaging in *C. elegans*

A number of techniques have been explored in the literature to map the biodistribution of nanoparticles within C. *elegans*. For example, an advantage in using microbeam synchrotron radiation X-ray fluorescence (μ-SRXRF) over sectioning and TEM histology is that μ-SRXRF allows in situ mapping of elements in *C. elegans*. After a 36 hour exposure of 100 μM of CuNP (23.5 nm) and 100 μM of $CuCl_2$ in PBS, biodistribution was measured. Gao, *et al.,* found accumulation of Cu in the head and partially in the midsection of the body; whereas, Cu^{2+} accumulated near the tail for excretion.[36] Cu was mapped in situ using μ-SRXRF,[36] but the transparent body of C. elegans also provides the convenience of using fluorescence microscopy with pixel density measure to quantify nanoparticle uptake.[30]

Mohan et al., monitored the biotransfer of 120 nm bare nanodiamonds as a fluorescent marker in *C. elegans* under a fluoresce microscope. Different biodistributions resulted between feeding and microinjection of fluorescent nanodiamonds (FND).[37] After

feeding bare FNDs, they accumulated in the intestinal lumen; whereas, conjugated FNDs adsorbed through the intestinal cells. Microinjection delivered FNDs to the embryos of the following generation where they transferred into progeny as hatched larvae.[37]

Because of the transparent bodies of nematodes, in vivo showed the biotransfer of bare FNDs in the lumen during a 12 h exposure by feeding. Without food, the FNDs remained in the body, but with food, the FNDS were excreted within 1 h. Conjugated FNDs absorbed into intestinal cells. Then, with food, conjugated FNDs remained within in the cells. In addition, microinjected FNDs resided in the gonad and passively passed through to the embryo, commonly seen with other ENPs, such as Ag, Al_2O_3, and graphite nanoplatelets.[18,31,38] Interestingly, the authors found that with FND exposure, second generation progeny were not affected.[37]

Graphite nanoplatelets (GNPs) were also not toxic to lifespan and reproduction.[38] Using Fourier transform infrared spectroscopy (FTIR), GNPs were mapped in the intestine and embryo where biotransfer from the intestine into the gonad occurred after a 24 h exposure. Moreover, just as Zn and Ag are antibacterial, GNP is an antimicrobial, too.[18,20,39] Zanni, *et al*., used a GFP-expressing bacterium that fluoresced in the intestine of untreated worms. When exposed to GNPs, bacterium fluorescence in the intestine decreased after 30 m. The authors speculate that the antibacterial effect may stem from the likelihood of forming agglomerates while in the digestive tract, becoming lethal.[38]

2.6. Conclusion

A number of tools to diagnose and identify toxicants that hinder *C. elegans* development and fitness can be monitored using biochemical assays, quantified physiological endpoints and genetics. In this study, *C. elegans* were used in ecotoxicological research to assess the toxicity and biodistribution of ENPs and their more toxic ion form from ENP dissolution. This illustrates how feeding on bacteria, *C. elegans* can consume nanoparticles through its food chain and contribute to nanoparticle accumulation high in the food web. Toxicity studies using *C. elegans* can provide information to asses risks from ENP exposures in humans.

Chapter 3

Experimental Method: *Caenorhabditis elegans* as a Tool for Nanotoxicity

3.1. *In Vivo* Nanoparticle Exposure

Caenorhabditis elegans is the most thoroughly studied organism in the scientific literature. A key animal model, *C. elegans* provide a wealth of information in genetic, neurology, muscle, movement, and physiology in order to study ageing, neurological and muscular degenerative diseases, and sex-related studies. In this thesis, the use of physiological assays, such as lifespan and physiological endpoints in order to study changes in fitness after chronic exposures to nanoparticles.

In addition to instruments and tools available to monitor stress in nematodes that cause physiological changes that can be quantified allowed us to measure changes in fitness as well. Parameter endpoints measured in this thesis include the mean lifespan, fertility, growth and locomotion parameters, such as flex, velocity, amplitude and

velocity. Lifespan and fertility for each nematode was followed using a compound microscope and physically sitting for hours scoring observations. In contrast, parameters such as movement and locomotion were quantified using a computer-controlled tracking system. For the many locomotion parameters, the coefficient of variability was negligible and not significantly different for untreated nematodes, which served as the control.

The short lifespan and large brood size rendered most indefinitely the opportunity to score measurements with a microscope. Another key point is that the a study on toxicity effects over the span of up to four generations, illustrates how the results for parent worms cannot be used to predict the tolerance of stress in the next generation.

3.1.1. *C. elegans* Maintenance

The wild type N2 strain was obtained from the *Caenorhabditis* Genetics Center (MN, USA). *C. elegans* were cultured at 20 °C on nematode growth medium agar, using *Escherichia coli* strain OP50 as the food source following standard cultivation protocols.[17,40] To obtain a synchronized population, gravid nematodes were collected and treated with hypochlorite.[40]

3.1.2. Multigenerational Toxicity

In the multi-generation experiment, first-generation *C. elegans* were continuously exposed to nanoparticles or reference chemical toxicants at the fourth larval (L4) stage. L4 is the larval stage when germs cells start to divide and develop. In subsequent generations, *C. elegans* L4s were randomly selected from the first-day progeny of the

previous generation and continuously exposed to nanoparticles or reference chemical toxicants throughout their life span (Figure 3.).

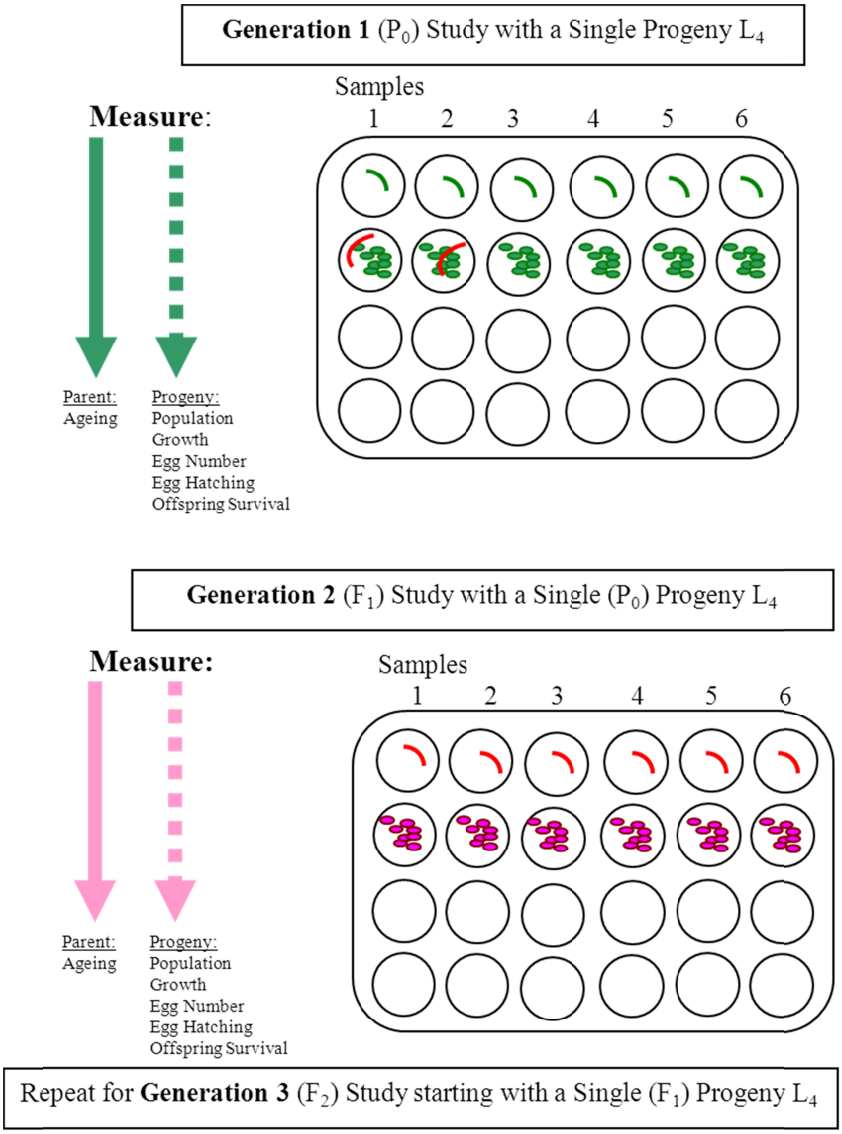

Figure 3. Multi-generation scheme for plate transfer. Generation 1 L4s are moved daily for 4 days into the next row in order to manage nematode population in each well and to prevent starvation. After three days, eggs hatch and are allowed to become L4s, which are then used to start the next generation in a separate 24-well plate.

3.1.3. Assessment of *E. coli* Viability

To study the effects on food source, nanoparticle or reference chemical exposure plates were prepared as described above except that no C. elegans were placed on the plates. The plates were incubated at 20 °C for 24 h. After the inoculation time, 1 mL of sterile H_2O was used to rinse and collect the bacteria from the surface of each well to prepare serial dilutions. 20 µL of each dilution was spread onto a 6 cm LB plate and incubated overnight at 37 °C. The number of colonies was counted to evaluate the concentration of live bacteria in the original solution.

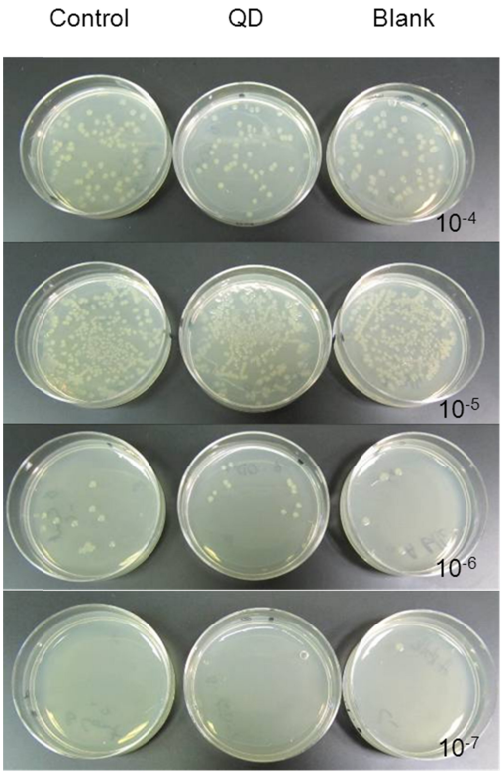

Figure 4. QD exposure in *E. coli*. After counting all colonies in each plate, colonies are counted to determine significant changes from effects of EPN on the food source.

3.1.4. Nanoparticle and Chemical Control Exposure

Experiments were carried out on 24-well plates with 1 mL of NGM-agar added into each well. The wells were seeded with 10 µL of fresh overnight-culture of *E. coli* OP50 and kept for 3 days at room temperature to form a bacterial lawn. To the surface of each well, 30 µL of the nanoparticle or reference chemical was added to cover the bacterial lawn. After about 30 min at 20°C, one *C. elegans* was placed into each well. The plates were cultivated in a 20°C incubator. *C. elegans* were transferred to freshly dosed plates every 24 h.

3.1.5. Quantification of Internalized Nanoparticle.

To determine the uptake rate, the exposure concentration for core and core-shell QDs used was 300 mg Cd/L. for the QD experiment an d100 mg Ag/L for the AgNP experiment. The metal content of exposed adults was measured using an inductively coupled plasma-optical emission spectroscopy instrument (Perkin Elmer, ELAN9000 ICP-OES) and reported as milligrams of metal ion in the solution.

One-hundred nematodes were picked and transferred to clean NGM-plates to remove the bacteria. The nematodes were rinsed off with water and transferred into pre-weighed glass tubes to digest in a block heater at 90 °C for 4 h after addition of 1 mL of 70% HNO_3. After digestion the samples were filtered and transferred to polypropylene tubes and diluted with ultrapure water to achieve a final acid concentration of 1% by volume.

3.2. Life-Cycle Analysis

3.2.1. Life Span and Fertility Assessment

Life span was measured as the number of days that a nematode was alive: from egg to time of death. Fertility was measured as the total progeny number (brood size) of each nematode.

3.2.2. Body Length and Locomotive Behavior Assessment

If cadmium leaches from QDs it may have neurotoxic effects.[41] For this reason we analyzed the body length and locomotive behavior of adult nematodes using an automated WormTracker to measure sinusoidal movement and velocity(**Table 4**).[13]

The hardware of the system consisted of a dissecting microscope (Unitron) equipped with a motorized stage (Prior) and a Firewire camera (Unibrain Fire-i). The same computer controlled the motorized stage and the camera. The entire setup was placed at a constant temperature of 20 °C. To start the measurement, a first-day adult nematode was transferred to the middle of a 10 cm NGM plate that was spread with fresh OP50. The software suite tracked the *C. elegans* and recorded a video of the nematode movement for 4 minutes. This video was then analyzed for body length and several motility parameters: amplitude, wavelength and velocity.

3.2.2.1. Locomotion Parameter

The movement of the *C. elegans* is sinusoidal. Using a tracking computer attached to a motorized stage and a compound, the movements of nematodes can be monitored. Flex is the measure of the number of times that the body bends; velocity is the change in

speed in one direction, for amplitude and wavelength the worm moves intrinsically as a nematode; and for velocity, it is the change in forward trajectory.

Since the nanoparticles were suspended in borate buffer, this solution was used as untreated and negative controls for multiple generations to examine variations for each endpoint measured of the Worm Tracker **(Table 4).**

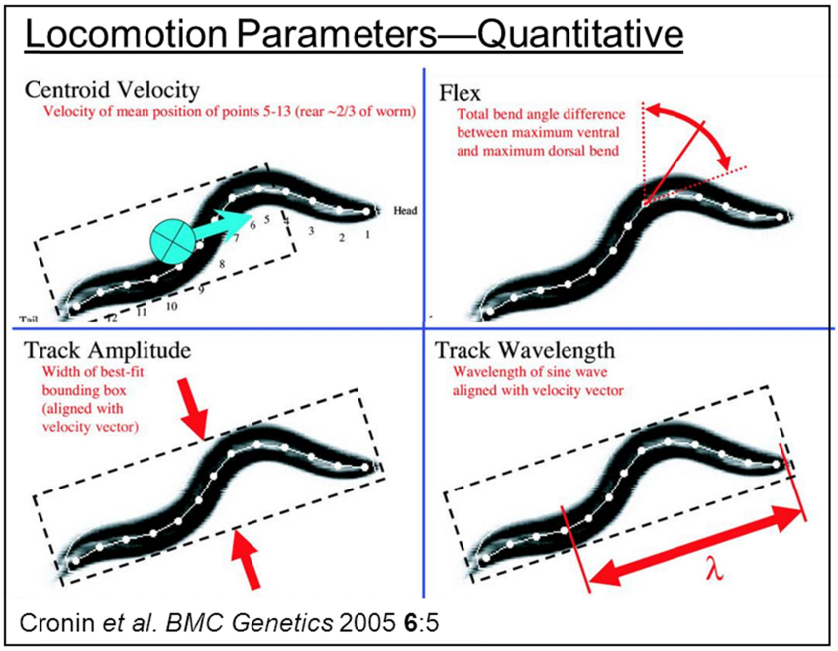

Figure 5. Sinosodial locomotion parameters measured by an automated computer tracking system. Four parameters are used to determine adverse effects from ENP exposure in nemoatdes. The measure of body length (growth) is also measured. Reprinted from BMC Genetics [13]

Table 4. Percent coefficinet of variation (%CV) of locomotive measurements of wild-type N2 nemoatdes that are untreated with ENPs (control) using an automated tracking system. This computer system tracked nemoatdes for 4 generations, n=125 total.

Generation	1	2	3	4	Average
Length	5.8	8.4	7.2	4.9	6.8
Amplitude	7.8	7.7	9.6	8.4	8.4
Wavelength	6.4	10.0	8.9	6.9	8.8
Flex	11.7	16.8	12.7	13.0	13.8
Velocity	25.9	29.5	22.8	17.1	24.7

3.2.2.1. Coefficient of Variation

The coefficient of variation (CV) is defined as the ratio of the standard derivation σ to the mean μ, or $CV = \sigma/\mu$. A CV of 10% or less indicates homogeneity of the parameter measured.

Except for flex and velocity with an average %CV of 13.8 and 24.7%, respectively, all other parameters measuring the motility of untreated nematodes over four generations show no significant variation.

3.3. Analysis of Variance and Statistics

All samples were analyzed using OrginPro 8.5.1 (OriginLab Corporation, USA). Data was compared against the buffer control by one-way ANOVA *post-hoc* Tukey test at 99% confidence interval.

Chapter 4

Toxicity of quantum dots and cadmium salt to *Caenorhabditis elegans* after multigenerational exposure

To fully understand the biological and environmental impacts of nanomaterials requires studies which address both sub-lethal endpoints and multigenerational effects. Here we use a nematode to examine these issues as they relate to exposure to two different types of quantum dots, core (CdSe) and core-shell (CdSe/ZnS), and to compare the effect to those observed after cadmium salt exposures. The strong fluorescence of the core-shell QDs allowed for the direct visualization of the materials in the digestive track within a few hours of exposure. Multiple endpoints, including both developmental and locomotive, were examined at QD exposures of low (10 mg/L Cd), medium (50 mg/L Cd), and high concentrations (100 mg/L Cd). While the core-shell QDs showed no effect on fitness (lifespan, fertility, growth, and three parameters of motility behavior), the core QDs caused acute effects similar to those found for cadmium salts. Over multiple

generations, we commonly found that for lower life-cycle exposures to core QDs the parents response was generally a poor predictor of the effects on progeny. At the highest concentrations, however, biological effects found for the first generation were commonly similar in magnitude to those found in future generations

4.1. Introduction

The study of the biological effects of engineered nanoparticles is limited by the challenges associated with rapidly collecting comprehensive toxicological data. While *in vitro* studies are fast and well suited for evaluating NP libraries, they are limited in capturing more subtle organism impacts particularly over multiple generations.[42,43] More informative *in vivo* experiments can more accurately capture biological impact, but most animal models require too much time for facile evaluation of tens or hundreds of relevant nanoparticles. The low throughput of animal studies is a severe problem for multi-generational studies where data on multiple biological endpoints (e.g. fertility, development, neuromotive) is desired. Such information is precisely the most valuable for ecotoxicological studies where degenerative or adaptive behaviors in progeny may be the most critical impacts.

To address these issues, we present here studies of the nematode *Caenorhabditis elegans*. Quantitative methodologies are applied to assess multiple endpoints relevant to their fitness after long-term exposures to NPs at three different environmentally-relevant and sub-lethal concentrations. Specifically, automated image analysis is applied to measure the body size and locomotive behavior of *C. elegans*, which moves in a

sinusoidal pattern. Changes in the wavelength, amplitude, and velocity of their movements can indicate adverse neurological effects.[16]

These studies can be continued over multiple generations due to the short lifespan and large brood size per worm. To study toxicity at all life stages, two generations of exposure are often required because the early embryonic stage of an animal starts when inside the parent.[44] Multigenerational studies can reveal cumulative damage, acclimation or adaptive responses.[33-35] Cumulative damage in progeny is evident when the parent has no change in fitness but the progeny fitness gets progressively worse. Acclimation occurs when progeny, having been exposed to sublethal concentrations during embryogenesis, has no change in its fitness.[33,35,45-48]

C. elegans has been the subject of a number of toxicology studies focused on the acute effects of NPs such as silver, silica, ceria, titania, and zinc oxide.[3,12,31,32] However, none of this prior work has addressed the multi-generational impacts of engineered nanoparticle exposures. Here we explore the quantitative impact of both core and core-shell quantum dots over the span of four generations of *C. elegans*.

For the purposes of illustrating this multigenerational model, we used a standard NP type, quantum dots (QDs), both because they can be imaged within organisms and because of their use in emerging nanomaterial commercial products (QD Vision, Watertown, MA, USA). QD toxicity has been studied *in vivo;* the materials can be toxic when their largely organic surface coatings are compromised.[49-51] Most have attributed this toxicity to the release of soluble cadmium from the CdSe core.[52,53] QDs with an outer ZnS shell, referred to as core-shell QDs, are generally more chemically stable and preferred in products due to their longer lifetime and brighter fluorescence.[54] The few *in*

vivo toxicity studies of these core-shell systems have found low or no toxicity in rats.[55,56] In Daphnia and fish, researchers also observed low toxicity unless surface coatings were degraded.[52,57] None of these *in vivo* studies have yet addressed multigenerational effects.

We report for the first time a multigenerational study of the sub-lethal biological effects of both core and core-shell QDs in a nematode. Core QDs had impacts similar but less pronounced than cadmium salts, while the core-shell QDs had little impact on a multitude of endpoints over multiple generations

4.1. Methods

4.1.1. Quantum Dot Preparation and Characterization

The CdSe core and the CdSe/ZnS core-shell quantum dots (QDs) used in this study were prepared following procedures described in our previous work.[54] To ensure their stability in biologically relevant conditions, the amphiphilic copolymer poly(maleic anhydride-alt-1-octadecene, Sigma) (PMAO) (Mn = 30,000-50,000) - PEG (Mn = 1000, Sigma) (molar ratio PMAO:PEG=1:10) was formed through an anhydride coupling reaction to coat and to water-solubilize the QDs from organic solutions.[58]

Before beginning these toxicity studies, we carefully evaluated the physicochemical properties of these systems. Transmission electron microscopy (Joel 2010 TEM) revealed monodisperse core QDs with 3.4 nm core diameter and core-shell QDs with 4.1 nm core diameter (Figure 6). Dynamic light scattering (Malvern Zetasizer Nano-ZS) showed that both core and core-shell QDs had a

hydrodynamic diameter of approximately 17 nm (**Figure 6**); the polymer coating contributes substantially to the size of the particles in water.[54,58] The cadmium concentration was determined by inductively coupled plasma-optical emission spectroscopy (Perkin Elmer, ELAN9000 ICP-OES). Concentrations were reported as milligrams of the cadmium ion in the solution. Three sub-lethal concentrations of [Cd] = 10, 50, and 100 mg/L were tested for each QD sample.

A

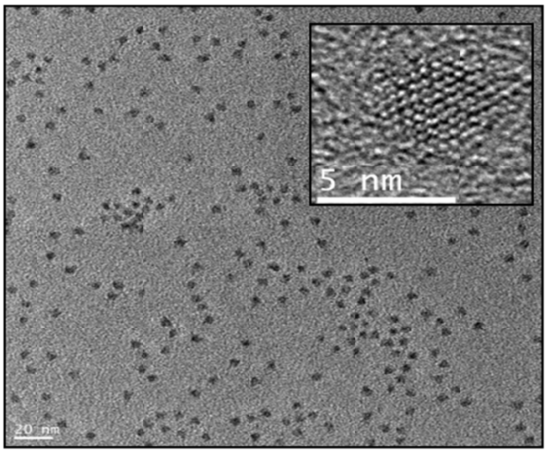

B

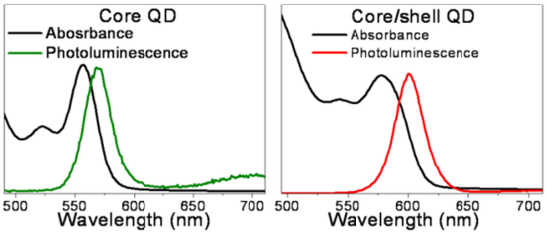

C

Quantum dot	Core	Core-shell
Composition	CdSe	CdSe/ZnS
Core diameter (nm)	3.4 ± 0.72	4.1 ± 1.1
Hydrodynamic diameter (nm)	16.5 ± 3.9	17.4 ± 0.5
Zeta-potential (mV)	-22.5 ± 12	-29.0 ± 16

Figure 6. QD characterization. (A) TEM image showing CdSe/ZnS QDs coated with PMAO-PEG copolymers. The QDs are uniform in size with a 4.1 nm core diameter (non-aggregated, scale bar = 20 nm). Inset: High-resolution TEM image of the crystalline structure of a single QD core particle. (B) UV-vis absorbance (black line) and

photoluminescence with a peak at 569 nm (green line) for the core QDs and at 600 nm (red line) for the core-shell QDs. (C) Quantum dot characterization table. The concentration is the measured atomic concentration of cadmium in buffered media; the core diameter was determined from TEM images, while the last two rows indicate the hydrodynamic size and charge of the polymer coated materials in buffer.

4.1.2. Exposure and Uptake of Quantum Dots

Exposure and uptake experiments were carried out on 24-well plates with 1 mL of NGM-agar as described in chapter 2. Briefly, 30 μL of the QD in borate buffer solution (50 mM, pH=10) or chemical controls was added to cover the bacterial lawn.

Sub-lethal concentrations for the multi-generational study were set at 10, 50, and 100 mg Cd/L. All reagents were of analytical grade and supplied by Aldrich.

4.1.3. Bioimaging and Microscopy

To visualize red fluorescence from internalized NPs, the exposure concentration for core and core-shell QDs used was [Cd] = 300 mg/L. After the inoculation time, *C. elegans* were immobilized with 10% sodium azide (NaN_3, Sigma) and mounted on slides following standard procedures.[59] The nematodes were imaged using a compound microscope (Axio Imager M2m, Carl Zeiss) with Nomarski objectives. Core-shell QD fluorescence was detected using a Texas Red filter (Carl Zeiss). Fluorescence and Nomarski images were acquired using a CCD camera (AxioCam, Carl Zeiss). All images were acquired and processed using the AxioVision

(Rel.4.8, Carl Zeiss) software. Core QDs could not be directly imaged inside the *C. elegans* due to their low quantum yields (data not shown).

4.2. Results and Discussion

Toxicity studies in *C. elegans* are directly relevant to the assessment of the environmental impact of NPs because nematodes are one of the most abundant animals in the soil. Also, NPs are often engineered for good dispersion in water as this is important for many of their applications; such modifications also have the consequence of increasing NP accessibility to terrestrial ecosystems, land disposals or wastewater treatment plants containing NPs.[60-62] In such an exposure scenario, nematodes are likely to be among the first organisms to encounter nanomaterial waste.

4.2.1. Uptake of Quantum Dots and Reference Toxicant

For these studies, we designed polymer-coated QDs to be monodisperse and non-aggregating under aqueous conditions. But before any QD toxicity could be interpreted, it was necessary to evaluate the impact of these NPs on the bacteria which are the food source for this organism.

E. coli growth showed no change after exposure to core QD, core-shell QD, or the cadmium salt controls after 24 h (**Table 5**). QD materials can be anti-microbial which can lead to starvation and developmental defects in nematodes.[50,63] However, these particular QDs and respective control solutions pose no threat to the food

source allowing a straightforward interpretation of the biological impact of the QDs on *C. elegans*. Because the QD materials were added to the surface of an agar plate supporting the worms, we anticipated that the main route of exposure would be through the digestive tract.

Table 5. Bacterial viability. Number of live cells after 24 hrs exposure to high [Cd] = 300 mgL^{-1} and low [Cd] = 10 mgL^{-1} concentrations of chemical control solutions and to nanoparticles at [Cd] = 10 mgL^{-1}. The results are expressed as the log of CFU/mL (colony-forming units/mL). Data shown are mean + SE from four independent experiments; p-values are derived from student t-test.

Sample	CFU	Log CFU	p-value
Buffer (Control)	1.5E+09	9.2	-
300 mgL^{-1} $CdSO_4$	1.2E+09	9.1	0.07
10 mgL^{-1} $CdSO_4$	1.5E+09	9.2	0.76
Core QD	1.5E+09	9.2	0.80
Core/shell QD	1.8E+09	9.3	0.13

We confirmed this exposure route by using fluorescent microscopy. The transparent body of *C. elegans* and the red fluorescence from core-shell QDs enabled us to directly visualize them in a live, intact animal. Over the timescale of these experiments we only found red fluorescence in the digestive tissue of the nematodes (Figure 7) which suggests there is no substantial assimilation of intact particles. Moreover, the emission remained bright and consistently red over the duration of

the study which indicates the core-shell QD do not appreciably change while ingested (Figure 7D).[53] This is in agreement with other studies of QDs in aquatic organisms such as crustaceans and *Daphnia magna*.[57,64]

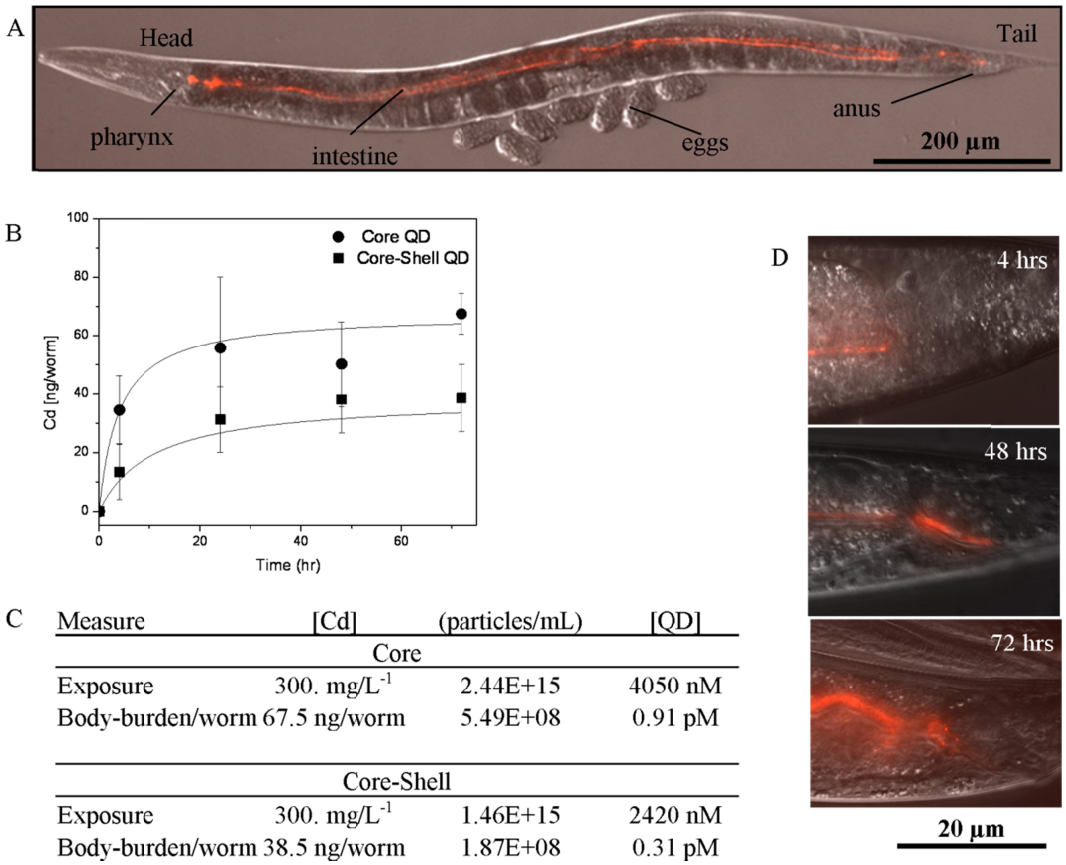

C

Measure	[Cd]	(particles/mL)	[QD]
Core			
Exposure	300. mg/L^{-1}	2.44E+15	4050 nM
Body-burden/worm	67.5 ng/worm	5.49E+08	0.91 pM
Core-Shell			
Exposure	300. mg/L^{-1}	1.46E+15	2420 nM
Body-burden/worm	38.5 ng/worm	1.87E+08	0.31 pM

Figure 7. (A) Internalized QDs. DIC image with color overlay of the entire nematode showing the anatomy: head, body, and tail. (B) The uptake profile of QDs based on body burden of internalized cadmium and (C) the exposure concentrations for each QD by ICP-OES. Data shown are mean + SE (n = 5). (D) Red fluorescence channel showing the tail region near the anus of the worm after 4, 48 and 72 h of exposure. The exposure concentration was [Cd] = 300 mg/L. Anterior is left and dorsal is up in all of the figures.

To complement the imaging observations which are semi-quantitative and applicable only to core-shell QDs, we also quantitatively assessed the total cadmium body-burden by ICP-OES. After 72 hours of continual exposure, we found an average of 67.5 ng Cd/worm for core QDs and 38.5 ng Cd/worm for core-shell QDs (Figure 7B, C). The higher body burden for the core QD reflects that this material is more soluble and likely to leach cadmium into the organism in a molecular form.[53] Also, we note that these body burdens are similar to studies of PEG conjugate PMAO QDs in organisms such as *D. magna,* where Lewinski, *et al.* found that the average uptake was 41 ng Cd/daphnia.[57] More comprehensive biokinetics studies that address the time dependence of the uptake, and the compartmentalization of cadmium in the gut as opposed to whole body, are underway.

4.2.2. Range-Finding Toxicity Response

The sub-lethal effects of the core QD on these organisms are similar to the effects of $CdSO_4$, but generally occur at net higher doses of QD. Figure 2 shows that after 72 h of exposure to core QDs (300 mg/L Cd), adult nematodes have a significantly decreased ($p < 0.01$) lifespan. Similarly, $CdSO_4$, the acute reference toxicant, caused a similar effect on lifespan albeit at even lower concentrations (Figure 8A, black). When exposed to core QDs (20 mg/L), brood size decreased ($p < 0.01$) by 25.8% (Figure 8B, red), with a dose-response relationship similar to $CdSO_4$. In stark contrast, core-shell QD exposures at concentrations up to 100 ppm had no impact on lifespan or brood size.

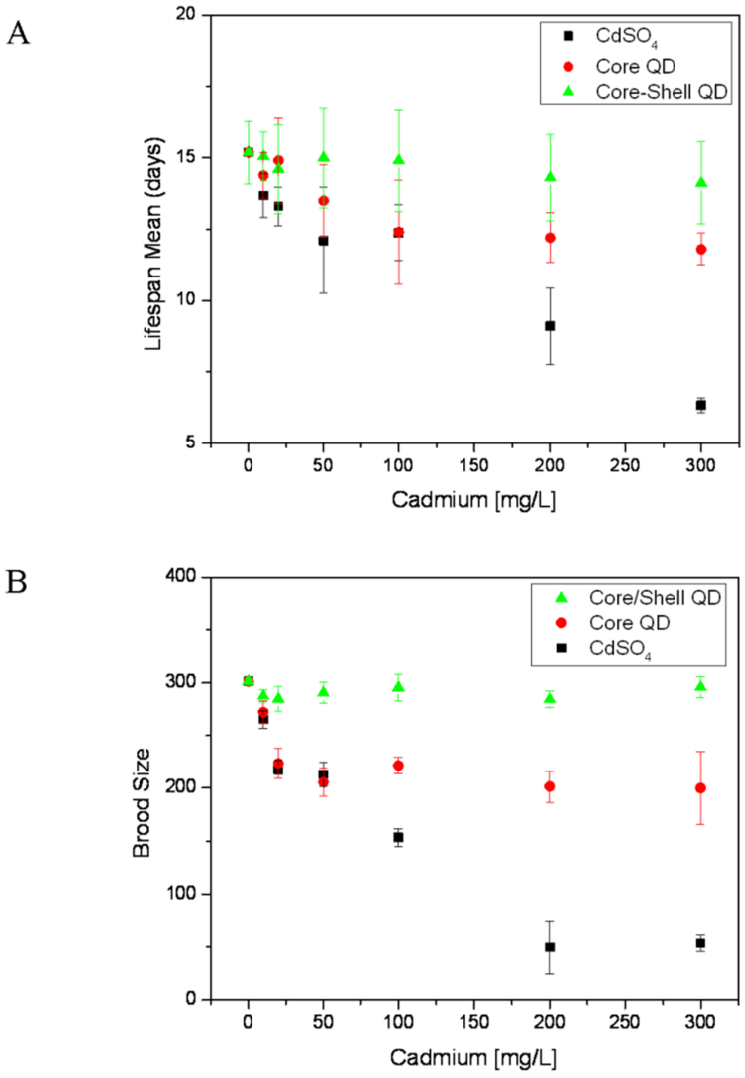

Figure 8 Range-finding toxicity response curves. (A) *C. elegans* life span mean of generation 1 after QD and chemical acute exposures. (B) Exposure related effect on brood size of adult nematodes of generation 1. Error bars indicate standard error of means from 12 independent experiments for each data point.

One mode of toxicity suggested for quantum dots is the release of soluble cadmium from the CdSe core into solution; even small amounts of leached cadmium

could have significant effects as this heavy metal is acutely toxic.[52] We find in this data a similar pattern of biological response in multiple endpoints to both the positive cadmium salt control and the core QDs. The primary difference is that the core QD caused these impacts at higher doses than the cadmium salt. These observations suggest that not all cadmium in the core QD is biologically available in contrast to the cadmium derived from soluble salts.

The lack of toxicity of core-shell QDs as compared to core QDs can be attributed to the zinc-containing shell of the core-shell QD. As zinc is incorporated into cadmium sulfide, the overall solubility of both metals decreases.[53,65] These data are consistent with other *in vivo* studies showing that QDs have low or no toxicity if their surfaces are appropriately designed to stabilize the nanoparticle and prevent dissolution.[50,58]

From these dose-response data, it was possible to select sub-lethal exposures for the multi-generational study; these correspond to cadmium concentrations of 10, 50, and 100 mg Cd/L for the positive control, core QD and core-shell QD.

4.2.3. Multigenerational Toxicity Response

Figure 3 shows multigenerational toxicity data for several biological endpoints after QD exposures. These data illustrate that at higher toxicant exposures, the biological response of the first generation is commonly mirrored in subsequent generations. For example, multigenerational exposure to the positive control, $CdSO_4$, showed significant adverse toxicity in fertility (brood size) and

length at high concentration [Cd] =100 mg/L (**Figure 9**). This significant change in population and growth may be due to the bioaccumulation of the heavy metal toxicant. Similar to the impact of cadmium salts, exposure to low (10 mg/L), medium (50 mg/L) and high (100 mg/L) concentrations of core QDs had the most notable impact on fertility. For fertility, a normal progeny count for unaffected adult worms is 300 offspring, but with a chronic exposure to core QDs at high concentrations [Cd] = 100 mg/L, brood size decreased significantly ($p < 0.01$) by 20% or more in population for all generations (**Figure 9**).

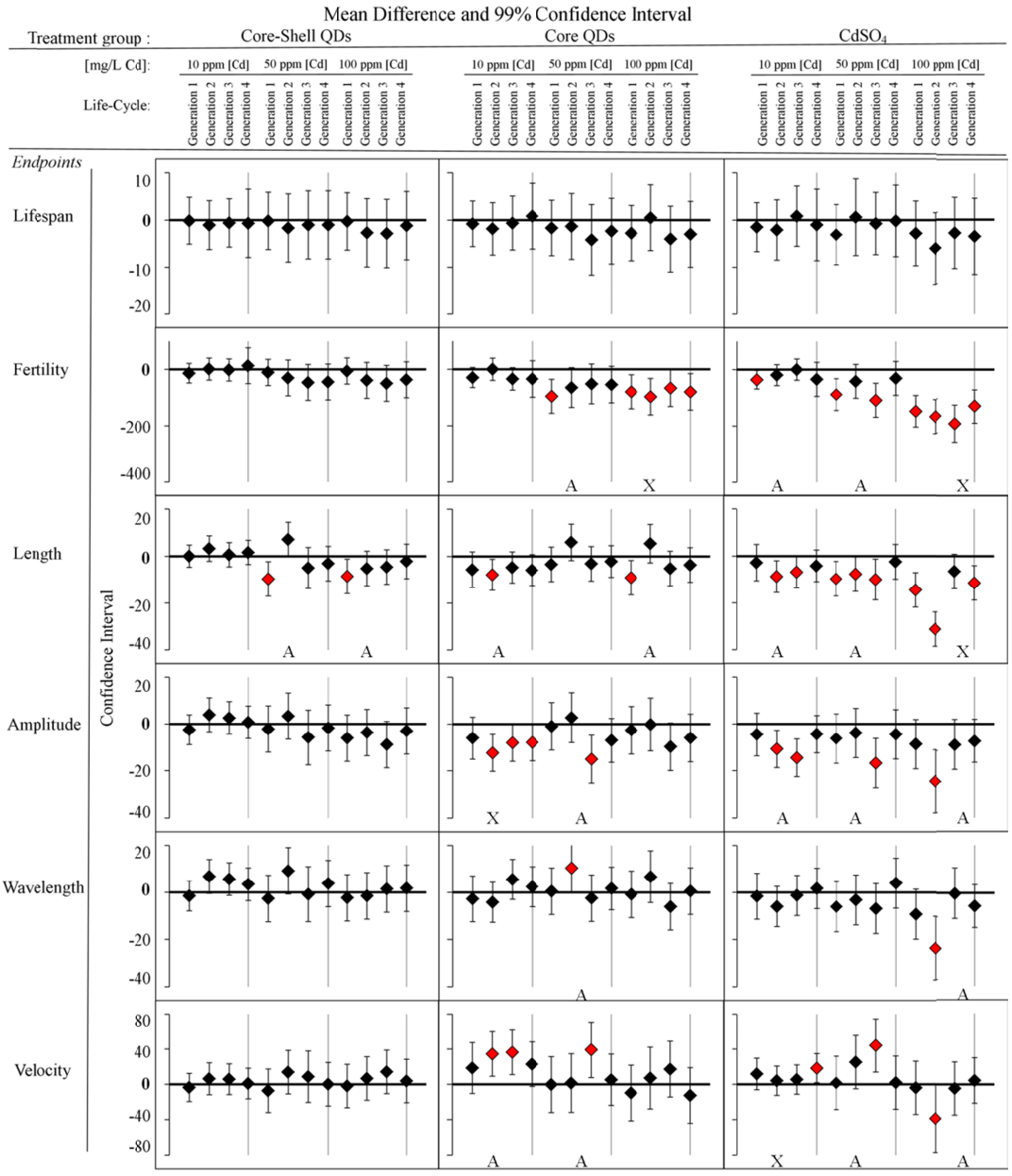

Figure 9 Multigenerational chronic exposure effects in multiple endpoints: lifespan, fertility, growth, and locomotion (amplitude, wavelength, velocity) for four generations at low (10 mg/L) medium (50 mg/L), and high (100 mg/L) concentrations of equivalent cadmium for each sample tested: core-shell QDs, core QDs, and $CdSO_4$. An A represents multi-generational data in which the effect in subsequent generations is different than the first generation. An X indicates continual adverse effects over multiple generations. Each horizontal bar represents the mean differences against the untreated control (ANOVA and

post-hoc Tukey test with 99% confidence interval). If the interval excludes 0, then the difference is considered significant (red marker) for that pair-wise comparison (n=12).

This agrees with previous reports of a 20% inhibition in fertility (brood size) of *C. elegans* in highly metal-contaminated soils.[10] Even the core QDs caused consistent impact on fertility at the highest exposures (100 mg/L Cd). Also, growth abnormality is a common indicator of developmental and metabolic defects.[63] Höss *et al.* (2009) investigated the growth of *C. elegans* in sediments polluted with heavy metals and showed a similar magnitude of effect on such parameters as length and fertility.[10] Qualitatively, of the three samples studied $CdSO_4$ caused the most significant changes to fertility, growth and to locomotive behaviors. In contrast, the multi-generational data for the core-shell QDs showed no evidence of any biological impact both in the first generation or subsequent generations.

While at the higher exposures, the first generation response predicted the response in subsequent generations, at the lower exposures for the core and core-shell QD first generation effects did not reflect the changes in subsequent generations.[45] In particular, it was commonly observed that when the first generation had a significant response ($p < 0.01$) to cadmium salt, core QDs, or core-shell QDs, subsequent generations had either less of an effect or no effect at all (Figure 9). This is most clearly seen in the core-shell QD exposures, particularly the measure of nematode length (**Figure 9**). The first generation in the 50 and 100 ppm exposures both had significantly reduced ($p < 0.01$) length, but this effect was not seen in subsequent generations. For core QD at medium concentration [Cd] = 50

mg/L, fertility significantly changed ($p < 0.01$) in the first generation, but returned to normal by generation 2. Similarly, nematodes exposed to $CdSO_4$ at varying Cd concentrations had more notable changes in the first generation than in subsequent ones. This was true at low concentrations with respect to fertility.

Such data may reflect that over generations nematodes can acclimate to low QD exposures as much as they acclimate to heavy metal contaminants in their environment.[21,35] Acclimation of aquatic organisms to heavy metal exposures has been linked to the upregulation of metallothionein-like proteins that bind to heavy metals and lower their bioavailability.[21,34,64] This phenomenon has been seen in other multi-generational toxicity studies of chemical agents such as endocrine disrupters and pharmaceutical waste.[34,46,48] Further studies to test whether and how the organisms are acclimating to the presence of core QDs are ongoing with a particular focus on the hypothesis that this acclimation is linked to regulation of metallothionein-like proteins.

4.3. Conclusion

To conclude, the biological effects of QDs of different surface coating and their precursor salts were extensively evaluated in this first multigenerational study of *C. elegans*. From this study, we conclude that QDs do not fully dissolve in nematodes as their biological effects are far less severe than cadmium salts; they are in effect much less toxic than free cadmium, a fact we attribute to the low solubility of cadmium selenide and the even lower solubility of cadmium selenide surrounded

by zinc sulfide.[53,65] We note, however, that any biological or environmental process that results in the full dissolution of these QDs could have significant and exaggerated consequences for this organism due to the intrinsic toxicity of their constituent cadmium. The multi-generational data suggests that nematodes may have the capacity to adapt or acclimate to the presence of low levels of heavy metals. It illustrates the importance of considering effects over multiple generations and provides one effective animal model well suited for evaluating different types of engineered nanomaterials.

Chapter 5

Size Effects of Silver Nanoparticles on the Fitness of *Caenorhabditis elegans* after Multigenerational Exposure

Here we present the use of *Caenorhabditis elegans* as an animal model to assess the size-dependent toxicity from four generations of exposure to silver nanoparticles. In this multi-generational study, we evaluated the biological effects of silver nanoparticles (AgNPs) of different sizes in nematode for four generations. AgNP with mPEG-SH coating had no effect on the bacterial food source. Size-dependent adverse effects on lifespan and brood size occurred, though with opposite trend. For example, 2 nm AgNP impacted fertility more than any larger particle tested of 5 and 10 nm. This may be due to the higher bioavailability of smaller nanoparticles to fertile eggs. In contrast, the largest particles, 10 nm, significantly reduced the lifespan of first generation *C. elegans* by 28.8%. This may be due to higher retention of larger nanoparticles within the body or adverse effect to the biological surface of the nematode, becoming lethal. Finally, no

evidence of adaptation occurred in lifespan and fertility, but rather, the impacts became more pronounced over subsequent generations. Additionally, a computer vision system automatically measured the adverse effects in body length and motility, which in contrast, were not size-dependent, suggesting a different mode of toxicity.

5.1. Introduction

Water-stability of nanoparticles increases its bioavailability to plants and animals in aquatic and terrestrial environments.[66] The abundance of nanoparticle waste currently derived from consumer products and materials into the environment already poses a toxic threat.[2,67] One of the most commercially relevant nano-size particles is AgNP which is currently incorporated into a many products from textiles to antibacterial cleaning solutions. Silver waste into the environment is projected to grow, such as from the wash of textiles, and to adversely affect the food web.[2]

A model organism to evaluate environmental impact is the terrestrial nematode *Caenorhabditis elegans* which come into contact with material waste in the soil. With its short lifespan and large brood size, studies with *C. elegans* may reveal how the nematode acclimates over several generations to exposure from nanoparticles. A few studies using *C. elegans* to investigate the impact of AgNPs have been reported.[3,11,18,19] Currently, no *in vivo* study has yet addressed the adverse effects after multigenerational exposures on a number of fitness endpoints, such as lifespan, fertility, growth and locomotion parameters (flex, amplitude, wavelength, and velocity).

Two key modes of toxicity for AgNP result from either ionic effect of silver ions or particle effect.[68,69] Toxicity from Ag ions causes ionic gradient changes across

membranes, malfunctioning organelles and disrupting peptide function by oxidative stress, as well.[19,68,69] Particle (or size-dependent) effect occurs from the actual presence of a hard chafing material physically embedded within the organism that causes significant structural damage and infections without remedy, for example.[70,71] Both ionic and particle-effect by AgNPs are common modes of toxicity *in vitro* and *in vivo*. In this study, mPEGSH-coated particles with negligible dissolved ionic silver provided the opportunity to examine true particle effects on OP50 *E. coli* and nematodes as opposed to impacts caused by substantial amounts of leaching Ag ions.

Particle effect is dependent on its bioavailability to the organism. Nano-specific toxicity consist of reactive oxygen species (ROS) or free ion dissociation.[72] Smaller particles of 10 nm or smaller increase bioavailability and easily transfer through embryonic cell walls and tissue, for example.[18,72,73] Meyer *et al.* showed 7 nm citrate coated AgNPs in K-media in *C. elegans* transfer through the cell membrane of parent eggs, causing adverse effect and offspring death, and illustrating transgeneration adverse effects.[18] In addition to surface charge and a number of other parameters, particle size can increase bioavailability and facilitate NP biodistribution into different tissues and organs.[31,74]

Both small and large particle aggregates can cause adverse effects but by different toxicity modes. Smaller nanoparticles have been found to be more toxic because of increased total surface area. Greater total surface area allows for increased reactivity that can damage proteins and organelles *in vivo*. Extensive damage occurs when smaller nanoparticles diffuse through cells and tissue. Once internalized within cells, small sized nanoparticles may have the tendency to aggregate with other nanoparticles by

intermolecular forces of attraction.[74] Aggregation within the cell prevents the small particles to diffuse back out and instead damage the cell more.

Once aggregated, larger particle size was more toxic than smaller particles.[74] For example, Lee et al., described how clotting occurred after smaller particles passing passively through the transmembrane pores of embryonic cells aggregated with larger particles. Intracellular clotting prevented NPs from diffusing out which caused developmental delays, deformities, and offspring death in Zebrafish.[75] These authors illustrated how aggregate-sized NPs when measured *in situ*, can become more toxic than smaller sized NPs.[74,75]

C.elegans do not discern between bacteria and nanoparticles of any size when feeding.[76] Larger particles greater than 10 nm can also cause exogenous structural damages, influencing molting and becoming lethal.[11,31] Kim *et al*. showed that AgNPs can not only cause damage when internalized, but can cause dermal effect to the exterior cuticle.[11] The authors introduced larger particles of 50.6 nm citrate-coated AgNPs to *C. elegans* by feeding. As seen in numerous scanning electron images, the AgNP fractured the biological surface of nematodes.[11] The cuticle of *C. elegans* became physically rigid from exposure to AgNP preventing molting, bursting, and becoming lethal.[11] Kim *et al*. described how *C. elegans* suffered from particle effect to the epidermis, but also once internalized, larger-sized nanoparticles can also cause lethal endogenous damage.[11]

In this study with *C. elegans*, we examined three different sizes (2, 5, and 10 nm) of AgNPs at three concentrations (low 1 mg Ag/L, medium 10 mg Ag/L, and high 100 mg Ag/L concentrations). For all sizes and concentrations, these PEGylated-AgNPs had no antibacterial properties and no effect on the food source. Four generations of *C. elegans*

were continuously exposed and analyzed for life span and fertility with size-dependent adverse effects. In addition, growth and motility parameters (velocity, flex, amplitude, and wavelength) were quantitatively analyzed using an automated computer vision system showing no size-dependent correlation with adverse effects. Here, for multiple generations, we quantitatively measure a number of fitness parameters to determine if cumulative damage or acclimation occurre when exposed to different sizes of AgNPs.

5.2. Method

5.2.1. Silver Nanoparticle Preparation and Characterization

Silver Nanoparticle Preparation and Characterization. To control size, silver nanoparticles (AgNPs) were prepared with $AgClO_4$ and an oleic acid coating following published procedures [77]. Briefly, $AgClO_4$ was reduced by oleylamine at varying temperatures to produce different sizes and then coated *in situ* with oleic acid for stability of monodispersed silver nanoparticles. These materials were made water soluble by coating with the amphiphilic polymer mPEG-SH (Mn = 5000, Sigma) through a ligand exchange reaction. After phase transfer into water, the mPEG-SH surface coating limits silver ion dissolution and the antibacterial property of AgNPs.

The size and chemical composition of AgNPs were carefully measured using several characterization tools (**Figure 10**). The silver core diameter was determined via transmission electron microscopy (Joel 2010 TEM). To measure the hydrodynamic diameter and zeta potential of the nanoparticles in solution, dynamic light scattering (Malvern Zetasizer Nano-ZS) was used (**Figure 10**). The silver ion concentration was determined by inductively coupled plasma-Mass spectrometer (ICP-MS). All

concentrations were based on milligrams of silver ion in solution. Three sub-lethal concentrations of 1, 10, and 100 mg Ag/L were tested for each AgNP sample.

5.2.2. Assessment of *E. coli* Viability

AgNPs were added to the bacterial lawn to measure their impact on OP50 *E. coli* food source for *C. elegans*.[78] Two reference toxicants: silver nitrate ($AgNO_3$, Sigma) and silver perchlorate ($AgClO_4$, Sigma) were tested and compared against the toxicity of AgNP on the bacterial food source, as well. In 24-well plates maintained at 20°C, 30 uL of respective sample was added to the bacterial lawn for a 24 hour exposure. After the inoculation time, the bacterium was washed with 1 mL of sterile H_2O to make serial dilutions. Onto a 6 cm LB plate, 20 μL of each dilution was added and maintained overnight at 37°C. Bacteria viability was determined by counting the colonies and calculating the initial concentration of live bacteria in solution.

5.2.1. Exposure and Uptake of AgNP

Exposure and uptake experiments were carried out on 24-well plates with 1 mL of NGM-agar as described in chapter 2. Briefly, 30 μL of the AgNP or chemical controls was added to cover the bacterial lawn.

Sub-lethal concentrations for the multi-generational study were set at 1, 10, and 100 mg Ag/L. All reagents were of analytical grade and supplied by Aldrich.

5.2.2. Quantification of Internalized Silver

The silver concentration within N2 nematodes was determined by inductively coupled plasma-Mass spectrometer (Perkin Elmer, ELAN9000 ICP-MS). Concentrations were reported as milligrams of the silver ion in the solution.

At the sublethal exposure concentration of 100 mg Ag/L, *C. elegans* on agar plates were treated to different sizes of AgNP: 2, 5, and 10 nm. Exposed since eggs, one-hundred L4 nematodes were collected and washed to remove bacteria and excess chemicals. The nematodes were placed in pre-weighed glass tubes and 1 mL of 70% HNO_3, followed by heat digestion in a block heater at 90 °C for 4 hours, and left over-night to cool. The solution was then diluted with ultrapure water to achieve a final acid concentration of 1%.

5.3. Results and Discussion

Because of the well-known antibacterial property of AgNPs, its use in this study with *C. elegans* that feed on *E. coli* can pose a major problem.[78] Any dissolution of silver ion from improperly coated, low-quality, or acid-decomposed AgNP can cause starvation and secondary adverse effect in *C. elegans.*[63] Since Ag ions are indisputably antibacterial, AgNPs were added to the bacterial lawn to measure their impact on food.[78]

5.3.1. AgNP characterization

AgNP were characterized thoroughly using TEM to measure cores size. All images illustrates AgNP that are monodispersed and non-aggregating. The core diameter of small, medium, and large sizes were 2.2 ± 0.8, 4.7±0.9, and 8.9±1.9, which are to be

labeled in this chapter as 2, 5 and 10 nm particles, respectively (**Figure 10**A). Further characterization using DLS indicates the presence of a polymer coating to render the AgNPs water soluble. In this study, NPs of less than 10 nm, are well below the detection limit of DLS; yet, change in diameter before and after a ligand exchange indicates that the reaction was successful.

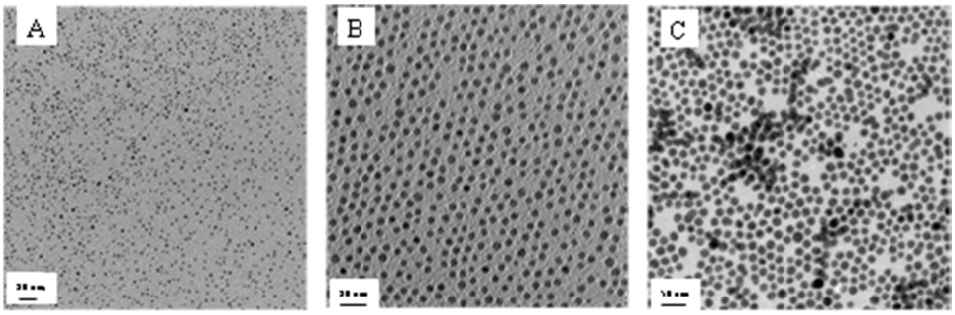

D

Parameters	2 nm	5 nm	10 nm
Core diameter (nm)	2.2 + 0.8	4.7 + 0.9	8.9 + 1.9
Surface area (nm^2)	15.2	69.5	249.1
DLS_{org} (nm)	16.3 + 1.8	18.6 + 1.5	26.5 + 4.1
DLS_{aq} (nm)	22.1 + 3.5	26.5 + 4.1	35.5 + 2.1

Figure 10. AgNP characterization of 2nm (A), 5 nm (B), and 10 nm (C) silver particles. The core diameter was determined from TEM images coated with mPEG-SH (non-aggregated, 0.12 mV, scale bar = 20-50 nm). (D) The surface area in nm^2 was calculated. The addition of mPEG-SH via a ligand exchange was measured by DLS in the organic and aqueous solutions. The amount of dissolution over two months is negligible and below the detection limit for ICP-MS.

5.3.2. Effects of soluble silver salts versus AgNPs on the growth of *E. coli*

Ionic silver introduced from either $AgNO_3$ or $AgClO_4$ was lethal to OP50 *E. coli* colonies. At extremely low concentrations, the LD_{50} for $AgClO_4$ was 0.02 mg Ag/L and

for $AgNO_3$, 0.06 mg Ag/L (**Figure 11**A). Ag ions are indisputably antibacterial.[78] In fact, the well-known antibacterial property of silver has been exploited in medicinal textiles and in many other consumer products.[79]

In contrast, when exposed to doses of 2, 5, and 10 nm AgNPs at 100 mg Ag/L, *E. coli* remained viable with no significant change ($p < 0.05$) compared to an untreated control over the span of 4 generations (**Figure 11**B). The absence of bactericidal property indicates that no lethal amount of silver ions leached from the nanoparticle. Therefore for these materials, the polymer surface coating decreased dissolution (**Figure 10**), even after two months. This shows there is no impact on the animal model due to starvation.

A

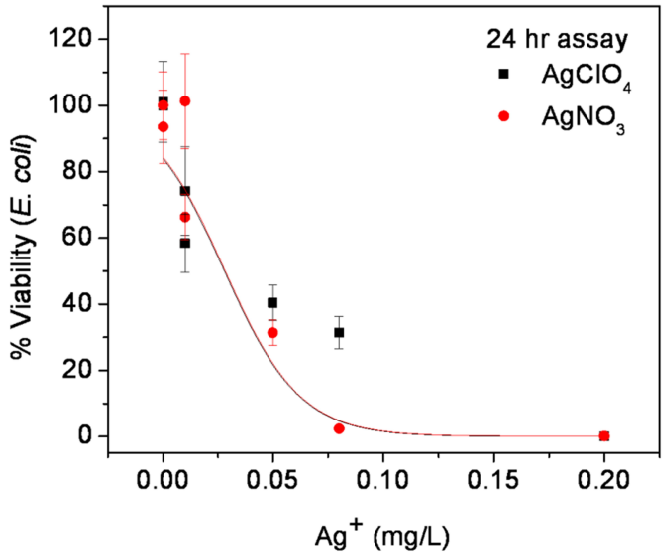

B

Sample	(mg/L)	CFU	Log CFU	p-value
Control	0	1.1E+09	9.0	-
	1	1.1E+09	9.0	0.78
2 nm	10	1.1E+09	9.0	0.93
	100	8.6E+08	8.9	0.08
	1	1.2E+09	9.1	0.73
5 nm	10	1.1E+09	9.1	0.76
	100	8.4E+08	8.9	0.12
	1	9.0E+08	9.0	0.18
10 nm	10	9.0E+08	9.0	0.17
	100	1.2E+09	9.1	0.67

Figure 11. Bacterial viability after 24 hour exposure to nanoparticles or silver salts. All AgNPs showed no antimicrobial activity. With LD50 values of 0.06 mg Ag/L for $AgNO_3$ and 0.02 mg Ag/L for $AgClO_4$ (A), toxicity of silver ions was evident. However, no effects were observed with silver nanoparticles up to 100 mg Ag/L when compared to the untreated control (B).

.

5.3.3. AgNP Exposure and Uptake

We speculate that in addition to exogenous stress to the epidermis,[11] endogenous stress from quantitative amount of internalized AgNP adversely affected nematode mean lifespan because of cumulative adverse effects and transgenerational accumulation. At the exposure concentration of 100 mg Ag/L, internalized silver concentrations in *C. elegans* exposed since eggs to 2, 5, and 10 nm Ag particles were quantified by ICP-MS (**Figure 12**). Ag concentration was 1.84 ± 0.2 ng/nematode for nematodes exposed to 10 nm particles and 1.80 ± 0.1 ng/nematode for nematodes exposed to 5 nm particles. For 2 nm AgNP exposures, an internalized silver concentration was 1.30 ± 0.2 ng/nematode. This range of Ag concentrations in *C. elegans* were in agreement with Choi, *et al.* who treated zebra fish with 120 mg Ag/L AgNP and measured a silver concentration of 2.4 ng Ag/liver.[80] Because surface coating is the same, we attribute any toxicity to the different sizes of AgNP.

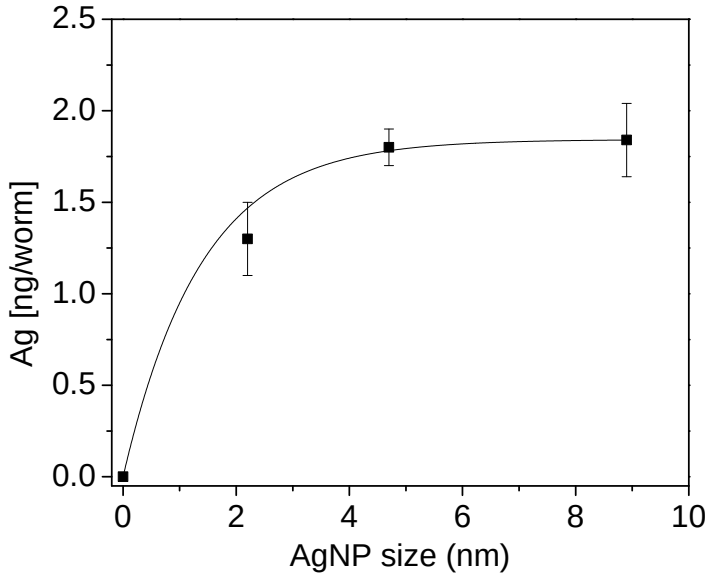

Figure 12. Size-dependent uptake measured using ICP-MS methods.

In this study, only nematodes that reached adulthood by day 4 were measured. Here, adverse effects on the mean lifespan and fertility were size dependent where the most adverse effect for lifespan occurred with the larger AgNPs and for fertility, smaller AgNPs. Less quantitative amount of Ag^{+} was detected in C. elegans exposed to 2 nm Ag particles when compared to larger particles of 5 and 10 nm. We speculate that the smaller size increase particle mobility out the body and into eggs,[18] whereas larger sized particles accumulate longer inside the body.

5.3.4. Multigenerational Toxicity Response

5.3.4.1. Lifespan Assay

Cumulative adverse effect on mean lifespan was size-dependent at 100 mg Ag/L (**Figure 13**A). For untreated *C. elegans*, have a mean lifespan of 14.2 days.[81] At 100 mg/L Ag/L, 2 and 5 nm particles caused no significant change in parent (P0) mean lifespan (**Figure 13**A). Whereas, at 100 mg/L, 10 nm Ag particles decreased the mean lifespan for P0 nematodes by 28.8%; and over the span of three generations, 10 nm Ag particles continued to significantly decrease ($p < 0.01$) mean lifespan when compared to smaller sized AgNPs. Ultimately at 100 mg/L, all AgNPs in this study caused a significant decrease in mean lifespan.

For F1 progeny (first generation), mean lifespan of nematodes exposed to 10 nm AgNPs [100 mg/L] significantly decreased ($p < 0.01$) by 58.7%; while exposure to 2 and 5 nm AgNPs decreased mean lifespan by 30.8 and 34.6%, respectively (**Figure 13**A). For second generation progeny (F2), 10 nm AgNPs caused the most adverse effect, reducing mean lifespan by 52.5%. Whereas, AgNP of 2 and 5 nm reduced F2 mean lifespan by 21.5 and 49%, respectively (**Figure 13**A). In fact, AgNP of 5 nm at 100 mg/L for F2 (49% reduced mean lifespan) was comparable to 10 nm particles (52% reduced mean lifespan). Also at 100 mg Ag/L, mean lifespan for 5 nm particles for F1 and F2 is also much more significant than for 2 nm particles.

F2 mean lifespan exposed to 5 and 10 nm AgNP (49 and 52% decrease) correlates with similar amounts of internalized Ag concentrations. We found that after three generations (F3) of chronic exposure to 100 mg Ag/L, accumulated adverse effects of AgNPs caused nematode population to decrease to low or absent sample size (**Figure 13**, red lines). We

speculate that AgNPs absorbed to the cuticle, decreased motility, prevented molting, and became lethal.[11,76] In contrast, smaller nanoparticles would have increased bioavailability as they are easier to absorb than larger ones and translocate easier within and between cells and tissues in nematodes, resulting in higher toxicity, parent sterility or death,[31,74] or offspring developmental delay or death.[3]

5.3.4.2. Fertility Assay

In contrast to lifespan, 2 nm AgNPs caused the greatest adverse effect on fertility over three generations, in comparison to larger sized AgNPs (**Figure 13**B). An untreated (control) single worm has about 300 offspring over its lifetime.[81] At 10 mg Ag/L, adverse effect on *C. elegans* brood size was inversely size-dependent. For example, the smallest (2 nm) AgNPs at 10 mg/L significantly decreased $(p < 0.01)$ all nematode populations for P0, F1 and F2 generations to an average of 185 nematodes (**Figure 13**B). However, at the same exposure concentration, for 5 nm AgNP at 10 mg/L, a change in brood size was not noticeable until F2 where brood size significantly decreased $(p < 0.01)$ to 197 nematodes. Lastly, 10 nm AgNP at 10 mg/L did not adversely affect brood size for three generations (**Figure 13**B). This is in agreement with Meyer et al, who illustrated how smaller AgNPs transferred past embryonic cell walls causing transgenerational toxicity, developmental delays or death in progeny.[18]

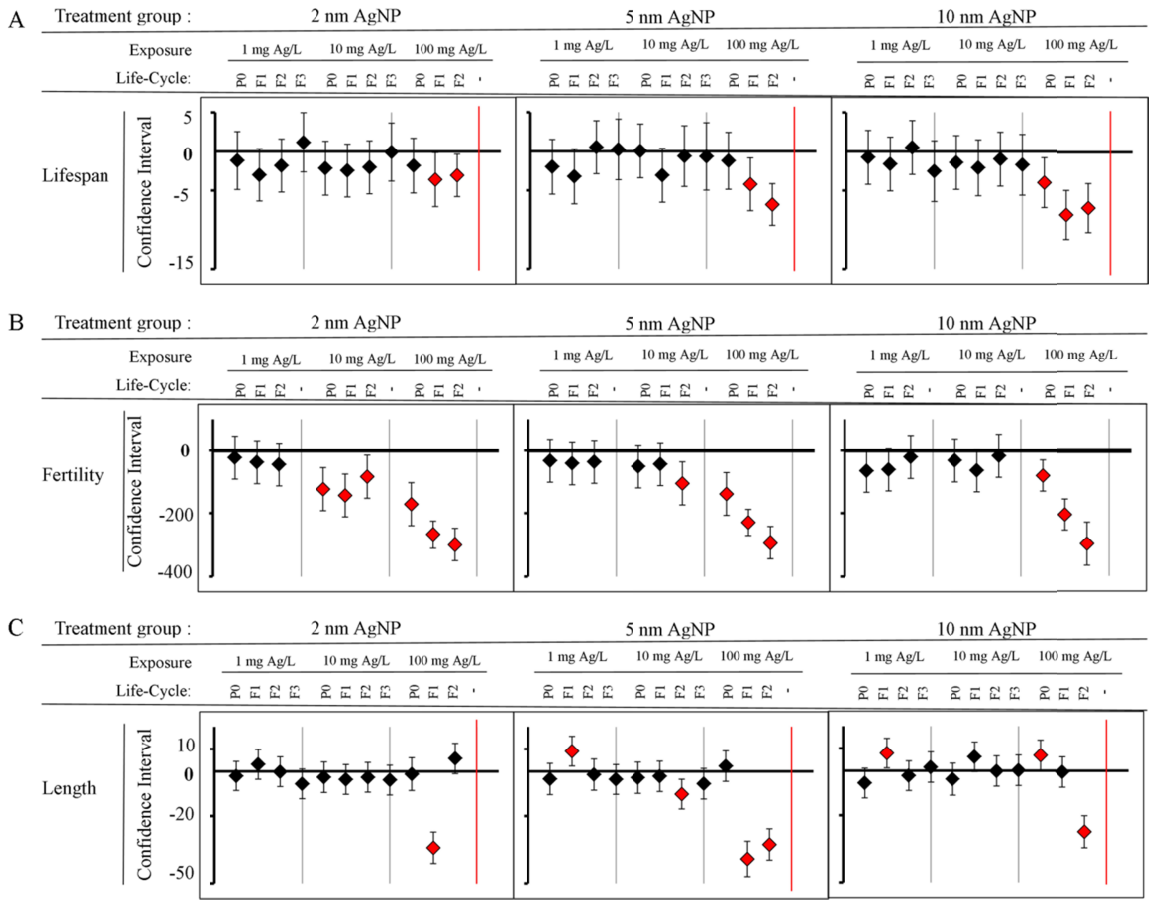

Figure 13. Size-dependent adverse effect on A) lifespan, B) fertility, and C) length after multigenerational chronic exposure for three generations at low (1 mg Ag/L), medium (10 mg Ag/L), and high (100 mg Ag/L) concentrations for each diameter of 2, 5, and 10 nm. Each vertical bar represents the mean differences against the untreated control (ANOVA and *post-hoc* Tukey test with 99% confidence interval). If the interval excludes 0, then the difference is considered significant (red marker) for that pair-wise comparison (n=12). Red vertical bars represent no data as F3 nematodes did not survive exposure.

At 100 mg Ag/L, reduced brood size for three generations was cumulative and size-dependent (**Figure 13**B). For smaller particle sizes, 2 nm caused brood size to decrease from 56.8% for P0 to 98.9% by F2 at a decrease rate of 64 nematodes/generation. For 5 nm AgNP, brood size decreased at a rate of 77 nematodes/generation. Exposure to the

largest AgNP (10 nm) caused a significant decrease ($p < 0.01$) in brood size of 26.4% for P0 to 98.2% by F2, with a decrease rate of 108 nematodes/generation. For all AgNPs tested, F2 brood size was similar and F3 extinction occurred due to either low or no sample size (**Figure 13**, F3 red lines). We speculate that these size-dependent toxicities for both lifespan and brood size accumulated with each generation that led to serious F3 mortality rates. In this study, parameters such as lifespan and fertility gave more distinct and linear results from AgNP exposure than growth and locomotion.[32]

5.3.4.3. Growth Assay

When exposed to 5 and 10 nm AgNPs, body length of first-day adults were adversely affected, but with opposite trends of acclimation at low exposure concentrations and cumulative damage at high concentrations (**Figure 13**C). For example, acclimation at the low exposure concentration of 1 mg Ag/L occurred when F1 progeny body length was significantly greater ($p < 0.01$) than average, but by generation F2, body length returned to normal (**Figure 13**C). Another example of physiological acclimation to AgNPs occurred at 10 mg Ag/L when 5 nm AgNP caused shorter body lengths in F2 progeny, but returned to normal by generation F3 (**Figure 13**C). Cumulative adverse effects are seen at the high concentration (100 mg Ag/L), occurred when multiple generations of chronic exposure to 2, 5 and 10 nm AgNPs increasingly caused developmental delays and stunted the growth of offspring (**Figure 13**C).[18,31] The adverse effect on growth (body length) caused by AgNPs was not size-dependent, as with lifespan and fertility.

5.3.4.4. Locomotion Assay

Using an automated tracking microscope, locomotion parameters (flex, amplitude, wavelength, and velocity) were quantitatively measured and adverse effects were not size-dependent (**Figure 14**). With the exception of one amplitude endpoint for 2 nm AgNP, at the highest sub-lethal concentration [100 mg Ag/L] for all sizes of AgNP, significant impact *($p < 0.01$)* and cumulative adverse effect on amplitude, wavelength, and velocity occurred exclusively, with no acclimation (**Figure 14**, denoted as X). That is, nematodes exposed for multiple generations to 100 mg Ag/L had decreased body movement and forward trajectory. These impediments to locomotion behaviors could result from adverse epidermal damage to the cuticle by AgNP, limiting movement, or from neurotoxicity by silver ions.[11]

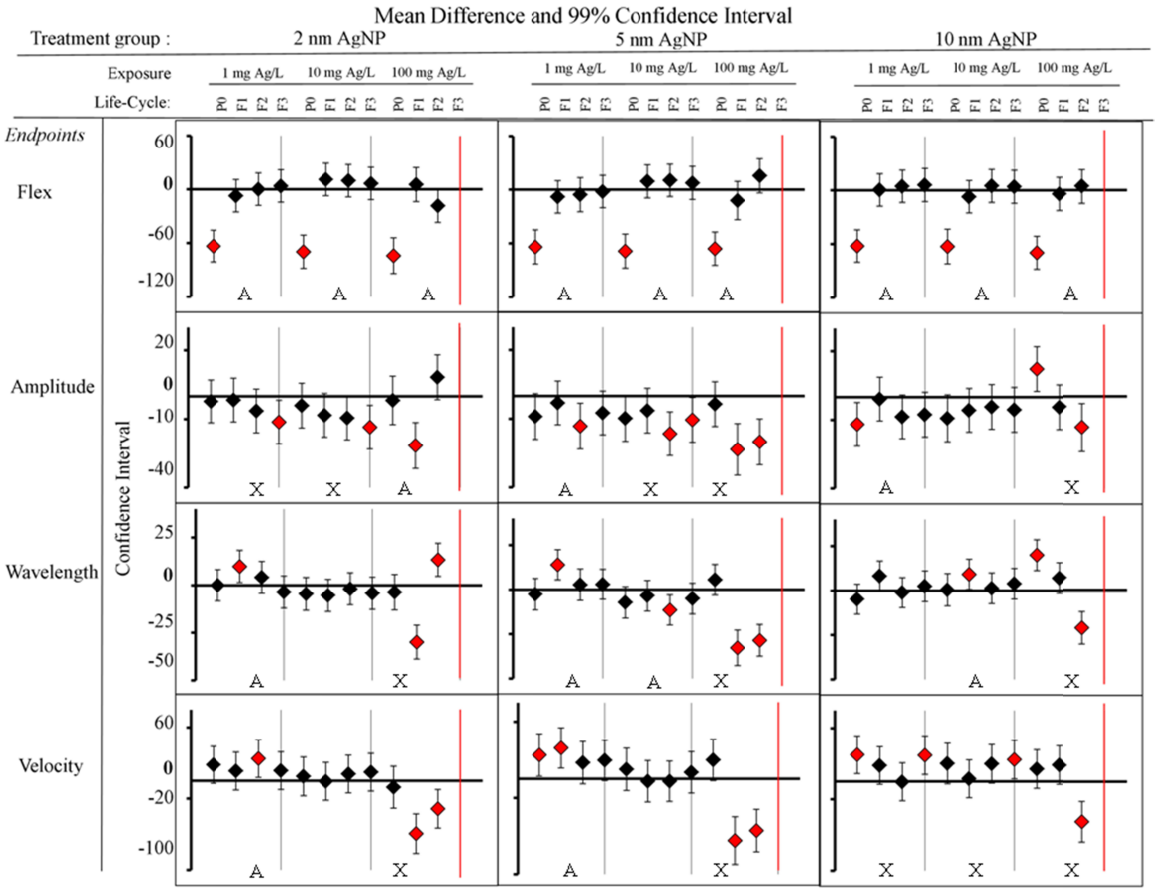

Figure 14. Multigenerational chronic exposure effects in multiple endpoints in neurological behaviors (flex, amplitude, wavelength, and velocity) for four generations at low (1 mg Ag/L) medium (10 mg Ag/L), and high (100 mg Ag/L) concentrations of silver nanoparticles tested: 2nm, 5 nm, and 10nm. An 'A' represents multi-generational data in which the effect in subsequent generations is different than the first generation. An 'X' indicates continual adverse effects over multiple generations. Each vertical bar represents the mean differences against the untreated control (ANOVA and *post-hoc* Tukey test with 99% confidence interval). If the interval excludes 0, then the difference is considered significant (red marker) for that pair-wise comparison (n=12). For F3 for lifespan, fertility and length at high concentration, has no data for the fourth generation was available as nematodes did not survive exposure.

In contrast, at lower exposure concentrations of 1 and 10 mg Ag/L, acclimation in nematode progeny occurred with all locomotion endpoints measured (**Figure 14,** denoted as A), except for amplitude and velocity. Specifically, acclimation occurred when parent (P0) locomotion behavior became impaired, but then returned to normal in progeny. For example, when monitoring the flex parameter, or the number of times that the body bends, nematode progeny (F1) acclimated and flex behavior returned to normal (**Figure 14**).

When nematodes were exposed to AgNPs of 5 nm, the amplitude cumulatively worsened in a dose-dependent manner in F2 and F3 generations. While at 1 mg Ag/L, nematodes acclimated by F3 to AgNP chronic exposures, but at 10 mg Ag/L, the opposite is true. At 10 mg Ag/L, amplitude began to decrease after two generations of chronic exposure, as with 100 mg Ag/L. Another example of dose-dependent cumulative adverse effect occurred with amplitude when exposed to 2 nm AgNP and with velocity when exposed to 10 nm AgNP.

5.3.1. *C. elegans* Acclimation to AgNP Toxicity

Toxicity from AgNP exposure in *C. elegans* can have a dire effect on the organism, food web and ecosystem. Results from the present study are far from conclusive and future research should consider a variety of assays, from physiological endpoints to genotoxicity, to elucidate AgNP toxicity. There exist the possibility of randomness in these endpoints, but this data also lends to the possibility of long-term cumulative adverse effect after multi-generation exposures to water-soluble nanoparticles where the polymer coating are expected to increase bioavailability and exposure.

Environmental threats and heavy metal contaminants commonly cause endogenous and exogenous stresses to organisms. In order to defend against lethal stresses and to acclimate to a toxic environment, *C. elegans* have the capability of producing metal-binding proteins, such as metallothionein, to purge its body of heavy metal contaminates. It can also increase protein scavengers, such as glutathione peroxidase and superoxide dismutase, to remove stress-induced reactive oxygen species in order to decrease internal damages.[82] Another coping mechanism consists of regulating the trade-off between fertility and lifespan, for example, in order to maintain homeostasis.[3,83] Measuring proteins are common methods for monitoring environmental threats and issues. In this study, we introduce a quick and high-throughput method to measure fitness endpoints in *C. elegans* that are sensitive to toxicants and AgNP exposures. These endpoints, along with nanobiotoxicology studies, can unravel modes of toxicity that are prudent to monitor the health of organisms and their environment.

5.4. Conclusion

For four generations, C. *elegans* and *E. coli* were continuously exposed to either a low, medium, or high concentration of silver nanoparticles (AgNPs) of three different sizes: 2, 5, and 10 nm. The AgNP caused no adverse effect to *E. coli* and to the food of *C. elegans* demonstrating no immediate bactericidal properties from leaching Ag ions. Yet, these nanoparticles have size-dependent effects on *C. elegans* lifespan and fertility after multigenerational exposure with opposing trends. At 100 mg Ag/L, the largest diameter AgNP significantly shortened the lifespan of *C. elegans* causing the most lethal damage*;* whereas, the smallest diameter AgNP significantly affected fertility. In measuring growth

and neurodegenerative endpoints, silver nanoparticles had no size-dependent adverse effect. Overall, for all the AgNP sizes, the nematodes acclimated at lower exposure concentrations but suffered cumulative damage at high exposure concentrations.

Chapter 6

Experimental Methods: ROS Measurements *In Vitro*

6.1. Mammalian Cell Cultivation and Exposure.

Human dermal fibroblasts (HDF, Cambrex, USA) were cultured in Dulbecco's Modified Eagle's Medium (ATCC, USA), supplemented with 2 mM L-glutamine, 1% penicillin, 1% streptomycin, and 10% fetal bovine serum. Cells were incubated at 37°C under 5% CO_2 and detached from culture with trypsin and re-suspended in media for passaging to wells. HDF cells were grown to 70% confluency in multi-well plates before testing.

The cells were inoculated with C_{60}/THF nanoaggregate samples. This experiment was repeated a second time with UV-irradiation. In the same way for cells dosed with irradiated C_{60}/THF, the solution of titania was irradiated separately for 10 m in 2 m increments, and then added to the cells.

6.1.1. Assessing Qualitative Cellular Response

The Live/Dead kit (Promega, USA) gave immediate qualitative analysis of adverse effects to HDF cells. After the incubation time, the supernatant containing the nanoparticles was removed and replaced with the Live/Dead assay following the manufacture's protocol. After incubation at room temperature for 60 m, live and dead cells were imaged using a fluorescence microscope, which consisted of an inverted Zeiss Axiovert 135 phase-contrast microscope (Carl Zeiss, USA) equipped with a Nikon digital camera.

6.1.2. Plate Reader to Assess Cellular Viability

Colorimetric, fluorescence, and chemiluminescence were measured using a SpectraMax M5 Multi-Mode Microplate Reader (Molecular Device, USA) with SoftMax Pro Software (Molecular Device, USA).

6.1.2.1. Assessing Mitochondrial Activity

The mitochondrial activity of viable cells was assessed by the colorimetric MTS assay (CellTiter 96® AQ_{ueous} Non-Radioactive Cell Proliferation Assay, Promega, USA). The cells were treated in a 96-well, clear plate. The cells were inoculated with gradient concentrations of C_{60}/THF, with one set used as the untreated control. After a 24 and 48 h exposure, the supernatant containing the nanoparticles was replaced with 100 µL of fresh, phenol red-free DMEM (Gibco/Invitrogen)and 20 µL MTS stock solution. After incubating at 37 °C for 1 h, the absorbance at 490 nm and the reference at 680 nm were measured with a plate reader.

6.1.2.2. Assessing Membrane Integrity

To assess lethality, a fluorescent dye, acetyoxymethyl ester (Calcein AM, Invitrogen, USA), was used following the manufacture's protocol. The cells were treated in a 96-well, black with clear bottom plate. The cells were inoculated with gradient concentrations of C_{60}/THF, with one set used as the untreated control. After a 24 and 48 h exposure, the supernatant containing the nanoparticles was replaced with 300 μL Calcein AM. After incubation at room temperature in the dark for 45 m, live cells fluoresced green and was quantitatively measured (ex/em 495 nm/515 nm) with a plate reader.

6.2. Flow Cytometer to Assess Cellular Stress.

Flow cytometery was done using a FACScan (Beckman Coulter, USA) with Power Mac G3 and BD CellQuest Pro software (BD Biosciences, USA).

6.2.1.1. Assessing Oxidative Stress

This assay was used to quantify oxidative stress *in vitro* by measuring the oxidation of 2'7'-dichlorofluorescin (DCFH) to 2'7'-dichlorofluorescein (DCF), a fluorescent product (ex/em 485 nm/530 nm) (**Figure 15**) [84]. A 1 mM stock of 2'7'-dichlorofluorescin (DCFH, 4091-99-0, Sigma, US) was diluted into a working concentration of 40 μM in 0.01 N NaOH and kept in the dark at room temperature for 30 m before adding 10 mL of 25 mM phosphate buffer solution (PBS, pH=7.2).

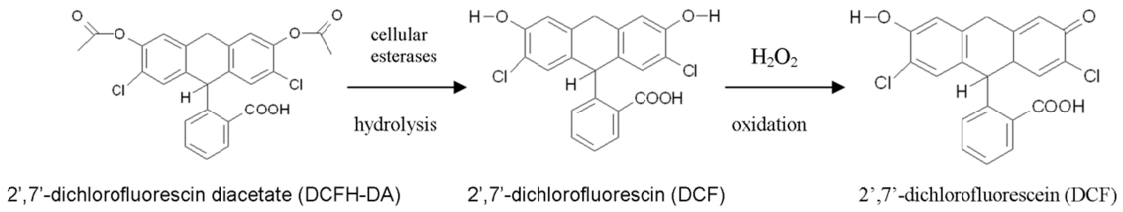

Figure 15. DCFH is oxidized in the presence of ROS to DCF and fluoreescence

After inoculation in a 24-well plate with C_{60}/THF, the cells were centrifuged to remove the supernatant and resuspended in 500 µL of 2.5 µM DCFH solution for 30 m at 37 °C. The cells were centrifuged to remove the dye and resuspended in phosphate buffer solution (PBS) for analysis with the flow cytometer.

6.2.1.2. Assessing Membrane Integrity.

To assess lethality, propidium iodide (PI, Molecular Probes, USA) fluoresces at 575 nm when it passes through the damaged nuclear membrane of dead cells and binds to nucleic acids. After inoculation with gradient concentrations of C_{60}/THF, the cells were resuspended in 500 µL of 5 µg/mL PI working solution for analysis with the flow cytometer.

6.3. Preparation of Cell Free Assays

6.3.1. Luminol

The luminol cell-free assay reacts with ROS impurities in solution to produce chemiluminescence (**Figure 16**).[85] A 10 mM luminol solution (3-aminophthalhydrazide, Sigma) in a 10 mM tris(hydroxymethyl)aminomethane buffer solution (pH=10, Sigma) was stirred for 1 h at room temperature until completely dissolved. The catalyst in this assay was optimized to 90 mM potassium ferricyanide (Sigma), which was prepared fresh daily. The reagents were added to a total volume of 100 μL in each well of a 96-well white opaque-plate, where luminol was added last.

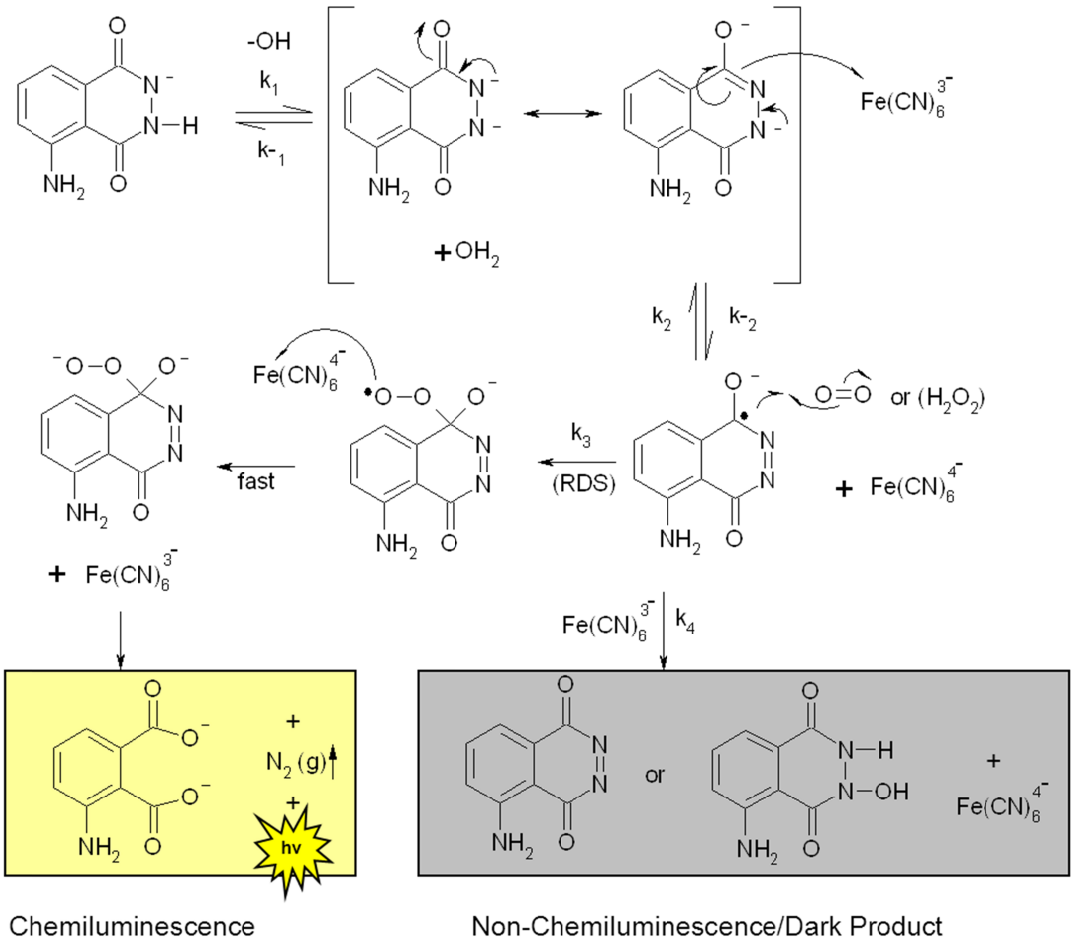

Figure 16. Reaction mechanism of the oxidation of luminol by an ROS to produce chemiluminescece.

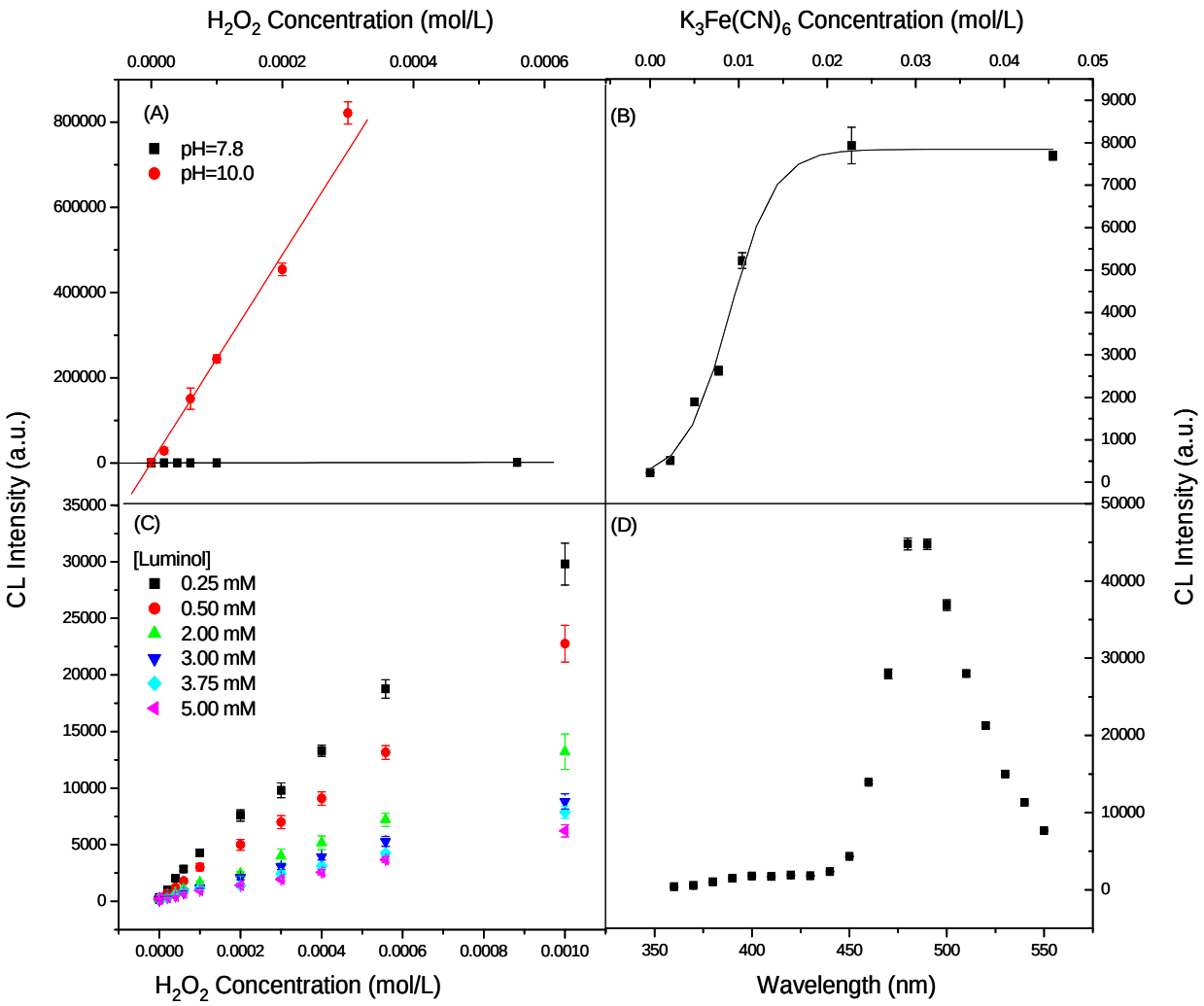

Figure 17. Parameter optimization on the lumino-H_2O_2 CL system. (A) Effects of hydrogen peroxide concentration and of the pH of assay: 0.50 mmol/L luminol, 0.03 mol/L $K_3Fe(CN)_6$, pH=7.8 and pH=10.0 (B) Effects of catalyst concentration: 3 X 10^{-3} mol/L luminol, 0.15 mol/L H_2O_2, (C) Concentration-response curve of luminol oxidation in the presence of H_2O_2.: 0.01 M $K_3Fe(CN)_6$ was held constant. (D) Optimal wavelength for emission of chemiluminescence is at 485 nm: 3 X 10^{-3} mol/L luminol, 0.03 mol/L $K_3Fe(CN)_6$, 0.15 mol/L H_2O_2.

ROS in solution oxidized the luminol instantly to produce chemiluminescence. This chemiluminescence was measured with a plate reader at 468 nm, at exactly 5 s after adding the luminol. A gradient concentration of chemical reference toxicant, hydrogen peroxide, was used to make a concentration-response curve.

6.3.2. Dichlorofluorescin

The DCFH-DA assay is versatile in that it can also be used as a *cell-free* assay with the addition of horse radish peroxidase. A 1 mM stock of 2'7'-dichlorofluorescin (DCFH, 4091-99-0, Sigma, US) was diluted into a working concentration of 40 μM in 0.01 N NaOH and kept in the dark at room temperature for 30 m before adding 10 mL of 25 mM phosphate buffer solution (PBS, pH=7.2). As a cell-free assay, 0.2 U/mL coenzyme, horse radish peroxidase (HRP, 9003-99-0, add 1.2 mg to 100 ml of PBS (pH=7.2), Sigma, USA), was added.

A gradient concentration of C_{60}/THF was introduced to the DCF assay in a 96-well black-with-clear-bottom plate to produce fluorescence that can be measured (ex/em 485 nm/520 nm) with a plate reader.

6.4. Statistical Analysis

Each experiment was repeated four times to obtain the average value expressed as percentage of the unexposed control $\pm$ standard of measure (SM). The LD_{50} value, which gives the lethal dose required for half of the cells to die, was

determined by calculating the percent viability of the cells. Control values were set as 100%. Statistical significant differences were set at $p < 0.05$.

Chapter 7

In vitro Toxicity of Fullerene Nanoaggregate: Differences in Sample Purity and UV-Irradiation

Highly purified C_{60} nanoaggregates by solvent exchange (C_{60}/THF) were found to be non-toxic when the impurities in solution were removed by a stir-cell. Even after UV-irradiated, C_{60}/THF remained non-toxic to HDF cells. The additional purification step with a stir-cell efficiently removed THF and autoxidized byproducts in solution and rendered this sample inert. Whereas, samples loaded with residual solvent THF served as the source for reactive oxygen specie (ROS) that caused the adverse effect and lethality in human dermal fibroblast (HDF) cells. The biocompatibility of C_{60}/THF was quantified using a number of commercially available assays to indirectly measure reactive oxygen species by absorbance, chemiluminescence, and fluorescence. In this paper, we propose a suite of *in vitro* and cell-free assays to test the biocompatibility of C_{60} nanoaggregates and other nanoengineered materials. Improvements in nanobiotoxicity

testing have prompted efforts to make C_{60} nanoaggregates and other nanoengineered materials safer.

7.1. Introduction

With its discovery, C_{60} in organic solvent showed unique chemical and photosensitizing properties that would soon prompt four creative techniques to disperse pristine C_{60} into water and to exploit for biological and medicinal applications. Four methods to disperse pristine C_{60} into water include: (1) functionalizing with polar groups, such as amines and hydroxyl groups (C_{60}-X); (2) encapsulating C_{60} within a surfactant or an amphiphilic polymer, such as polyvinyl pyrrolidone (C_{60}/PVP); (3) stirring rigorously for days until C_{60} forms enthalpically favorable aggregates in water (C_{60}/water); and, (4) using polar organic solvents, such as tetrahydrofuran (THF) and toluene, to phase transfer C_{60} into water (C_{60}/THF).[86,87] In this study, we used the latter method using an organic solvent, THF, in which both water and C_{60} are soluble. Then THF was evaporated to obtain nano-sized aggregated C_{60} dispersed in water (<10-200 nm).

For nanoC_{60} in water, fullerene toxicity in the literature is vast, and data inconsistent when the details are fragmented and other physical properties are incomplete (Table 6).[88] Briefly, depending on the dispersion method and surface coating, researchers have found that polymer-coated C_{60} nanoaggregates can be toxic and even photosensitized in water when coated with γ-cyclodextrin (γ-CyD/C_{60})[89-91] or polyvinyl pyrrolidone (PVP/C_{60}),[92-95] due to tendencies to form reactive oxygen species (ROS) at the particle surface when irradiated under ultraviolet light. ROS causes adverse effects and lethality by

malfunctioning membranes, splicing DNA, and disrupting peptide function by oxidative stress. In contrast, pristine C_{60} simply stirred for days are found to be nontoxic.

With solvent-exchange, researchers have reported C_{60}/THF nanoaggregates to be both toxic[96-102] and nontoxic[87,91,94,95,103-107]. Henry *et al.* in 2007, proposed that the nanoaggregated C_{60} from C_{60}/THF was not toxic but instead that *in vivo* toxicity stemmed from significant amounts of residual THF from the phase transfer solvent, instead.[97] Specifically, they described the easily formed byproducts from the autoxidation of THF, such as gamma-butyrolactone and peroxides that were even more toxic than the parent molecule (Figure 18). THF during production, rendered the sample to be safe.[97] The fundamental tendency of THF to autoxidize was first demonstrated by Hara *et.al,* who used headspace tandem gas-chromatography mass-spectroscopy (GC-MS), to identify these byproducts.[108]

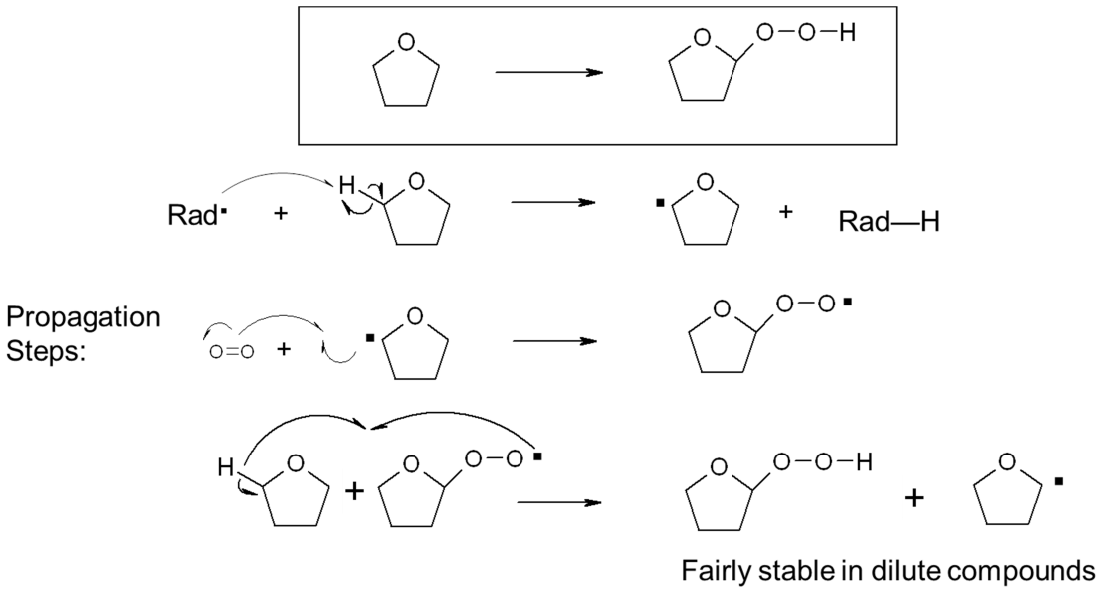

Figure 18. Autoxidation of THF into an ether peroxide, impurities and other ROS. Reprinted from *Advanced Organic Chemistry: Reaction Mechanisms* [99]

Table 6. Literature summary up to 2009 of observed biological effects by different aqueous fullerene systems and nano-aggregates.

Fullerene System		Photosensitized	ROS	Biological System	Biological Effect	Ref.
Derivatized	C_{60}-Malonic acid (C_n)	No	None	Liposomes, mammalian cells, Swiss mice	Nontoxic: anti-apoptotic; antioxidant; neuro-protection; liver-protective	107, 110, 111, 103, , ,
	C_{60}-OH_n (n=22-26)	No	None	Mammalian cells, Liposomes, *Escherichia coli*	Nontoxic: antioxidant; prevents lipid peroxidation	107, 112, 113, 114, 104, ,
	C_{60}-OH_n (n=22-26)	15-W lamp (310-400 nm)	$^1O_2$, $O_2^{\bullet-}$	Mammalian cells, *Escherichia coli*	Toxic*: viral inactivation; antibacterial	112, 115, , 105, 94, , 91
Polymer-coated	γ-CyD/C_{60}	Laser photolysis (532 nm)	$^1O_2$, $O_2^{\bullet-}$	Plasmid DNA	Toxic*: DNA-cleavage, mammalian cells	89, 90, 91
	PVP/C_{60}	4-W, 15-W lamp (365 nm)	$^1O_2$, $O_2^{\bullet-}$ $HO^{\bullet}$	*Escherichia coli*, *Baciullus subtilis*, plasmid DNA	Toxic*: antibacterial, DNA-cleavage	92, , 93, 95, 94
Solvent-exchanged (uncoated)	THF/C_{60}	No	None	Mammalian cells, *Escherichia coli*, *Daphnia magna*	Nontoxic‡: antioxidant; no cell death	107, 87, 104, 106, , , 90, Table 7
	THF/C_{60}	4-W, 15-W lamp (350-400 nm)	None	Mammalian cells	Nontoxic	105, 95, 94, 90, Table 7
	THF/C_{60}	No	Peroxides	Mammalian cells, largemouth bass	Toxic**: acute; ROS production causes lipid peroxidation, protein oxidation	101, 100, 102, 96, , , 97, 99
	THF/C_{60}	No	None	*Escherichia coli*, *Baciullus subtilis*	Toxic (oxidant): via chemical interaction, ROS-independent oxidative stress	116,
	THF/C_{60}	14-W lamp (310-400 nm), 30 h	None	*Escherichia coli*, *Baciullus subtilis*	Toxic (oxidant): via ROS-independent oxidative stress	117
	Toluene/C_{60}	No	None	Liposomes	Nontoxic: antioxidant; prevents lipid peroxidation	107
	Alcohol/C_{60}	40-W light; no UV	None	Bacterium	Nontoxic: lacks genotoxicity effects	118
Sonicated and/or Stirred	aq/C_{60}	No	None	Mammalian cells, Zebrafish	Nontoxic	99, 104, 97, , , 94, 90
	aq/C_{60}	4-W lamp, 9-W lamp, 15-W (~365 nm)	None	Mammalian cells, *Escherichia coli*	Nontoxic	115, 119, 95, 114, , , 90

Toxic: only in the presence of reducing agent, NADH; Toxic**: nC_{60}/THF system lack extra washing step with stir-cell to remove residual THF; Nontoxic‡: nC60/THF system with extra washing step with stir-cell to remove residual THF; PVP-C_{60} polyvinylpyrrolidone-coated C_{60}; γ-CyD: gamma cyclodextrin-bicapped C_{60}

Furthermore, when Arbogast, et al., discussed the photophysical properties of the hydrophobic form of C_{60} and showed the excitation of its double bonds in organic solvent,[120] the photosensitization of a carbaceous molecule prompted vast efforts to replicate this phenomenon in a aqueous solvent for many medicinal applications. Yet, it has been reported that when pristine C_{60} begins to aggregate in the presence of water, the aggregate are no longer photosensitized. Two theories have been published, including that quenching occurs because of the proximity of neighboring molecular cages in an aggregate,[115,121] and that the UV-irradiation process itself causes the photodegradation of the molecule C_{60}. [95] Still, researchers have found that only polymer-encapsulated C_{60} water-stable systems (γ-CyD/C_{60} and PVP/C_{60}) can function as an acceptor photodopant when embedded into a conducting polymer matrix[122] and can be photosensitized in aqueous solvents when irradiated by UV energy.[123]

In this study, the toxicity of C_{60} nanoaggregate by solvent exchange (C_{60}/THF) was compared to hydrogen peroxide and to the photocatalytic nanomaterial, TiO_2, to support and validate the final result that C_{60} nanoaggregates are neither cytotoxic nor photosensitized. The results from this research also further supports the finding and conclusions of Arbogas,[120] that the unique photochemical and nanobiotoxicity properties of hydrophobic C_{60} are not retained once it is made soluble in water. Ultimately in this paper, the results from a variety of assays may elucidate how system preparation, surface chemistry and soluble impurities may affect biocompatibility and toxicity.

7.2. Experimental Method

7.2.1. C_{60} Nanoaggregate Preparation and Characterization

Pristine C_{60} nanoparticles were water-dispersed by forming crystalline aggregates in tetrahydrofuran (THF), following Deguchi's solvent-exchange method.[86] The final aqueous solution (C_{60}/THF) was filtered through a 0.22 μm cellulose acetate filter, sparged with argon, and stirred overnight to yield a working C_{60} nanoaggregate suspension. C_{60} concentrations range from 0 to 6.5 mg/L. Fullerene concentration in these experiments is measured by the absorption spectra of isolated C_{60} extracted back into toluene from its aqueous aggregate form.

Samples of different purities were prepared. One sample of C_{60} water-dispersed solutions (99.9%, MER Corp., Tucson, AZ) included an additional purification step to remove impurities from THF autoxidation (purified) using a stirred-cell membrane unit (Amicon, 10,000 MW cutoff, 10 psi N2 UHP) for 6 hours to remove >99% of the residual solvent.[124] For comparison, all samples were analyzed before (unpurified) and after (purified) purification by a stir-cell. Both samples were further characterized by instrumental analysis for size distribution and sample quality. The diameters of the nanoparticles were sized by transmission electron microscopy (200 kV, JEOL 2010 FasTEM, JEOL, USA) where 30 μL was dropped onto a 300-mesh copper carbon grid (Ted Pella, USA). To measure the hydrodynamic diameter and zeta potential of the nanoparticles in solution, dynamic and phase analysis light scattering (Malvern Zetasizer Nano-ZS), were used.[54,58,125] Purity was determined by gas chromatograph mass spectroscopy (GC-MS, Agilent

Technologies, USA) equipped with a headspace sampler (Agilent G1888).[108,126] Also samples were irradiated with UV light (λ=365 nm) from a hand-held UV lamp in order to study the photosensitization and their adverse effects *in vitro*.

7.2.2. Reference Toxicant Preparation

In this study, the reference nanoparticle toxicant was TiO2 (P25, Degussa), a photocatalyst. A 1 mg/mL solution of titania nanoparticle was sonicated for 3 m and stirred for 1 h for thorough dispersion in water. Gradient concentrations of hydrogen peroxide (30% H2O2, Sigma), a chemical reference toxicant, was prepared fresh daily.

7.3. Results and Discussion

7.3.1. C_{60} nanoaggregate Characterization and Purification

Sample preparation and characterization is central for nanotoxicity studies. Towards this end, C_{60}/THF nanoaggregates were prepared by solvent-exchange using THF to produce colloidally stable C_{60}/THF nanoaggregates in biologically relevant aqueous conditions. TEM imaging revealed crystalline C_{60} nanoaggregates with less than 100 nm core diameter (Figure 19). Headspace gas chromatography coupled with mass spectroscopy (GC-MS) measured highly volatile impurities in the samples following Hara's method; 99.1% of impurities were removed using a stir-cell (Figure 19).[108,126,124]

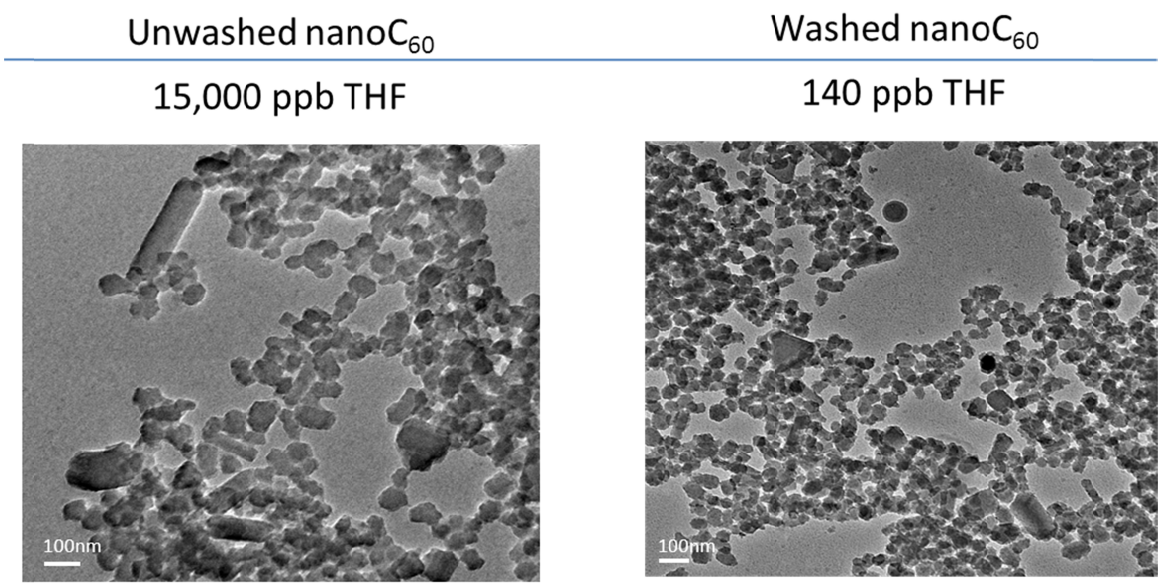

Figure 19. (A) Unpurified sample was not washed to remove THF and impurities; and (B) purified sample after 4 washes in a stir-cell significantly, which removed THF residue concentrations as measured by GC-MS. TEM images of nanoC60 aggregates in water (86.80 ± 36.2 nm) cast on carbon coated films and imaged at 100 k .Scale bars: 100 nm

7.3.2. Suite of Assays

Because of the evident presence of autoxidized byproducts, unpurified C_{60}/THF samples caused adverse effect by forming reactive oxygen species (ROS) and causing cellular death, which also increased after UV irradiation (**Table 7**). Researchers have published that UV irradiation of C_{60}/THF produces ROS. Here, C_{60}/THF samples were irradiated to produce ROS that was quantified indirectly using a suite of *in vitro* and cell-free assays. ROS can cause adverse effects *in vitro* and using a suite of assays to indirectly measure three byproducts: absorbance,

chemiluminescence and fluorescence, differences between purified and unpurified samples were quantified. Results from the purified C_{60}/THF solution showed a significantly different toxicity result when added to human dermal fibroblasts (HDF) cells; these *in vitro* results were further corroborated by cell-free assays. Additional testing of the effects when the particles are also UV-irradiated is important as particles may have photochemical properties as well.

Table 7. Summary of observed biological effects by different fullerene systems.

C_{60} nanoaggregates	Purified		Unpurified	
In-Vitro (LD_{50})	DARK	UV	DARK	UV
MTS	Non-toxic		1.8 ppm	1.3 ppm
Calcein AM	Non-toxic		1.6 ppm	1.1 ppm
PI	Non-toxic		1.6 ppm	2.0 ppm
DCF	Non-toxic		2.1 ppm	1.3 ppm
Cell-free	DARK	UV	DARK	UV
Luminol	-	-	+	+
DCF	-	-	+	+

7.3.3. In vitro assays

Specifically, the *in vitro* assays included both the standard tetrazolium-based assay (MTS) and the calcein AM assay to measure cell viability, and both the propidium iodide (PI) and the dichlorofluorescein (DCF) assay to measure cell death. But first, the commercially available Live/Dead Kit was first used to image the impact of cell viability by fluorescence and then to quantify cell viability (Figure 20).

The Live/Dead assay qualitatively showed that purified C_{60}/THF nanoaggregates were not toxic and fluoresced green; whereas, nanoaggregates prepared without the purification step (Figure 20), caused cellular death and fluoresced red. After UV irradiation, the purified fullerene solutions behaved similarly with no photosensitization and no toxicity. Differences in these samples derived from the presence of toxic residual THF solvent and byproducts in unpurified samples. The Live/Dead assay kit (Molecular Probe, USA) enabled us to quickly visualize the lethality of C_{60}/THF before and after purification. Using fluorescence microscopy, the cells were examined after a 24 hour exposure. In this assay, acetoxymethyl ester enters the cells and is cleaved by esterases in live cells to yield calcein, producing a green fluorescence. Also in this kit, dead cells were permeable to ethidium homodimer-1, which passed through damaged nuclear membranes and bonded to the nucleic acids, causing dead cells to fluoresce red.

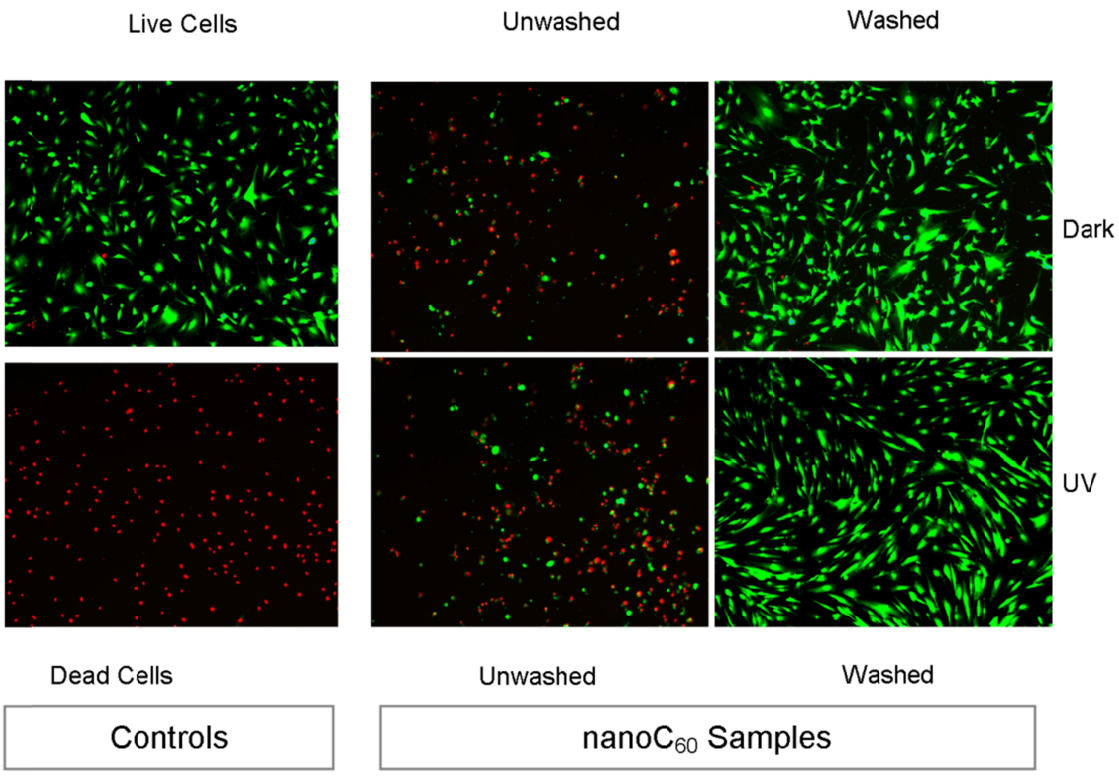

Figure 20. Live/Dead assay. Fluorescence is the indicator that differentiates between live and dead cells. Here, the purified samples fluoresce green, even after irradiation with UV light.

The MTS assay, mitochondrial activity of cells inoculated with purified C_{60}/THF nanoaggregates for 24 hours sustained colorimetric product when compared to untreated sample, even when irradiated by UV light (Figure 21). In contrast, unpurified sample gave an LD_{50} value of 1.46 mg/L, which indicates significant damage to the mitochondria and to cellular function. When irradiated, unpurified C_{60}/THF nanoaggregates gave an LD_{50} =1.32 mg/L. After purification, C_{60}/THF nanoaggregates at 1-5 mg/L were rendered non-toxic and had no impact on mitochondrial activity when compared to untreated cells. Whereas, samples of poorer quality caused a decrease in mitochondrial activity as sample concentration increased (Figure 21). The MTS assay is a colorimetric assay (468 nm) that measures the mitochondrial activity of viable cells. Only viable cells will produce the water soluble crystalline, purple formazan by mitochondrial oxidation.

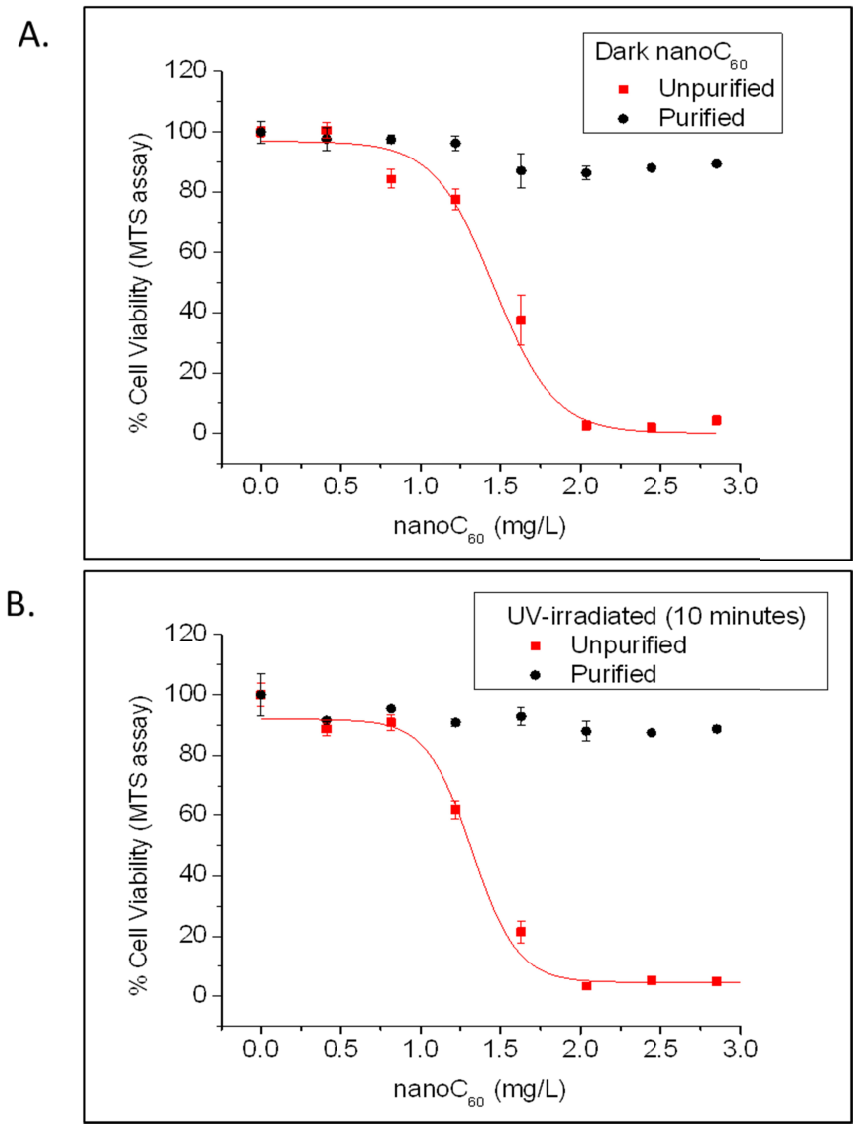

Figure 21. MTS assay. Dose-dependent effects of $nanoC_{60}$ aggregates at different concentrations (from 0.01–3.0 mg/L) on HDF cell growth for 24 hours. Data are percentage of cell viability $\pm$ SD from four independent experiments. A) Sterile $nanoC_{60}$ aggregates were introduced to the cells. B) Sterile $nanoC_{60}$ aggregates were irradiated with a UV-light for ten minutes and introduced to the cells. No change in effect from UV-irradiation was noted.

As with the MTS assay, the calcein AM assay showed the same outcome that purified C_{60}/THF sample were non-toxic and caused no cellular death, even when irradiated (**Figure 22**). But, unpurified samples were tested *in vitro* with a consequence of cellular death at higher concentrations (LD_{50}=1.62 mg/L). When irradiated with UV for 10 minutes, the unpurified sample gave an LD_{50} value of 1.13 mg/L (**Figure 22**). This second lethality assay, calcein AM, fluoresced green (ex/em 485 nm/530 nm) as calcein was hydrolyzed by intracellular esterases in live cells; but in dead cells, the dye leaked through the damaged membrane. Two additional *in-vitro* assays that measures fluorescence using a flow cytometer was used to measure toxicity.

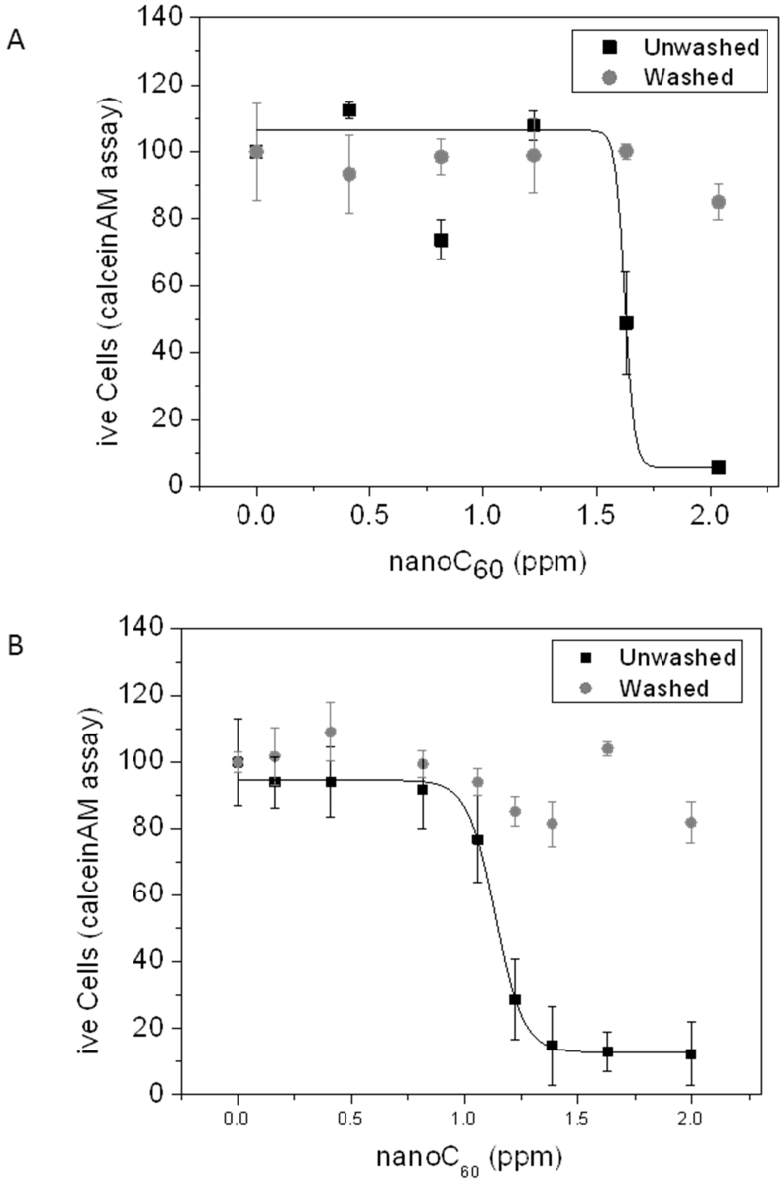

Figure 22. Calcein AM assay. Dose-dependency effects of nanoC_{60} aggregates (aq) at different concentrations (from 0.01–3.0 ppm) on the cell growth of human dermal fibroblast cells for 24 hours without UV (A) and with 10 minutes of UV irradiation (B). Percentage of cell viability was determined by the calcein-acetyoxymethyl assay. Data are means $\pm$ S.D. from four independent experiments.

A total of five *in vitro* assays showed similar results (Figure 23**Error! Reference source not found.**) where unwashed samples caused cellular toxicity with similar LD50 values and washed samples had no lethal oxidative activity to cells. Propodium iodide (PI) and 2'7'-dichlorofluorescin diacetate (DCFH-DA) both corroborated previous results (Table 7). After a 24 hr exposure, the purified samples caused no adverse effect when compared with untreated HDF cells, even when irradiated (Table 7); but unpurified samples caused cellular death by ROS (Figure 23). Both assays measured the probability of cellular death by two different mechanisms.

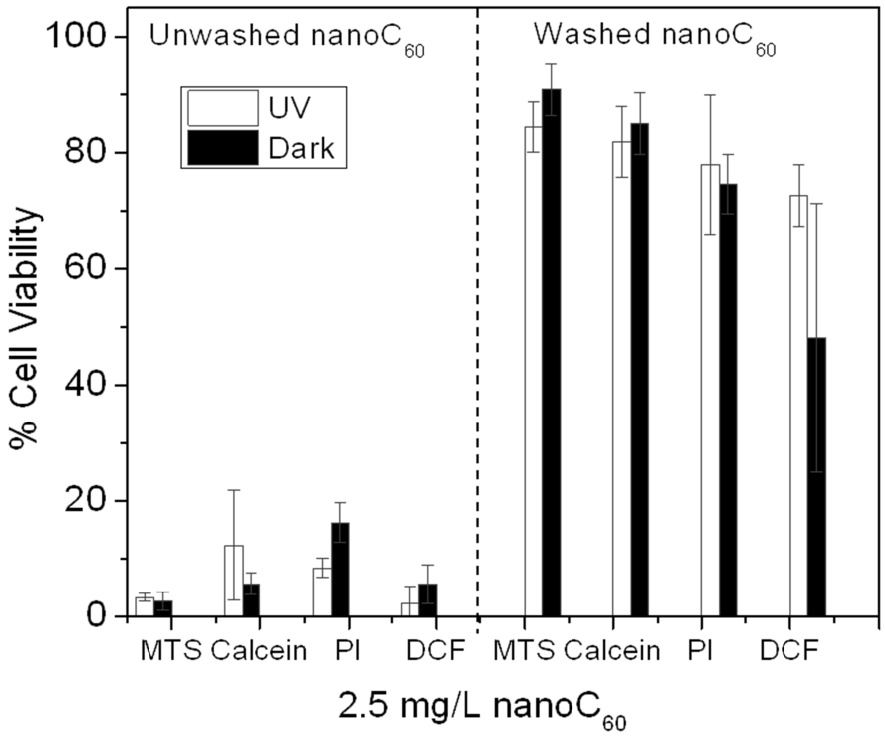

Figure 23. Using five different in-vitro assay to test the differences between purified and unpurified samples of 2.5 mg/L C_{60} nanoaggregates in water. (A) LD_{50} values for

parameters testing unwashed (left) vs. washed (right) nanoC_{60} samples of UV-irradiated (white bars) or dark (black bars) samples.

7.3.4. Cell-free assays

In the same way after a 24 hr exposure, the versatile DCFH-DA assay showed that unpurified samples produced fluorescence. Whereas, in the absence of THF-peroxides, purified samples caused no fluorescence and was non-toxic (Figure 24). This implies that in the absence of THF autoxidation byproducts, as described by Henry *et al.*,[97] the assay was not oxidized to form a fluorescing product in both the *in-vivo* and *cell-free* study (Figure 24). A second cell-free assay uniquely chemiluminesced after oxidation by ROS.

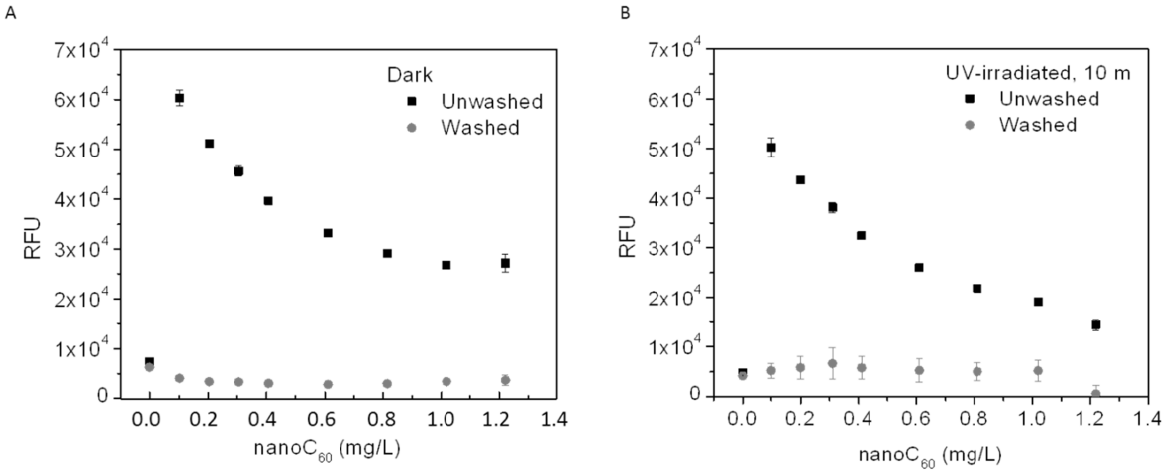

Figure 24. Concentration-response curve of the enzyme-catalyzed Dichlorofluorescin diacetate (DCFH) fluorescence in the presence of nanoC_{60} aggregates. (A) A positive linear trend with an increase of a reactive oxygen specie that oxidizes the DCFH-DA into DCFH is evident with unwashed samples, whereas fluorescence is not evident with washed samples. (B) The results remain the same after irradiating samples for 10 minutes

with UV. The curve becomes saturated at low concentrations because the HRP is saturated and destroyed with great amounts of peroxides and ROS found in solution of unwashed samples. Further optimization is not possible as this biological enzyme is not effective at high concentrations of ROS.

As expected, the luminol assay showed that C_{60}/THF nanoaggregates themselves do not produce ROS, even when irradiated with UV (Figure 25). When both purified and unpurified samples were irradiated with UV energy, only the unpurified samples provided the ROS needed to react with the luminol assay to produce quantitative amounts of chemiluminescence. That is, as the concentration of unpurified C_{60}/THF sample increased, chemiluminescence also increased in a linear direct relationship. Luminol chemiluminesces when oxidized by any peroxide (H_2O_2) or ROS in the presence of an iron catalyst.

Lastly, over than span of more than 3 years (100 weeks), unpurified samples from THF degradents (ether peroxides and ROS) increasingly oxidized luminol to produce chemiluminesce over time (Figure 26A). Whereas, samples that had residual THF initially removed with a stir-cell, produced no THF degradent to oxidize luminol, even after 17 months (Figure 26B). Therefore, we conclude that toxicity in prior studies[96-102] were a result of THF degradents and not C60 nor residual THF, but that caused oxidative stress to HDF cells.

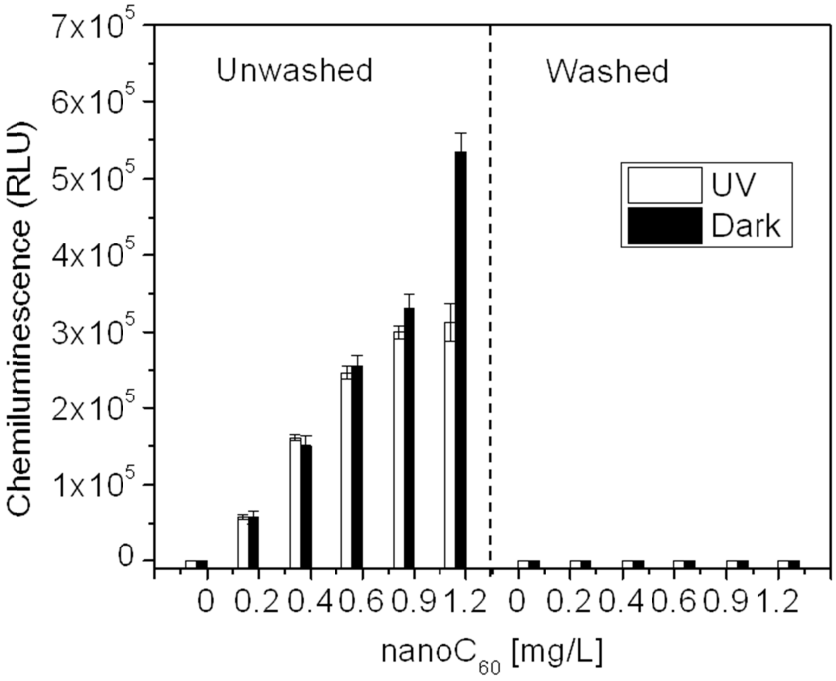

Figure 25. Concentration-response curve of Luminol oxidation in the presence Chemiluminescence was used to detect differences between two samples of purified and unpurifed C_{60}. A positive linear trend with an increase of reactive oxygen specie (ROS) that oxidized the luminol for unpurified samples (left, black bars), whereas chemiluminescence is not evident with washed samples (right, black bars). The results remain the same after irradiating samples for 10 minutes with UV (white bars). Because of the ROS impurities, unwashed samples becomes lethal with and without UV-irradiation.

The Luminol and $K_3Fe(CN)_6$ concentration were held constant at 0.50 mmol/L and 0.03 mol/L, respectively, at pH=10. The data was obtained from four independent experiment and are expressed as the mean $\pm$ SM. Chemiluminescence measurements are reported after five seconds (λ_{EM}=485 nm). The absence of an *error bar* indicates the error is not visible within the symbol.

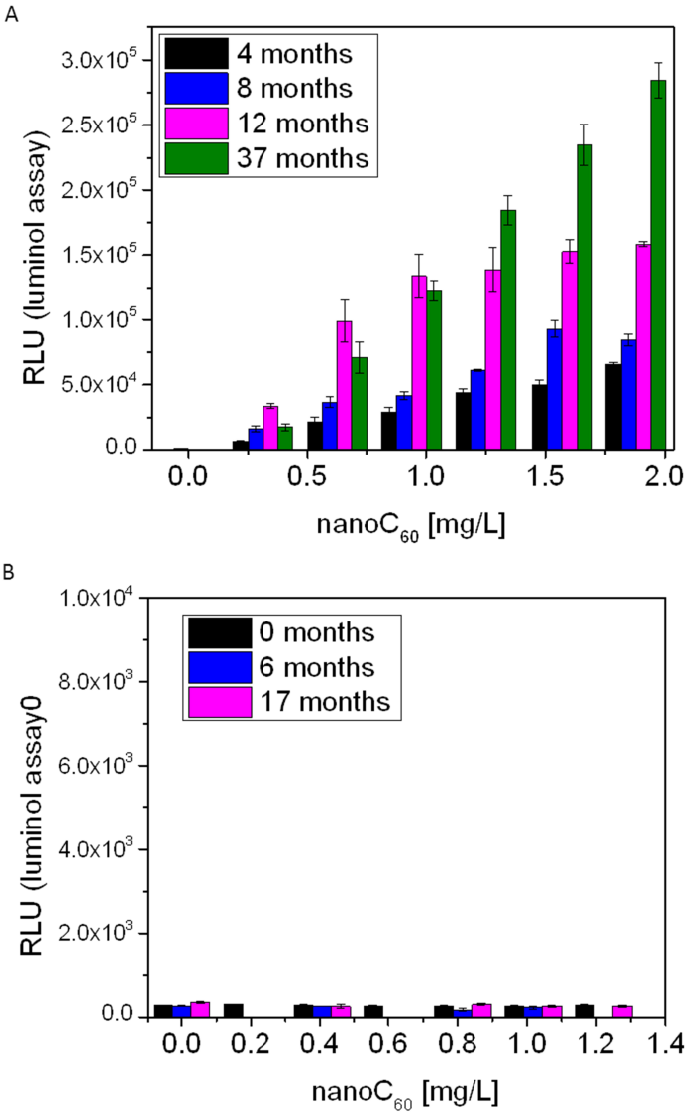

Figure 26. Concentration-response analysis of luminol oxidation in the presence of unwashed (A) and washed (B) nanoC_{60} aggregates over the span of a year, at pH=10.0. A positive linear trend with an increase of a reactive oxygen specie that oxidizes the luminol is evident with unwashed samples over the span of 162 weeks, (or 3 years, 1 month, 14 days). The Luminol and $K_3Fe(CN)_6$ concentration was held constant at 0.50 mmol/L and 0.03 mol/L, respectively.

The data was obtained from four independent experiment and are expressed as the mean $\pm$ SM. Chemiluminescence measurements are reported after five seconds (λ_{EM}=485 nm). The absence of an *error bar* indicates the error is not visible within the symbol.

7.3.5. UV irradiation of Photocatalytic nanoTiO_2

The luminol-hydrogen peroxide reaction gave a concentration-dependent control curve to quantitatively measure ROS in solution. In addition, UV irradiation also converted peroxides into hydroxyl radicals, to produce chemiluminescence. In this paper, the nanoparticle titania that photocatalytically produces ROS, was irradiated with UV-light as a reference toxicant.

The luminol-titania reaction produced chemiluminescence only upon irradiation; as with the luminol assay, MTS assay showed an increase in ROS from UV irradiation of titania that became lethal to HDF cells (**Figure 27**). Unlike C_{60}/THF nanoaggregate after UV-irradiation, titania produced ROS to oxidize luminol and to increase chemiluminesces as UV irradiation time increased, increasing ROS concentration in solution. The fact that TiO_2 can produce ROS upon irradiation by UV-energy prompted a study of the lethality effects from exposure of photosensitized nano TiO_2 and to compare to cells inoculated with C_{60}/THF. Titania was irradiated to form hydroxyl radicals at the surface and peroxides in solution.

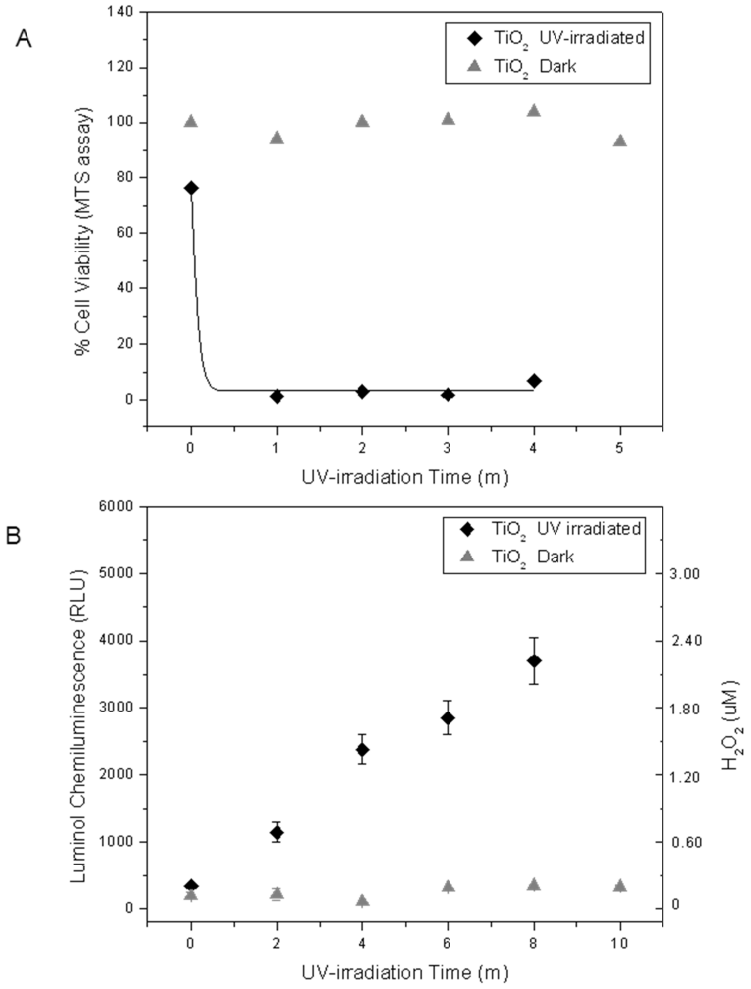

Figure 27. Comparison experiments with TiO_2 (P_{25}). The 1 ($^{g}/_{L}$) TiO_2 water suspension was successfully irradiated to produce reactive oxygen species (ROS) and peroxides. (A) Graph shows the effect of UV-irradiation time of TiO_2 particle on human dermal fibroblast cell proliferation as determined by the MTS assay after 24 hours. Viability is expressed as a percentage of control (untreated) cells. TiO_2 irradiated for <1 minute had fatal effects on the cells. (B) As the time of irradiation increases, the TiO_2 suspension produced an increasing amount of ROS that increases the chemiluminescence (λ_{EM}=485 nm).

7.4. Conclusion

In conclusion, we recently demonstrated a method by solvent-exchange to produce non-toxic C_{60} nanoaggregate (C_{60}/THF) using an additional purification step with a stir-cell to remove the THF autoxidized byproducts in solution. This resulted in C_{60} nanoaggregates (C_{60}/THF) that was non-toxic. C_{60}/THF nanoaggregate samples were also irradiated with UV-energy and remained non-toxic to HDF cells. We chose assays that measured indirectly lethality and ROS by quantifying absorbance, chemiluminescence, and fluorescence. Positive controls included samples loaded with residual solvent THF to indirectly quantify the adverse effect and lethality in HDF cells also using the same suite of assays, both *in vitro* and cell-free. These assays verified the presence of impurities and prompted additional measures with a stir-cell to make the nanomaterial safe by removing toxic impurities in solution.

References

(1) Nanoscience and nanotechnologies: opportunities and uncertainties. *Royal Society* [Online Early Access]. Published Online: 2004.

(2) Benn, T. M.; Westerhoff, P. *Environ. Sci. Technol.* **2008**, *42*, 4133.

(3) Roh, J.-y.; Sim, S. J.; Yi, J.; Park, K.; Chung, K. H.; Ryu, D.-y.; Choi, J. *Environ. Sci. Technol.* **2009**, *43*, 3933.

(4) Sutphin, G. L.; Kaeberlein, M. *The Journal of Visualized Experiments* **2009**, e1152.

(5) Boyd, W. A.; McBride, S. J.; Rice, J. R.; Snyder, D. W.; Freedman, J. H. *Toxicol. Appl. Pharmacol.* **2010**, *245*, 153.

(6) Kim, J.; Shirasawa, T.; Miyamoto, Y. *Biomaterials* **2010**, *31*, 5849.

(7) Kim, J.; Takahashi, M.; Shimizu, T.; Shirasawa, T.; Kajita, M.; Kanayama, A.; Miyamoto, Y. *Annals of Nutrition and Metabolism* **2008**, *53*, 4.

(8) Kim, J.; Takahashi, M.; Shimizu, T.; Shirasawa, T.; Kajita, M.; Kanayama, A.; Miyamoto, Y. *Mechanisms of Ageing and Development* **2008**, *129*, 322.

(9) Sakaue, Y.; Kim, J.; Miyamoto, Y. *International Journal of Nanomedicine* **2010**, *5*, 687.

(10) Höss, S.; Jänsch, S.; Moser, T.; Junker, T.; Römbke, J. *Ecotoxicol. Environ. Saf.* **2009**, *72*, 1811.

(11) Kim, S. W.; Nam, S.-H.; An, Y.-J. *Ecotoxicol. Environ. Saf.* **2012**, *77*, 64.

(12) Pluskota, A.; Horzowski, E.; Bossinger, O.; von Mikecz, A. *PLoS One* **2009**, *4*, e6622.

(13) Cronin, C.; Mendel, J.; Mukhtar, S.; Kim, Y.-M.; Stirbl, R.; Bruck, J.; Sternberg, P. *BMC Genetics* **2005**, *6*, 5.

(14) Johnstone, I. L. *Trends Genet.* **2000**, *16*, 21.

(15) Myllyharju, J.; Kivirikko, K. I. *Trends Genet.* **2004**, *20*, 33.

(16) Dhawan, R.; Dusenbery, D. B.; Williams, P. L. *Journal of Toxicology and Environmental Health, Part A: Current Issues* **1999**, *58*, 451.

(17) Brenner, S. *Genetics* **1974**, *77*, 71

(18) Meyer, J. N.; Lord, C. A.; Yang, X. Y.; Turner, E. A.; Badireddy, A. R.; Marinakos, S. M.; Chilkoti, A.; Wiesner, M. R.; Auffan, M. *Aquat. Toxicol.* **2010**, *100*, 140.

(19) Yang, X.; Gondikas, A. P.; Marinakos, S. M.; Auffan, M.; Liu, J.; Hsu-Kim, H.; Meyer, J. N. *Environ. Sci. Technol.* **2011**, *46*, 1119.

(20) Ma, H. B.; Bertsch, P. M.; Glenn, T. C.; Kabengi, N. J.; Williams, P. L. *Environ. Toxicol. Chem.* **2009**, *28*, 1324.

(21) Swain, S. C.; Keusekotten, K.; Baumeister, R.; Stürzenbaum, S. R. *J. Mol. Biol.* **2004**, *341*, 951.

(22) Wang, H.; Joseph, J. A. *Free Radical Biol. Med.* **1999**, *27*, 612.

(23) Valembois, P.; Seymour, J.; Lassègues, M. *Cell Tissue Res.* **1994**, *277*, 183.

(24) Zhang, H. F.; He, X. A.; Zhang, Z. Y.; Zhang, P.; Li, Y. Y.; Ma, Y. H.; Kuang, Y. S.; Zhao, Y. L.; Chai, Z. F. *Environ. Sci. Technol.* **2011**, *45*, 3725.

(25) Tsyusko, O. V.; Unrine, J. M.; Spurgeon, D.; Blalock, E.; Starnes, D.; Tseng, M.; Joice, G.; Bertsch, P. M. *Environ. Sci. Technol.* **2012**, *46*, 4115.

(26) Ellegaard-Jensen, L.; Jensen, K. A.; Johansen, A. *Ecotoxicol. Environ. Saf.* **2012**, *80*, 216.

(27) Lim, D.; Roh, J.-y.; Eom, H.-j.; Choi, J.-Y.; Hyun, J.; Choi, J. *Environ. Toxicol. Chem.* **2012**, *31*, 585.

(28) Bar-Ilan, O.; Albrecht, R. M.; Fako, V. E.; Furgeson, D. Y. *Small* **2009**, *5*, 1897.

(29) Wu, S.; Lu, J. H.; Rui, Q.; Yu, S. H.; Cai, T.; Wang, D. Y. *Environ. Toxicol. Pharmacol.* **2011**, *31*, 179.

(30) Li, Y.; Yu, S.; Wu, Q.; Tang, M.; Pu, Y.; Wang, D. *J. Hazard. Mater.* **2012**, *219–220*, 221.

(31) Wang, H. H.; Wick, R. L.; Xing, B. S. *Environ. Pollut.* **2009**, *157*, 1171.

(32) Roh, J.-Y.; Park, Y.-K.; Park, K.; Choi, J. *Environ. Toxicol. Pharmacol.* **2010**, *29*, 167.

(33) Lock, K.; Janssen, C. R. *Environ. Pollut.* **2002**, *117*, 89.

(34) Reinecke, S. A.; Prinsloo, M. W.; Reinecke, A. J. *Ecotoxicol. Environ. Saf.* **1999**, *42*, 75.

(35) Spurgeon, D. J.; Hopkin, S. P. *Environ. Pollut.* **2000**, *109*, 193.

(36) Gao, Y.; Liu, N. Q.; Chen, C. Y.; Luo, Y. F.; Li, Y. F.; Zhang, Z. Y.; Zhao, Y. L.; Zhao, B. L.; Iida, A.; Chai, Z. F. *J. Anal. At. Spectrom.* **2008**, *23*, 1121.

(37) Mohan, N.; Chen, C.-S.; Hsieh, H.-H.; Wu, Y.-C.; Chang, H.-C. *Nano Lett.* **2010**, *10*, 3692.

(38) Zanni, E.; De Bellis, G.; Bracciale, M. P.; Broggi, A.; Santarelli, M. L.; Sarto, M. S.; Palleschi, C.; Uccelletti, D. *Nano Lett.* **2012**, *12*, 2740.

(39) Sonkar, S. K.; Ghosh, M.; Roy, M.; Begum, A.; Sarkar, S. *Materials Express* **2012**, *2*, 105.

(40) Stiernagle, T. *The C. elegans Research Community, WormBook* **2006**, doi/10.1895/wormbook.1.101.1.

(41) López, E.; Figueroa, S.; Oset-Gasque, M. J.; González, M. P. *Br. J. Pharmacol.* **2003**, *138*, 901.

(42) Choi, J. Y.; Lee, S. H.; Bin Na, H.; An, K.; Hyeon, T.; Seo, T. S. *Bioprocess Biosyst. Eng.* **2010**, *33*, 21.

(43) Sohaebuddin, S. K.; Thevenot, P. T.; Baker, D.; Eaton, J. W.; Tang, L. P. *Particle and Fibre Toxicology* **2010**, *7*.

(44) Wright, P. L. *Environ. Health Perspect.* **1978**, *24*.

(45) Brennan, S. J.; Brougham, C. A.; Roche, J. J.; Fogarty, A. M. *Chemosphere* **2006**, *64*, 49.

(46) Clubbs, R. L.; Brooks, B. W. *Ecotoxicol. Environ. Saf.* **2007**, *67*, 385.

(47) Muyssen, B. T. A.; Janssen, C. R. *Environ. Toxicol. Chem.* **2001**, *20*, 2053.

(48) Tominaga, N.; Kohra, S.; Iguchi, T.; Arizono, K. *Journal of Health Science* **2003**, *49*, 459.

(49) Kirchner, C.; Javier, A.; Susha, A.; Rogach, A.; Kreft, O.; Sukhorukov, G.; Parak, W. *Talanta* **2005**, *67*, 486

(50) Mahendra, S.; Zhu, H.; Colvin, V. L.; Alvarez, P. J. *Environ. Sci. Technol.* **2008**, *42*, 9424.

(51) Ryman-Rasmussen, J.; Riviere, J.; Monteiro-Riviere, N. *J. Invest. Dermatol.* **2007**, *127*, 143

(52) Pelley, J. L.; Daar, A. S.; Saner, M. A. *Toxicol. Sci.* **2009**, *112*, 276.

(53) Barrett, K. A.; McBride, M. B. *Soil Sci. Soc. Am. J.* **2007**, *71*, 322.

(54) Zhu, H. G.; Prakash, A.; Benoit, D. N.; Jones, C. J.; Colvin, V. L. *Nanotechnology* **2010**, *21*, 255604.

(55) Hauck, T. S.; Anderson, R. E.; Fischer, H. C.; Newbigging, S.; Chan, W. C. W. *Small* **2010**, *6*, 138.

(56) Zhang, Y. B.; Chen, W.; Zhang, J.; Liu, J.; Chen, G. P.; Pope, C. *J. Nanosci. Nanotechnol.* **2007**, *7*, 497.

(57) Lewinski, N. A.; Zhu, H.; Jo, H.-J.; Pham, D.; Kamath, R. R.; Ouyang, C. R.; Vulpe, C. D.; Colvin, V. L.; Drezek, R. A. *Environ. Sci. Technol.* **2010**, *44*, 1841.

(58) Yu, W. W.; Chang, E.; Falkner, J. C.; Zhang, J.; Al-Somali, A. M.; Sayes, C. M.; Johns, J.; Drezek, R.; Colvin, V. L. *J. Am. Chem. Soc.* **2007**, *129*, 2871.

(59) Shaham, S., *ed. The C. elegans Research Community, WormBook* **2006**, doi/10.1895/wormbook.1.49.1.

(60) Balbus, J. M.; Maynard, A. D.; Colvin, V. L.; Castranova, V.; Daston, G. P.; Denison, R. A.; Dreher, K. L.; Goering, P. L.; Goldberg, A. M.; Kulinowski, K. M.; Monteiro-Riviere, N. A.; Oberdorster, G.; Omenn, G. S.; Pinkerton, K. E.; Ramos, K. S.; Rest, K. M.; Sass, J. B.; Silbergeld, E. K.; Wong, B. A. *Environ. Health Perspect.* **2007**, *115*, 1654.

(61) Colvin, V. L. *Nat. Biotechnol.* **2003**, *21*, 1166.

(62) Navarro, E.; Baun, A.; Behra, R.; Hartmann, N. B.; Filser, J.; Miao, A. J.; Quigg, A.; Santschi, P. H.; Sigg, L. *Ecotoxicology* **2008**, *17*, 372.

(63) Boyd, W. A.; Cole, R. D.; Anderson, G. L.; Williams, P. L. *Environ. Toxicol. Chem.* **2003**, *22*, 3049.

(64) Bodar, C. W. M.; van der Sluis, I.; van Montfort, J. C. P.; Voogt, P. A.; Zandee, D. I. *Aquat. Toxicol.* **1990**, *16*, 33.

(65) de Livera, J.; McLaughlin, M. J.; Hettiarachchi, G. M.; Kirby, J. K.; Beak, D. G. *Sci. Total Environ.* **2011**, *409*, 1489.

(66) Dur; n, N.; Marcato, P. D.; De Souza, G. I. H.; Alves, O. L.; Esposito, E. *J. Biomed. Nanotechnol.* **2007**, *3*, 203.

(67) Kaegi, R.; Sinnet, B.; Zuleeg, S.; Hagendorfer, H.; Mueller, E.; Vonbank, R.; Boller, M.; Burkhardt, M. *Environ. Pollut.* **2010**, *158*, 2900.

(68) Auffan, M.; Rose, J.; Bottero, J.-Y.; Lowry, G. V.; Jolivet, J.-P.; Wiesner, M. R. *Nat Nano* **2009**, *4*, 634.

(69) Kawata, K.; Osawa, M.; Okabe, S. *Environ. Sci. Technol.* **2009**, *43*, 6046.

(70) Morones, J. R.; Elechiguerra, J. L.; Camacho, A.; Holt, K.; Kouri, J. B.; Ramírez, J. T.; Yacaman, M. J. *Nanotechnology* **2005**, *16*, 2346.

(71) Mueller, N. C.; Nowack, B. *Environ. Sci. Technol.* **2008**, *42*, 4447.

(72) Oberdorster, G.; Oberdorster, E.; Oberdorster, J. *Environ. Health Perspect.* **2005**, *113*, 823.

(73) Bowman, C. R.; Bailey, F. C.; Elrod-Erickson, M.; Neigh, A. M.; Otter, R. R. *Environ. Toxicol. Chem.* **2012**, *31*, 1793.

(74) Ma, H.; Kabengi, N. J.; Bertsch, P. M.; Unrine, J. M.; Glenn, T. C.; Williams, P. L. *Environ. Pollut.* **2011**, *159*, 1473.

(75) Lee, K. J.; Browning, L. M.; Nallathamby, P. D.; Desai, T.; Cherukuri, P. K.; Xu, X.-H. N. *Chem. Res. Toxicol.* **2012**, *25*, 1029.

(76) Donkin, S. G.; Dusenbery, D. B. *Arch. Environ. Contam. Toxicol.* **1993**, *25*, 145.

(77) Hiramatsu, H.; Osterloh, F. E. *Chem. Mater.* **2004**, *16*, 2509.

(78) Kim, J. S.; Kuk, E.; Yu, K. N.; Kim, J.-H.; Park, S. J.; Lee, H. J.; Kim, S. H.; Park, Y. K.; Park, Y. H.; Hwang, C.-Y.; Kim, Y.-K.; Lee, Y.-S.; Jeong, D. H.; Cho, M.-H. *Nanomedicine: Nanotechnology, Biology and Medicine* **2007**, *3*, 95.

(79) Tolaymat, T. M.; El Badawy, A. M.; Genaidy, A.; Scheckel, K. G.; Luxton, T. P.; Suidan, M. *Sci. Total Environ.* **2010**, *408*, 999.

(80) Choi, J. E.; Kim, S.; Ahn, J. H.; Youn, P.; Kang, J. S.; Park, K.; Yi, J.; Ryu, D.-Y. *Aquat. Toxicol.* **2010**, *100*, 151.

(81) Wood, W. B. *The Nematode Caenorhabditis elegans*; Cold Spring Harbor Laboratory Press: New York, 1988.

(82) Aschner, E. J. M.-F. a. M. *Journal of Toxicology* **2011**, *2011*.

(83) Motola, D. L.; Cummins, C. L.; Rottiers, V.; Sharma, K. K.; Li, T.; Li, Y.; Suino-Powell, K.; Xu, H. E.; Auchus, R. J.; Antebi, A.; Mangelsdorf, D. J. *Cell* **2006**, *124*, 1209.

(84) LeBel, C. P.; Ischiropoulos, H.; Bondy, S. C. *Chem. Res. Toxicol.* **1992**, *5*, 227.

(85) Zhang, Z.-F.; Cui, H.; Lai, C.-Z.; Liu, L.-J. *Anal. Chem.* **2005**, *77*, 3324.

(86) Deguchi, S.; Alargova, R. G.; Tsujii, K. *Langmuir* **2001**, *17*, 6013.

(87) Scrivens, W. A.; Tour, J. M.; Creek, K. E.; Pirisi, L. *Journal of the American Chemical Society* **1994**, *116*, 4517.

(88) Stone, V.; Johnston, H.; Schins, R. P. F. *Critical Reviews in Toxicology* **2009**, *39*, 613.

(89) Nakanishi, I.; Fukuzumi, S.; Konishi, T.; Ohkubo, K.; Fujitsuka, M.; Ito, O.; Miyata, N. *The Journal of Physical Chemistry B* **2002**, *106*, 2372.

(90) Zhao, B.; Bilski, P. J.; He, Y.-Y.; Feng, L.; Chignell, C. F. *Photochemistry and Photobiology* **2008**, *84*, 1215.

(91) Zhao, B.; He, Y.-Y.; Bilski, P. J.; Chignell, C. F. *Chemical Research in Toxicology* **2008**, *21*, 1056.

(92) Kai, Y.; Komazawa, Y.; Miyajima, A.; Miyata, N.; Yamakoshi, Y. *Fullerenes, Nanotubes and Carbon Nanostructures* **2003**, *11*, 79

(93) Yamakoshi, Y.; Umezawa, N.; Ryu, A.; Arakane, K.; Miyata, N.; Goda, Y.; Masumizu, T.; Nagano, T. *Journal of the American Chemical Society* **2003**, *125*, 12803.

(94) Brunet, L. n.; Lyon, D. Y.; Hotze, E. M.; Alvarez, P. J. J.; Wiesner, M. R. *Environ. Sci. Technol.* **2009**, *43*, 4355.

(95) Lee, J.; Fortner, J. D.; Hughes, J. B.; Kim, J. H. *Environ. Sci. Technol.* **2007**, *41*, 2529.

(96) Harhaji, L.; Isakovic, A.; Raicevic, N.; Markovic, Z.; Todorovic-Markovic, B.; Nikolic, N.; Vranjes-Djuric, S.; Markovic, I.; Trajkovic, V. *European Journal of Pharmacology* **2007**, *568*, 89.

(97) Henry, T. B.; Menn, F. M.; Fleming, J. T.; Wilgus, J.; Compton, R. N.; Sayler, G. S. *Environmental Health Perspectives* **2007**, *115*, 1059.

(98) Lyon, D. Y.; Fortner, J. D.; Sayes, C. M.; Colvin, V. L.; Hughes, J. B. *Environ. Toxicol. Chem.* **2005**, *24*, 2757.

(99) Markovic, Z.; Todorovic-Markovic, B.; Kleut, D.; Nikolic, N.; Vranjes-Djuric, S.; Misirkic, M.; Vucicevic, L.; Janjetovic, K.; Isakovic, A.; Harhaji, L.; Babic-Stojic, B.; Dramicanin, M.; Trajkovic, V. *Biomaterials* **2007**, *28*, 5437.

(100) Oberdorster, E. *Environ. Helath Perspect.* **2004**, *112*, 1058.

(101) Sayes, C. M.; Fortner, J. D.; Guo, W.; Lyon, D.; Boyd, A. M.; Ausman, K. D.; Tao, Y. J.; Sitharaman, B.; Wilson, L. J.; Hughes, J. B.; West, J. L.; Colvin, V. L. *Nano Lett.* **2004**, *4*, 1881.

(102) Sayes, C. M.; Gobin, A. M.; Ausman, K. D.; Mendez, J.; West, J. L.; Colvin, V. L. *Biomaterials* **2005**, *26*, 7587.

(103) Gharbi, N. P., M.: Hadchouel, M.; Szwarc, H.; Wilson, S.R.; Moussa, F. *Nano Lett.* **2005**, *5*, 2578.

(104) Kovochich, M.; Espinasse, B.; Auffan, M.; Hotze, E. M.; Wessel, L.; Xia, T.; Nel, A. E.; Wiesner, M. R. *Environ. Sci. Technol.* **2009**, *43*, 6378.

(105) Pickering, K. D.; Wiesner, M. R. *Environ. Sci. Technol.* **2005**, *39*, 1359.

(106) Spohn, P.; Hirsch, C.; Hasler, F.; Bruinink, A.; Krug, H. F.; Wick, P. *Environmental Pollution* **2009**, *157*, 1134.

(107) Wang, I. C.; Tai, L. A.; Lee, D. D.; Kanakamma, P. P.; Shen, C. K. F.; Luh, T. Y.; Cheng, C. H.; Hwang, K. C. *Journal of Medicinal Chemistry* **1999**, *42*, 4614.

(108) Hara, K.; Nagata, T.; Kimura, K. *International Journal of Legal Medicine* **1987**, *98*, 49.

(109) Bruckner, R. *Advanced Organic Chemistry: Reaction Mechanisms* Academic Press; 1 edition, 2001.

(110) Monti, D.; Moretti, L.; Salvioli, S.; Straface, E.; Malorni, W.; Pellicciari, R.; Schettini, G.; Bisaglia, M.; Pincelli, C.; Fumelli, C.; Bonafè, M.; Franceschi, C. *Biochemical and Biophysical Research Communications* **2000**, *277*, 711.

(111) Dugan, L. L.; Lovett, E. G.; Quick, K. L.; Lotharius, J.; Lin, T. T.; O'Malley, K. L. *Parkinsonism & Related Disorders* **2001**, *7*, 243.

(112) Badireddy, A. R.; Hotze, E. M.; Chellam, S.; Alvarez, P.; Wiesner, M. R. *Environ. Sci. Technol.* **2007**, *41*, 6627.

(113) Xia, T.; Kovochich, M.; Brant, J.; Hotze, M.; Sempf, J.; Oberley, T.; Sioutas, C.; Yeh, J. I.; Wiesner, M. R.; Nel, A. E. *Nano Lett.* **2006**, *6*, 1794.

(114) Lee, J.; Mackeyev, Y.; Cho, M.; Li, D.; Kim, J.-H.; Wilson, L. J.; Alvarez, P. J. J. *Environ. Sci. Technol.* **2009**, *43*, 6604.

(115) Hotze, E. M.; Labille, J.; Alvarez, P.; Wiesner, M. R. *Environ. Sci. Technol.* **2008**, *42*, 4175.

(116) Lyon, D. Y.; Alvarez, P. J. J. *Environ. Sci. Technol.* **2008**, *42*, 8127.

(117) Lyon, D. Y.; Brunet, L.; Hinkal, G. W.; Wiesner, M. R.; Alvarez, P. J. J. *Nano Lett.* **2008**, *8*, 1539.

(118) Babynin, E. V.; Nuretdinov, I. A.; Gubskaya, V. P.; Barabanshchikov, B. I. *Russian Journal of Genetics* **2002**, *38*, 359.

(119) Lee, J.; Cho, M.; Fortner, J. D.; Hughes, J. B.; Kim, J. H. *Environ. Sci. Technol.* **2009**, *43*, 4878.

(120) Arbogast, J. W.; Darmanyan, A. P.; Foote, C. S.; Diederich, F. N.; Whetten, R. L.; Rubin, Y.; Alvarez, M. M.; Anz, S. J. *The Journal of Physical Chemistry* **1991**, *95*, 11.

(121) Guldi, D. M.; Prato, M. *Accounts of Chemical Research* **2000**, *33*, 695.

(122) Lee, S.; Park, J. Y.; Park, Y. S.; Park, Y. W.; Li, Y.; Zhu, D.; Tada, K.; Kawai, T.; Yoshino, K. *Solid State Communications* **1998**, *105*, 345.

(123) Vileno, B.; Sienkiewicz, A.; Lekka, M.; Kulik, A. J.; Forró, L. *Carbon* **2004**, *42*, 1195.

(124) Fortner, J. D.; Kim, D. I.; Boyd, A. M.; Falkner, J. C.; Moran, S.; Colvin, V. L.; Hughes, J. B.; Kim, J. H. *Environ. Sci. Technol.* **2007**, *41*, 7497.

(125) Yu, W. W.; Wang, Y. A.; Peng, X. *Chem. Mater.* **2003**, *15*, 4300.

(126) Adina M. Boyd, J. D. F., Elizabeth Quevedo, Jed Costanza, Sean Moran, Kurt D. Pennell, and Vicki L. Colvin *Submitted*.